Construction and Initial Characterization of the Densin Knockout Mouse

Thesis by
Andrew G.A. Medina-Marino

In Partial Fulfillment of the Requirements
for the Degree of
Doctor of Philosophy

California Institute of Technology
Pasadena, CA 91125

(Defended May 20, 2009)

To my parents, Olga and Gabriel Marino, for their lifetime of sacrifices so that I could have the strength and resources to accomplish all that I have. Without their love and support, I never would have made it this far.

To my husband, Jim Rhyne, for all of his love and support for the entirety of my Ph.D. program. His presence comforts me and his strength grants me stability.

To my dearest friend, Angela Mrema, who was killed in a car accident just as I was starting to write this dissertation. She always kept the faith even when mine waned. May her energy find eternal peace.

Acknowledgements

First and foremost, I would like to thank my advisor, Mary Kennedy. Whether she was conscious of it or not, she provided a near perfect balance of praise and tough love to keep me motivated and energized- I assure you, this was not an easy balance to achieve both because of my personality and hers. Furthermore, she provided me an environment that was conducive both to scientific and personal development. Ultimately, I am forever grateful for the training I received with Mary, and her support of my future career endeavors.

While all members of the Kennedy lab were wonderful, caring, and supportive colleagues, Leslie Schenker and Tinh Luong were of particular importance to my success. Both Tinh and Leslie provided a great deal of technical and experimental support for my thesis. Specifically, Leslie was an equal partner for the screening of the 496 ES cell clones for homologous recombination. Furthermore, she took over the genotyping of the Densin knockout and floxed lines from me, thus freeing me up to focus on other aspect of my thesis research. Leslie managed all of the timed matings for the NR2A tailless mutant, NR2B tailless mutant, NR2A x NR2B double tailless mutant, NR1 knockout, Densin knockout, and Densin x NR1 double knockouts. Furthermore, Leslie dissected and maintained all of the primary hippocampal culture that I have reported on. The sheer volume of work that she performed in support for my project is deserving of much thanks and recognition. No other Kennedy lab member was as integral to the totality of my work than Leslie. I am also indebted to Tinh Luong. Tinh helped me complete the construction of the targeting construct, aided in my quantitative immunoblot work, and was always willing to drop nearly everything she was doing to help me out on any aspect

of my project. Tinh's technical expertise and intellectual capacity far exceed that of any other biology graduate student I have known at Caltech. Consequently, she was of great importance as I thought through the relevance and context of my results.

I would like to thank Holly Carlisle for all of her support and work on the spine analysis. Holly and I performed the animal perfusions together, I took all of the images, and Holly processed and analyzed my images. Ultimately, this project is as much hers as it is mine.

I would like to thank Barbara Wold for entering into a collaboration with us to analyze the Densin knockout mouse using the RNA seq method. Her intellectual and financial support was crucial for the entirety of this project. Furthermore, I would like to thank Holly Beale and Ali Mortazavi for the generation of the RPKM values and critical discussions of my RNA seq analysis.

Abstract

Densin-180 is a core protein of postsynaptic densities (PSDs) in excitatory neurons. Densin is known to interact with Maguin-1 and PSD-95, suggesting that it plays a role in the NMDA receptor complex. Densin also interacts with δ-Catenin and N-Cadherin, an adhesion complex known to play a role in spine morphology. A ternary complex of Densin, CaMKII, and alpha-actinin suggests that Densin plays a key role in cytoskeleton dynamics. Finally, Densin can directly bind to shank, a core scaffolding molecule of the postsynaptic density. The association of Densin with such diverse complexes of proteins suggests that it acts as an integrator of numerous signaling cascades. Here I describe the construction and initial characterization of a Densin knockout mouse. Mice homozygous for the Densin deletion are prone to seizures induced by barbiturates. Also, Densin$^{-/-}$ animals have altered spine morphologies and show changes in the expression levels of other core PSD proteins. Densin$^{-/-}$ neurons in culture exhibit an overall decrease in their dendritic complexity. Furthermore, we show that in the absence of the NMDA receptor, Densin can act to bind CaMKII in the PSD. A new high-throughput method for studying changes in gene transcription, RNA seq, was also used to study the effect of the Densin deletion on the forebrain and the hippocampus. This work represents the first time RNA seq has been used to study an animal with a knockout mutation. Two candidate genes that may mediate the seizure sensitivity, Npas4 and $GABA_A\alpha2$, were identified by this method. Npas4 is known to directly affect the number of inhibitory synapses formed by neurons, and $GABA_A\alpha2$ is a major GABA receptor subunit that mediates the effects of Nembutal. These results suggest that Densin may play a role in maintaining the balance between inhibitory and excitatory networks. Together, our results demonstrate that Densin is important for dendritic arbor formation, spine morphology, CaMKII localization in the PSD, and seizure susceptibility.

Table of Contents

Chapter 3: Analysis of Dendritic Arborization and Spine Morphology

Chapter 4: The Role of Densin in the Postsynaptic Density and Docking of CaMKII

Chapter 5: Global Analysis of the Effect of Densin Knockout on Gene Transcription in the Brain

Introduction

1.1 History and Context

Within an evolutionary context, one can easily imagine that an ability to positively adjust decision-making processes relative to past experiences and environmental conditions would greatly increase the survival of an organism. Consequently, phylogenetically acquired mechanisms that allow an organism to adjust its behavior on the basis of information acquired ontogenetically have proven to be powerful adaptations. Information acquisition and utilization implies a close relationship between learning, memory, and behavior. Thus, it comes as no surprise that the biological mechanisms that underlie neural learning and memory have been intensely pondered and studied by philosophers, psychologists, and biologists since ancient times.

Evidence indicates that the number of neurons in an adult brain does not significantly increase with age, suggesting that the production of new neurons is not the cellular mechanism underlying learning and memory [1] . The theories put forth by Ramon y Cajal [2] and expanded upon by Donald Hebb [3] suggesting that changes in neuronal connectivity are the cellular and molecular basis of learning and memory have become the dominant paradigm for much of modern neuroscience. In particular, Hebb's neurophysiological postulate of learning states:

> *Let us assume that the persistence or repetition of a reverberatory activity (or "trace") tends to induce lasting cellular changes that add to its stability.... when an axon of cell A is near enough to*

> *excite a cell B and repeatedly or persistently takes part in firing it, some growth process or metabolic change takes place in one or both cells such that A's efficiency, as one of the cells firing B, is increased. [3]*

Hebb's postulate laid the initial theoretical framework that led subsequent researchers to identify long term potentiation- the cellular mechanism by which a neuron's excitatory response can be enhanced, or "potentiated," by previous high frequency stimulation, allowing neurons to respond more sensitively to subsequent low frequency stimulations.

Neural connectivity as a concept originated with Ramon y Cajal's identification of small protrusions extending away from the main dendritic axis (dendritic spines) and their contact points with the adjacent nerve fibers (axons; Fig 1.1a, panel a). However, the concept that the bulbous head of dendritic spines were likely to act as "receptors of current" was contributed by H.J Berkley (Fig 1.1a, panel b):

> *"The function of the gemmule is in all likelihood to receive nerve impulses from the ending of the numerous terminal nerve fibers that seem almost to touch them, and carry these impressions to the dendrite and by its medium on the cell body."*

Furthermore,

"…these spherical apparatus (terminal buttons) are closely adjusted against the bulbous tip of the gemmules, at times the application being so close as to give the impression of actual contact." [2]

In 1897, Sherrington united Ramon y Cajal's neuroanatomical and Berkley's physiological arguments into the single concept of the synapse. However, it was not until 1956 that the definitive identification of the synapse was made by Palay, and not until 1959 that dendritic spines were definitively identified as the postsynaptic units (Gray 1959 a, b); both utilized electron microscopes to illuminate these structures.

In 1959, Gray identified specific, conserved structural differences between the axo-somatic and axo-dendritic synapses [4]. In particular, he described the electron dense thickening of the postsynaptic membrane (Fig 1.1b):

"One very obvious feature of the cortical synapse is that in certain contacts with dendritic trunks of their spines a high proportion of the length over which the membranes are apposed shows a thickening and increased density. Also the thickening and density is much more pronounced in the post- than the pre-synaptic membrane." (p. 422, [4])

Ensuing biochemical fractionation methods were developed to isolate intact membranes containing the proteins of the postsynaptic densities (PSD) [5, 6] thus

ushering in an era during which the protein constituents of the PSD began to be identified.

Finally, in the late 1960s and early 1970s another set of seminal experiments were providing the first experimental description of long term potentiation. Specifically, in 1966, Lomo and colleagues reported that a series of conditioning trains of impulses could potentiate the size of synaptic potentials for periods ranging from 30 min to many hours. In their seminal work, Lomo and Colleagues wrote the following:

> *"Extracellular responses of dentate granule cells, evoked by repetitive stimulation of the entorhinal area or perforant path fibres, were recorded simultaneously with two microelectrodes. One electrode recording from the layer of perforant path synapses on the granule cell dendrites, the other from the layer of granule cell bodies.*
>
> *"After an initial depression, lasting for a few seconds, repetitive stimulation led to a large potentiated response, compared to the response evoked by a single volley. This effect, frequency potentiation, was seen as an increase of the amplitude and a decrease of the latency of the population spike and as an increase of the rate of rise and amplitude of the extracellular excitatory synaptic potentials.*

"This represents an example of a plastic change in a neuronal chain, expressing itself as a long-lasting increase of the synaptic efficiency. The effect, which may last for hours, is dependent upon repeated use of the system." [7]

Further experimentation by Bliss and Lomo showed that "one or more brief episodes of tetanic stimulation (15 sec $^{-1}$ for 10--15 sec) produces a potentiation of the monosynaptic response evoked by single shocks which may last for several hours." The full report of Lomo's work, published in 1973 [7] was the first quantitative description of LTP.

1.2 The Postsynaptic Density: Contents, Supramolecular Complexes, and Higher Order Structure

It has long been thought that synapses are the most suitable location of memory storage in the brain [3, 8]. Furthermore, many believed that a clear relationship existed between the morphology of dendritic spines and their functions during normal and diseased states [9]. However, the observation that spine head volume can increase and neck length vary during LTP [10, 11] helped establish the idea that there exist dynamic and plastic mechanisms within the spine that actively respond to synaptic activity. This work, together with that of Bliss and Lomo [7] helped lay the groundwork for the subsequent hypothesis that synaptic plasticity is critical to the underlying molecular basis of learning and memory.

1.2.1 Contents of the PSD

Understanding the activity dependent changes that occur in the PSD upon synaptic stimulation requires an integrated approach to identify its constituent proteins and then study their function and dynamic organization. Early efforts to identify components of the PSD utilized differential centrifugation and sucrose density gradients, followed by detergent extraction with non-ionic detergents such as Triton-X [6]. Protein separation and microsequencing techniques used by Mary Kennedy and co-workers resulted in the identification of numerous core PSD proteins, including αCaMKII [12], PSD-95 [13], the NR2B subunit of the NMDA receptor [14], Densin [15], SynGAP [16], and Citron [17]. Yeast two-hybrid screens using known PSD proteins as bait were used to identify other PSD proteins, among them GKAP [18-20], Shank [21, 22], GRIP/ ABP [23, 24], Homer [25], GRASP-1 [26], and SALMs (synaptic adhesion-like molecules) [27]. More recently, mass spectrometry methods have been used to detect a large number of putative PSD proteins [28-31]. Though proteomic based PSD identification studies have identified many proteins likely to play a role in postsynaptic reception, care needs to be taken when interpreting these findings. The spatial constraints, stoichiometry and organization of the PSD suggests that the number of different proteins in a single PSD is likely to be in the tens, not hundreds of different proteins [32, 33].

Recent work by Heintz and co-workers [33] used a mix of genetic engineering, biochemical fractionation, affinity purification, and mass spectrometry to identify the contents of the parallel fiber/ Purkinje cell PSD. This experimental approach identified approximately 60 proteins enriched in these PSDs. Previously identified PSD proteins such as Homer3, Shank1, Shank2, PSD-95, PSD-93, α and βCaMKII, and δ-catenin

where identified. However, other previously unidentified proteins were also isolated. This work suggests that a core group of PSD proteins are likely to exist at most PSDs. Moreover, the bulk proteomic identification of numerous proteins from whole brain PSDs speaks more to the diversity of synapses, their spatial and functional specificity, and their complex signaling pathways than the general contents of a PSD.

Identifying the protein-protein interactions and atomic structure of individual PSD proteins is necessary for modeling the spatial geometry of this integrated macromolecular complex. Together with data generated from systematic EM immunogold analysis [34], electron microscopy [35], EM tomography [36], and solid phase chemical cross-linking methods [37], a comprehensive 3-dimensional model of the PSD is beginning to emerge. Two major characteristics of all current models are 1) the clustering and scaffolding of supramolecular complexes immediately adjacent to the membrane, and 2) a matrix of proteins forming a platform upon which these supramolecular complexes sit.

1.2.2 Supramolecular Complexes of the PSD

The supramolecular complexes immediately adjacent to the membrane are composed of transmembrane proteins (receptors, ion channels, and adhesion molecules) and their downstream effectors (G-proteins, kinases, phosphatases, signaling proteins, as well as cytoskeletal and adaptor proteins). Three such supramolecular complexes are 1) the NMDA receptor complex, 2) the mGluR complex, and 3) the AMPA receptor complex. The main scaffolding protein for the NMDA complex is PSD-95. Homer specifically complexes the mGluR complex, while GRIP1/ APB and PSD-95 each work to cluster and localize AMPA receptors with potential downstream signaling pathways.

Cho et al. [38], identified the first PSD scaffolding protein, PSD-95. With its three PDZ domains, a SH3 domain, and a guanylate kinase domain, PSD-95 is the prototypical PSD scaffolding molecule, allowing for multiple and simultaneous protein-protein interactions. PSD-95 has been shown to nucleate a NMDA receptor signaling complex [39, 40] and synaptic adhesion complexes [41] within the PSD. Though PSD-95 has not been shown to nucleate AMPA receptor signaling complexes, it has been shown to localize and target AMPA receptors via Stargazin [42-44]. Furthermore, Gerrow et al. [45] showed that mobile, preformed complexes of PSD-95, GKAP, and Shank are transported to dendritic positions primed for synapse development. Such evidence suggests that PSD-95 acts as a major scaffolding protein for modular clusters of supramolecular complexes i.e., the PSD-95/ NMDA receptor complex and the PSD-95/ adhesion molecule complex.

A second major PSD scaffolding molecule, Homer, is known to interact with and cluster the group 1 metabotropic receptors (mGluR1 and mGluR5) and inositol trisphosphate receptors (IP3R) [22, 25, 46]. The Homer protein has two major splice variants, long and short [47]. The long form contains two major domains, 1) the N-terminal EVH1 PDZ-like target-binding domain that mediates interactions with mGluR and IP3R [22, 25, 48] and 2) the C-terminal self-assembly coiled-coil/ leucine zipper domain that mediates self-dimerization [49]. The short form of Homer contains only the N-terminal EVH1 PDZ-like target-binding domain and exhibits activity regulated expression, placing it in the family of immediate early genes [25, 50]. Furthermore, this short form of Homer (a.k.a. Homer1a) exerts a dominant-negative activity by impairing self-dimerization and Homer-mediated multi-protein complexes [49, 51-53].

The third scaffolding protein that mediates clustering of particular PSD proteins into supramolecular complexes is GRIP/ ABP (AMPA binding protein). GRIP1 and ABP/ GRIP2 were independently identified using the C-terminal tail of GluR2/3 as bait in yeast two-hybrid screens [23, 24]. In addition to binding and clustering GluR2/3 receptors, GRIP1 also binds to GRASP-1, a neuron specific guanine nucleotide exchange factor (GEF). Recent work by Ye et al. [54] shows that GRASP-1 is able to bind both JNK and the upstream kinase MEKK1 in neurons, and that these interactions facilitate JNK signaling. Though a complex specifically containing AMPA, GRIP1, and GRASP-1 has yet to be shown, or the direct activation of AMPA receptors leading to the activation of the JNK pathway scaffolded by GRASP-1, the suggestion that GRIP1 scaffolds an AMPA receptor complex is intriguing. Finally, like PSD-95, GRIP family proteins can cluster synaptic adhesion molecules into larger supramolecular complexes [55-57].

1.2.3 Higher Order Structure of the PSD

Current models of the PSD suggest that the supramolecular complexes adjacent to the membrane sit on a platform matrix formed by the protein Shank. Shank was originally identified by using the C-terminal residues of GKAP, a PSD protein that specifically co-localizes with PSD-95 and directly interacts with its guanylate kinase domain [19-21, 58], as bait in a yeast two-hybrid screen [21]. Shank contains multiple protein-protein binding domains, including numerous N-terminal ankyrin repeats, SH3 and PDZ domains, conserved proline-rich clusters, and a SAM (sterile alpha motif) domain at its C-terminus [21]. X-ray crystallography and electron microscopy showed that Shank can form polymer sheets through self-association of the SAM domain, and

that helical fibers formed by Shank can be crossed linked by Zn^{2+} [35]. More recently, Hayashi et al. [59] demonstrated that interactions between multimerized Shank and tetramerized Homer form higher-order-polymerized complexes with a mesh-like network structure. This higher-order structure was proposed to form the core structural framework and binding platform for PSD supramolecular complexes.

The multiple protein domains of Shank have been shown to bind the different PSD supramolecular complexes immediately adjacent to the membrane either by direct binding or via adaptor proteins [32]. In particular, the PSD-95/ NMDAR and the PSD-95/ synaptic adhesion molecule complexes can be directly linked to the Shank scaffolding via GKAP [21]. Homer is known to directly bind Shank, thus linking the mGluR/ Homer complex to the underlying Shank scaffold matrix [22]. Consequently, Shank is able to cross-link Homer and PSD-95 complexes in the PSD. Finally, though no interaction has been demonstrated between the GRIP/ AMPA complex and Shank, AMPA receptor complexes can interact with PSD-95 through the C-terminal PDZ binding motif of Stargazin, a transmembrane AMPA receptor regulatory protein [42, 60]. Ultimately, the ability of Shank to tether and nucleate numerous PSD supramolecular complexes supports the current models of a laminar organization of the postsynaptic density.

1.3 Densin is a Core Component of the Postsynaptic Density

Densin was first identified as a highly enriched protein in the insoluble PSD fraction following extraction with *N*-lauroyl sarcosinate (sarcosyl), thus defining it as a "core" PSD protein [15]. A 167kDa glycosylated protein originally thought to be brain

specific, Densin has been subsequently shown to be expressed at low levels in kidney [61-63], Testis [64], and the pancreas [61].

Densin contains two indisputable protein domains, 1) a N-terminal leucine-rich repeat (LRR) domain consisting of 16 canonical LRRs, and 2) a C-terminal PSD-95/ Dlg/ ZO-1 (PDZ) domain (Fig 1.3). Other proteins with this arrangement of domains were subsequently identified and designated a new protein family call LAP proteins (LRR and PDZ domains), of which Densin is the founding member [65]. Initial sequence analysis of Densin also identified a RGD motif, a Mucin homology domain and a putative transmembrane domain (Fig 1.3).

1.3.1 Cellular Localization and Tissue Expression

Immunofluorescent double labeling of Densin and Synapsin I, a presynaptic marker, reveals that Densin is localized to the synapse (Fig. 1.4a, top panel). Furthermore, co-staining neuronal cultures with antibodies to Densin and PSD-95 reveals a tight colocalization of these two proteins, supporting the hypothesis that Densin is a postsynaptic density protein (Fig. 1.4a, bottom panel). Interestingly, Densin was also identified in the axon initial segment (Fig. 1.4a, bottom panel) suggesting that it may play a role in the macromolecular complex of the axon hillock where action potentials are generation. Comparison of in situ hybridization images of Densin with those of αCaMKII (high expresser) and the NR2C subunit of the NMDA receptor (low expresser) show that Densin is highly expressed in all forebrain regions (Fig 1.4b; images taken from the Allen Brain Map, Allen Institute for Brain Science http://www.brain-map.org/). Though there is not always a direct relationship between gene and protein expression

patterns, these studies suggest that the Densin protein is likely to be widely expressed in the forebrain.

1.3.2 CaMKII Phosphorylation of and Association with Densin

Apperson et al. [15] showed that Densin is specifically phosphorylated by endogenous CaMKII within the PSD. Subsequent work by Strack et al. [66] identified Ser^{1397} and Walikonis et al. [67] identified Ser^{1293} and Ser^{1397} as sites phosphorylated by CaMKII. Both studies independently identified the region between the putative transmembrane domain and the PDZ domain as the region of CaMKII binding, with Walikonis specifically demonstrating that Densin directly interacts with the association domain of CaMKII. Walikonis et al. [67] also demonstrated that autophosphorylation of CaMKII on Thr^{286} significantly increases its binding affinity for Densin; non-phosphorylated CaMKII has a reduced, but still significant binding affinity for Densin. Furthermore, the phosphorylation of Densin by CaMKII does not dramatically alter the binding affinity between the two proteins. Strack et al. [66] similarly demonstrated that autophosphorylation of CaMKII is not required for its interaction with Densin, and that binding of CaMKII to either Densin or the NR2B tail of the NMDA receptor is non-competitive. Taken together, these data suggest that Densin may act as a docking site for CaMKII even after dephosphorylation of the kinase, and that phosphorylation of Densin by CaMKII may act to modulate binding interactions between Densin and other proteins in the PSD. Finally, Strack et al. [66] and Jiao et al. [68] further demonstrated that the exon containing the CaMKII binding site (exon 24) has a developmentally regulated

splice variant, suggesting that alternative splicing may act as a mechanism to regulate the docking of CaMKII to Densin.

1.3.3 Protein-Protein Interactions Between Densin and Other PSD Proteins

In addition to identifying CaMKII as a binding partner for Densin in a yeast two-hybrid screen, Walikonis et al. also identified α-actinin as a binding partner for the PDZ domain of Densin. Biochemical studies of the interactions between Densin, CaMKII, and α-actinin not only confirms that α-actinin and Densin bind to distinct regions within CaMKII, but that CaMKII and α-actinin interact with each other; thus, these proteins can form a ternary complex.

Using the PDZ domain of Densin as bait in a yeast two-hybrid screen, Ohtakara and coworkers [69] identified Maguin-1 as a binding partner of Densin. Maguin-1 directly interacts with the PDZ domain of Densin via a canonical class I PDZ binding motif, THV, located at its C-terminus. Maguin-1 was previously shown to interact with PSD-95, S-SCAM (synaptic scaffolding molecule) and Raf-1, an activator of MAPK/ ERK signal transduction [70, 71]. Immunoprecipitation studies revealed that Densin, Maguin-1, and PSD-95 interact in a complex, while immunofluorescent imaging demonstrated tight co-localization of all three at the tips of spines in dissociated hippocampal cultures. A C-terminal leucine rich region allows Maguin-1 to self-associate. This self-association allows Maguin-1 to simultaneously interact with both Densin and PSD-95. Taken together, these results suggest that Maguin-1 may link Densin to the PSD-95 receptor signaling complexes and to the MAPK/ ERK signaling pathway, both of which are known to be involved in synaptic plasticity [32, 72].

The PDZ domain of Densin was also shown to interact directly with the C-terminal SWV PDZ binding motif of δ-catenin/ NPRAP [73]. Izawa and co-workers [73] showed the following: 1) Densin, δ-catenin/ NPRAP, and N-Cadherin co-immunoprecipitate with each other, 2) all three proteins co-localize at the tips of spines in dissociated hippocampal cultures, and 3) δ-catenin/ NPRAP specifically mediates the association of Densin and N-Cadherin. These results provide strong evidence that Densin is linked to cadherin-catenin complexes and that it may be involved in organizing synaptic cell-cell junctions.

Another PSD protein found to interact with Densin is Shank. Quitsch et al. used the SH3 domain of Shank as bait in a yeast two-hybrid screen. Of the approximately one million clones screened, only the C-terminus of Densin, residues 1125-1542, was consistently identified. Further analysis determined that the membrane proximal region of Densin was require for binding to Shank. However, the putative transmembrane region and the PDZ domain enhance the interaction between Densin and Shank such that, in their absence, Densin and Shank no longer interact.

Though only identified in the glomerular podocytes of kidney thus far, two additional cell adhesion complex proteins known to directly interact with Densin are β-catenin and nephrin [62, 63]. In addition, Heikkila and co-workers [63] isolated δ-catenin and α-actinin from the same yeast two-hybrid screen using the entire putative intracellular region of human Densin. Immunoprecipitation studies showed that β-catenin, P-cadherin, and Densin precipitate as a complex. Ahola and co-workers [62] identified Densin as a key component of the nephrin mediated slit diaphragm complex of the kidney; the slit diaphragm complex is critical for the maintenance of podocyte

cytoarchitecture and connections to the cytoskeleton. Though these protein-protein interactions have yet to be identified in the brain, the fact that Densin directly interacts with nephrin and complexes with β-catenin and P-cadherin suggests a conserved role for Densin as part of cell adhesion complexes.

1.3.4 Functional Analysis of Densin.

The only analysis of Densin's function in neurons to date is the work by Quitsch and co-workers [74]. Overexpression of full length Densin in primary hippocampal cultures caused a striking increase in dendritic branching and in the number of branch points. Quitsch and co-workers further demonstrated that this enhanced branching phenotype could be induced only by overexpression of constructs containing the LRR domain of Densin. Interestingly, co-overexpression of Shank was able to abrogate Densin induced branching. However, the increased branching patterns induced by Densin overexpression are not reversed by Shank when the C-terminal region of Densin is not part of the construct. Thus, the ability of Shank to abrogate Densin induced enhancement of dendritic branching requires direct interaction between Shank and the C-terminal domain. Finally, Quitsch and co-workers demonstrated that the overexpression of Densin resulted in an increased number of presynaptic synaptophysin clusters. They interpreted these results to mean that more presynaptic release sites are formed when Densin is over-expressed. Consequently, these results, in combination with known interactions of Densin with adhesion complexes in the PSD suggest that Densin may play a crucial role in synaptogenesis as well as in dendritic arborization.

1.3.5 Membrane Topology of Densin

A recent review by Thalhammer and collegues [75] proposed a new, membrane associated, entirely cytosolic topology for Densin. Recent analysis of the *in vivo* phosphorylation state of PSD preps found that Densin contained a cluster of phosphorylation sites positioned N-terminal to the proposed transmembrane domain. These findings prompted Thalhammer and colleagues to suggest that the original transmembrane topology of Densin was incorrect, and that Densin was in fact entirely cytosolic. They further purport that current bioinformatic analysis does not support the existence of a signal peptide or other sequence motifs that suggests a transmembrane domain. Moreover, they argue that the inability to surface biotinylate the proposed extracellular portion supports its intracellular position. Finally, they suggest with much hand-waving, that the experimental evidence for glycosylation was "quite weak." On this point, we take serious issue.

Two enzymatic digestions were done to support the glycosylation state of Densin. The first enzymatic digestion used neuraminidase from *Arthrobacter ureafasciens.* Neuraminidases are glycohydrolases that catalyze the hydrolysis of sialic acid-α-ketosides [76]. When Densin was subjected to a neuraminidase digestion, its molecular weight was significantly shifted from ~180kDa to 148kDa. Neuraminidase from *Arthrobacter ureafasciens* has been reported to be very efficient and highly specific for hydrolyzing α-2,6 linked sialic acid [77-79]. Thalhammer and colleagues argue that "only prolonged incubation with neuraminidase suggested the presence of sialic acid modified residues." The 24 hour, 37^0C incubation that was conducted is a standard protocol and is supported by voluminous research and protocol development. As such,

Thalhammer and colleagues are quite mistaken in their biochemical protocol assumptions.

Second, these authors argue that "digestion with O-sialoglycoprotein endoprotease suggested possible positioning of O-sialoglycosylation within the Mucin domain." The suggestion here is that digestion with the O-sialoglycoprotein endoprotease from *Pasteurella haemolytica* lacks in specificity of its action. The *P. haemolytica* O-sialoglycoprotein endopeptidase cleaves only proteins that are heavily sialyated, in particular those with sialylated serine and threonine residues [80, 81]. It does not cleave unglycosylated proteins, desialylated glycoproteins or glycoproteins that are only N-glycosylated [82-84]. Ultimately, this is a highly specific endopeptidase. The observed cleavage products were identified by immunoblot to be Densin.

Colbran and colleagues recently published an extensive profile of alternatively spliced species of Densin [68]. Though it has yet to be shown, the numerous slice variants of Densin suggest that both a transmembrane and a entirely cytosolic topology is possible. Thalhammer and colleagues never once suggested this possibility-- a serious scientific oversight.

Based on current hard evidence, not inference alone, we believe that Densin may adopt alternative membrane topologies, and that both a transmembrane and a cytosolic membrane-associated orientation may exist.

References

1. Williams, R.W. and K. Herrup, *The control of neuron number.* Annu Rev Neurosci, 1988. **11**: p. 423-53.
2. Garcia-Lopez, P., V. Garcia-Marin, and M. Freire, *The discovery of dendritic spines by Cajal in 1888 and its relevance in the present neuroscience.* Prog Neurobiol, 2007. **83**(2): p. 110-30.
3. Hebb, D.O., *The organization of behavior.* 1949, New York: John Wiley & Sons.
4. Gray, E.G., *Axo-somatic and axo-dendritic synapses of the cerebral cortex: an electron microscope study.* J. Anat., 1959. **93**: p. 420-433.
5. Cotman, C.W., et al., *Isolation of postsynaptic densities from rat brain.* J. Cell Biol., 1974. **63**: p. 441-455.
6. Carlin, R.K., et al., *Isolation and characterization of postsynaptic densities from various brain regions: enrichment of different types of postsynaptic densities.* J. Cell Biol., 1980. **86**: p. 831-843.
7. Bliss, T.V.P. and T. Lomo, *Long-lasting potentiation of synaptic transmission in the dentate area of the anaesthetized rabbit following stimulation of the perforant path.* J. Physiol., 1973. **232**: p. 331-356.
8. Deutsch, J.A., *The cholinergic synapse and the site of memory.* Science, 1971. **174**(11): p. 788-94.
9. Fiala, J.C., J. Spacek, and K.M. Harris, *Dendritic spine pathology: cause or consequence of neurological disorders?* Brain Res Brain Res Rev, 2002. **39**(1): p. 29-54.
10. Fifkova, E. and C.L. Anderson, *Stimulation-induced changes in dimensions of stalks of dendritic spines in the dentate molecular layer.* Exp Neurol, 1981. **74**(2): p. 621-7.
11. Van Harreveld, A. and E. Fifkova, *Swelling of dendritic spines in the fascia dentata after stimulation of the perforant fibers as a mechanism of post-tetanic potentiation.* Exp Neurol, 1975. **49**(3): p. 736-49.
12. Kennedy, M.B., M.K. Bennett, and N.E. Erondu, *Biochemical and immunochemical evidence that the "major postsynaptic density protein" is a subunit of a calmodulin-dependent protein kinase.* Proc. Natl. Acad. Sci. U.S.A., 1983. **80**: p. 7357-7361.
13. Cho, K.-O., C.A. Hunt, and M.B. Kennedy, *The rat brain postsynaptic density fraction contains a homolog of the Drosophila discs-large tumor suppressor protein.* Neuron, 1992. **9**: p. 929-942.
14. Moon, I.S., M.L. Apperson, and M.B. Kennedy, *The major tyrosine-phosphorylated protein in the postsynaptic density fraction is N-methyl-D-aspartate receptor subunit 2B.* Proc. Natl. Acad. Sci. U.S.A., 1994. **91**: p. 3954-3958.
15. Apperson, M.L., I.-S. Moon, and M.B. Kennedy, *Characterization of densin-180, a new brain-specific synaptic protein of the O-sialoglycoprotein family.* J. Neurosci., 1996. **16**: p. 6839-6852.

16. Chen, H.-J., et al., *A synaptic Ras-GTPase activating protein (p135 SynGAP) inhibited by CaM Kinase II.* Neuron, 1998. **20**: p. 895-904.
17. Zhang, W., et al., *Citron binds to PSD-95 at glutamatergic synapses on inhibitory neurons in the hippocampus.* J Neurosci, 1999. **19**(1): p. 96-108.
18. Naisbitt, S., et al., *Characterization of guanylate kinase-associated protein, a postsynaptic density protein at excitatory synapses that interacts directly with postsynaptic density-95/synapse-associated protein 90.* J Neurosci, 1997. **17**(15): p. 5687-96.
19. Satoh, K., et al., *DAP-1, a novel protein that interacts with the guanylate kinase-like domains of hDLG and PSD-95.* Genes Cells, 1997. **2**(6): p. 415-24.
20. Takeuchi, M., et al., *SAPAPs. A family of PSD-95/SAP90-associated proteins localized at postsynaptic density.* J Biol Chem, 1997. **272**(18): p. 11943-51.
21. Naisbitt, S., et al., *Shank, a novel family of postsynaptic density proteins that binds to the NMDA receptor/PSD-95/GKAP complex and cortactin.* Neuron, 1999. **23**(3): p. 569-82.
22. Tu, J.C., et al., *Coupling of mGluR/Homer and PSD-95 complexes by the Shank family of postsynaptic density proteins.* Neuron, 1999. **23**(3): p. 583-92.
23. Dong, H., et al., *GRIP: a synaptic PDZ domain-containing protein that interacts with AMPA receptors [see comments].* Nature, 1997. **386**(6622): p. 279-84.
24. Srivastava, S., et al., *Novel anchorage of GluR2/3 to the postsynaptic density by the AMPA receptor-binding protein ABP.* Neuron, 1998. **21**(3): p. 581-91.
25. Brakeman, P.R., et al., *Homer: a protein that selectively binds metabotropic glutamate receptors.* Nature, 1997. **386**(6622): p. 284-8.
26. Ye, B., et al., *GRASP-1: a neuronal RasGEF associated with the AMPA receptor/GRIP complex.* Neuron, 2000. **26**(3): p. 603-17.
27. Wang, C.Y., et al., *A novel family of adhesion-like molecules that interacts with the NMDA receptor.* J Neurosci, 2006. **26**(8): p. 2174-83.
28. Yoshimura, Y. and T. Yamauchi, *Phosphorylation-dependent reversible association of Ca2+/calmodulin- dependent protein kinase II with the postsynaptic densities.* J Biol Chem, 1997. **272**(42): p. 26354-9.
29. Peng, J., et al., *Semiquantitative proteomic analysis of rat forebrain postsynaptic density fractions by mass spectrometry.* J Biol Chem, 2004. **279**(20): p. 21003-11.
30. Jordan, B.A., et al., *Identification and verification of novel rodent postsynaptic density proteins.* Mol Cell Proteomics, 2004. **3**(9): p. 857-71.
31. Cheng, D., et al., *Relative and absolute quantification of postsynaptic density proteome isolated from rat forebrain and cerebellum.* Mol Cell Proteomics, 2006. **5**(6): p. 1158-70.
32. Sheng, M. and C.C. Hoogenraad, *The postsynaptic architecture of excitatory synapses: a more quantitative view.* Annu Rev Biochem, 2007. **76**: p. 823-47.
33. Selimi, F., et al., *Proteomic studies of a single CNS synapse type: the parallel fiber/purkinje cell synapse.* PLoS Biol, 2009. **7**(4): p. e83.
34. Valtschanoff, J.G. and R.J. Weinberg, *Laminar organization of the NMDA receptor complex within the postsynaptic density.* J Neurosci, 2001. **21**(4): p. 1211-7.
35. Baron, M.K., et al., *An architectural framework that may lie at the core of the postsynaptic density.* Science, 2006. **311**(5760): p. 531-5.

36. Chen, X., et al., *Organization of the core structure of the postsynaptic density.* Proc Natl Acad Sci U S A, 2008. **105**(11): p. 4453-8.
37. Liu, S.H., et al., *Studying the protein organization of the postsynaptic density by a novel solid phase- and chemical cross-linking-based technology.* Mol Cell Proteomics, 2006. **5**(6): p. 1019-32.
38. Cho, K.O., et al., *The alpha subunit of type II Ca^{2+}/calmodulin-dependent protein kinase is highly conserved in Drosophila.* Neuron, 1991. **7**: p. 439-450.
39. Kennedy, M.B., *Signal-processing machines at the postsynaptic density.* Science, 2000. **290**: p. 750-754.
40. Sheng, M. and C. Sala, *PDZ domains and the organization of supramolecular complexes.* Annu Rev Neurosci, 2001. **24**: p. 1-29.
41. Han, K. and E. Kim, *Synaptic adhesion molecules and PSD-95.* Prog Neurobiol, 2008. **84**(3): p. 263-83.
42. Chen, L., et al., *Stargazin regulates synaptic targeting of AMPA receptors by two distinct mechanisms.* Nature, 2000. **408**(6815): p. 936-43.
43. Chetkovich, D.M., et al., *Phosphorylation of the postsynaptic density-95 (PSD-95)/discs large/zona occludens-1 binding site of stargazin regulates binding to PSD-95 and synaptic targeting of AMPA receptors.* J Neurosci, 2002. **22**(14): p. 5791-6.
44. Bats, C., L. Groc, and D. Choquet, *The interaction between Stargazin and PSD-95 regulates AMPA receptor surface trafficking.* Neuron, 2007. **53**(5): p. 719-34.
45. Gerrow, K., et al., *A preformed complex of postsynaptic proteins is involved in excitatory synapse development.* Neuron, 2006. **49**(4): p. 547-62.
46. Thomas, U., *Modulation of synaptic signalling complexes by Homer proteins.* J Neurochem, 2002. **81**(3): p. 407-13.
47. Shiraishi-Yamaguchi, Y. and T. Furuichi, *The Homer family proteins.* Genome Biol, 2007. **8**(2): p. 206.
48. Xiao, B., et al., *Homer regulates the association of group 1 metabotropic glutamate receptors with multivalent complexes of homer-related, synaptic proteins.* Neuron, 1998. **21**(4): p. 707-16.
49. Tadokoro, S., et al., *Involvement of unique leucine-zipper motif of PSD-Zip45 (Homer 1c/vesl-1L) in group 1 metabotropic glutamate receptor clustering.* Proc Natl Acad Sci U S A, 1999. **96**(24): p. 13801-6.
50. Kubik, S., T. Miyashita, and J.F. Guzowski, *Using immediate-early genes to map hippocampal subregional functions.* Learn Mem, 2007. **14**(11): p. 758-70.
51. Ciruela, F., M.M. Soloviev, and R.A. McIlhinney, *Co-expression of metabotropic glutamate receptor type 1alpha with homer-1a/Vesl-1S increases the cell surface expression of the receptor.* Biochem J, 1999. **341 (Pt 3)**: p. 795-803.
52. Roche, K.W., et al., *Homer 1b regulates the trafficking of group I metabotropic glutamate receptors.* J Biol Chem, 1999. **274**(36): p. 25953-7.
53. Ango, F., et al., *Agonist-independent activation of metabotropic glutamate receptors by the intracellular protein Homer.* Nature, 2001. **411**(6840): p. 962-5.
54. Ye, B., et al., *GRASP-1 is a neuronal scaffold protein for the JNK signaling pathway.* FEBS Lett, 2007. **581**(23): p. 4403-10.

55. Silverman, J.B., et al., *Synaptic anchorage of AMPA receptors by cadherins through neural plakophilin-related arm protein AMPA receptor-binding protein complexes.* J Neurosci, 2007. **27**(32): p. 8505-16.
56. Bruckner, K., et al., *EphrinB ligands recruit GRIP family PDZ adaptor proteins into raft membrane microdomains.* Neuron, 1999. **22**(3): p. 511-24.
57. Lin, D., et al., *The carboxyl terminus of B class ephrins constitutes a PDZ domain binding motif.* J Biol Chem, 1999. **274**(6): p. 3726-33.
58. Naisbitt, S., et al., *Characterization of guanylate kinase-associated protein, a postsynaptic density protein at excitatory synapses that interacts directly with postsynaptic density-95/synapse-associated protein 90.* J. Neurosci., 1997. **17**: p. 5687-5696.
59. Hayashi, M.K., et al., *The postsynaptic density proteins Homer and Shank form a polymeric network structure.* Cell, 2009. **137**(1): p. 159-71.
60. Schnell, E., et al., *Direct interactions between PSD-95 and stargazin control synaptic AMPA receptor number.* Proc Natl Acad Sci U S A, 2002. **99**(21): p. 13902-7.
61. Rinta-Valkama, J., et al., *Densin and filtrin in the pancreas and in the kidney, targets for humoral autoimmunity in patients with type 1 diabetes.* Diabetes Metab Res Rev, 2007. **23**(2): p. 119-26.
62. Ahola, H., et al., *A novel protein, densin, expressed by glomerular podocytes.* J Am Soc Nephrol, 2003. **14**(7): p. 1731-7.
63. Heikkila, E., et al., *Densin and beta-catenin form a complex and co-localize in cultured podocyte cell junctions.* Mol Cell Biochem, 2007. **305**(1-2): p. 9-18.
64. Lassila, M., et al., *Densin is a novel cell membrane protein of Sertoli cells in the testis.* Mol Reprod Dev, 2007. **74**(5): p. 641-5.
65. Bilder, D., et al., *Collective nomenclature for LAP proteins.* Nat Cell Biol, 2000. **2**(7): p. E114.
66. Strack, S., et al., *Association of calcium/calmodulin-dependent kinase II with developmentally regulated splice variants of the postsynaptic density protein densin-180.* J. Biol. Chem., 2000. **275**: p. 25061-4.
67. Walikonis, R.S., et al., *Densin-180 forms a ternary complex with the α-subunit of CaMKII and α-actinin.* J. Neurosci., 2001. **21**: p. 423-433.
68. Jiao, Y., et al., *Developmentally regulated alternative splicing of densin modulates protein-protein interaction and subcellular localization.* J Neurochem, 2008. **105**(5): p. 1746-60.
69. Ohtakara, K., et al., *Densin-180, a synaptic protein, links to PSD-95 through its direct interaction with MAGUIN-1.* Genes Cells, 2002. **7**(11): p. 1149-60.
70. Yao, I., et al., *MAGUIN, a novel neuronal membrane-associated guanylate kinase- interacting protein.* J Biol Chem, 1999. **274**(17): p. 11889-96.
71. Yao, I., et al., *Association of membrane-associated guanylate kinase-interacting protein-1 with Raf-1.* Biochem Biophys Res Commun, 2000. **270**(2): p. 538-42.
72. Impey, S., K. Obrietan, and D.R. Storm, *Making new connections: role of ERK/MAP kinase signaling in neuronal plasticity.* Neuron, 1999. **23**(1): p. 11-4.
73. Izawa, I., et al., *Densin-180 interacts with delta-catenin/neural plakophilin-related armadillo repeat protein at synapses.* J Biol Chem, 2002. **277**(7): p. 5345-50.

74. Quitsch, A., et al., *Postsynaptic shank antagonizes dendrite branching induced by the leucine-rich repeat protein Densin-180.* J Neurosci, 2005. **25**(2): p. 479-87.
75. Thalhammer, A., et al., *Densin-180: revised membrane topology, domain structure and phosphorylation status.* J Neurochem, 2009. **109**(2): p. 297-302.
76. Roggentin, P., et al., *The sialidase superfamily and its spread by horizontal gene transfer.* Mol Microbiol, 1993. **9**(5): p. 915-21.
77. Drzeniek, R., *Substrate specificity of neuraminidases.* Histochem J, 1973. **5**(3): p. 271-90.
78. Iwamori, M., et al., *Arthrobacter ureafaciens sialidase isoenzymes, L, M1 and M2, cleave fucosyl GM1.* Glycoconj J, 1997. **14**(1): p. 67-73.
79. Rogerieux, F., et al., *Determination of the sialic acid linkage specificity of sialidases using lectins in a solid phase assay.* Anal Biochem, 1993. **211**(2): p. 200-4.
80. Manning, G., et al., *Evolution of protein kinase signaling from yeast to man.* Trends Biochem Sci, 2002. **27**(10): p. 514-20.
81. Hanks, S.K., A.M. Quinn, and T. Hunter, *The protein kinase family: conserved features and deduced phylogeny of the catalytic domains.* Science, 1988. **241**(4861): p. 42-52.
82. Abdullah, K.M., et al., *A neutral glycoprotease of Pasteurella haemolytica A1 specifically cleaves o-sialglycoproteins.* Infect. Immun., 1992. **60**: p. 56-62.
83. Sutherland, D.R., et al., *Cleavage of the cell-surface 0-sialglycoproteins CD34, CD43, CD44, and CD45 by a novel glycoprotease from Pasteurella haemolytica.* J. Immunol., 1992. **148**: p. 1458-1464.
84. Mellors, A. and D.R. Sutherland, *Tools to cleave glycoproteins.* Trends Biotechnol, 1994. **12**(1): p. 15-8.

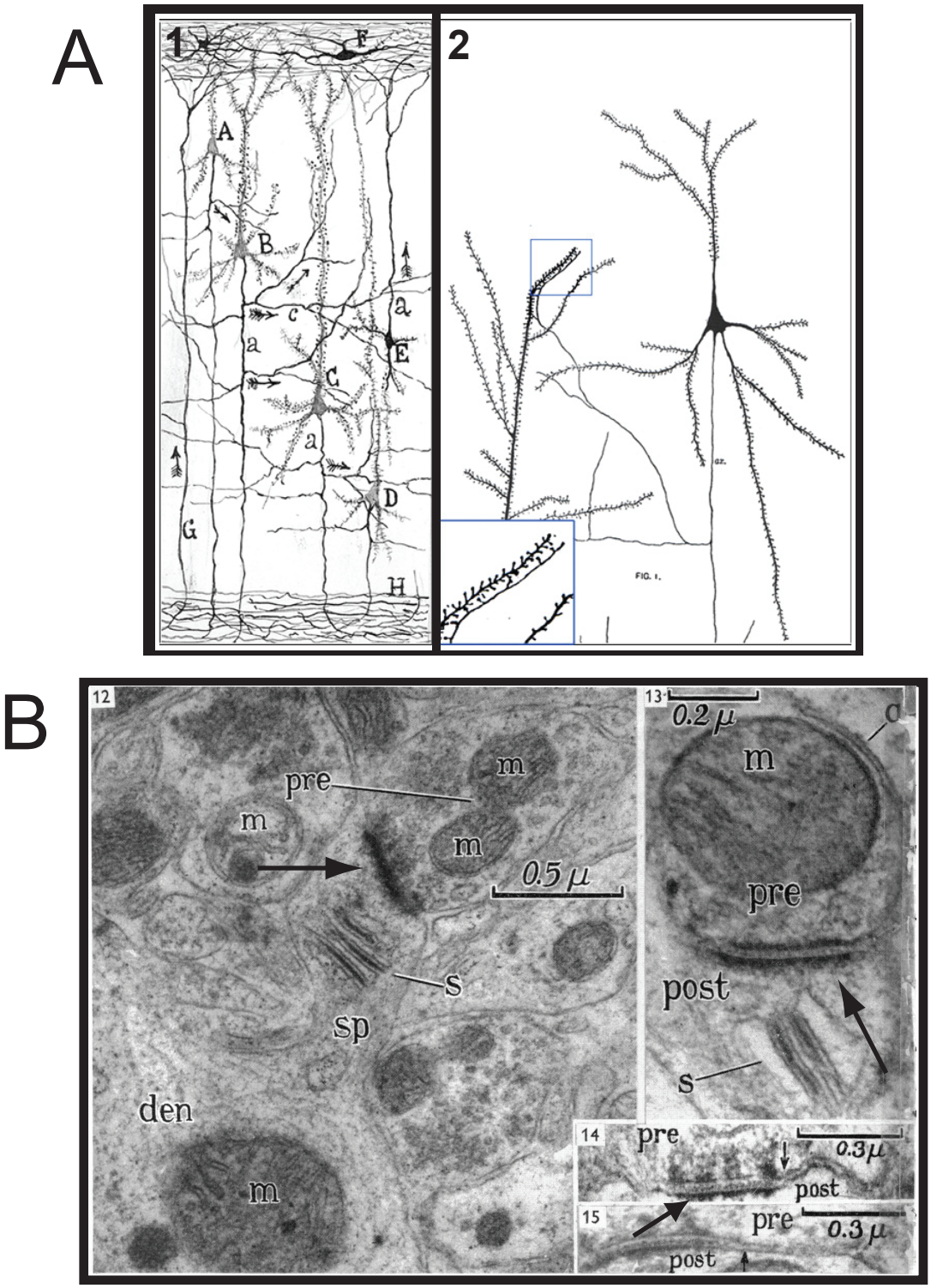

Figure 1.1 Hand drawing and electronmicrograph of synaptic connections between excitatory dendritic spines and axonal nerve fibers. (A) Comparative drawings from Ramon y Cajal (panel 1) and Berkley (panel 2) showing connections of axons with dendritic spines. Adapted from Garcia-Lopez et al. [2007]. (B) Electronmicrograph of presynaptic terminals forming glutamatergic synapses with dendritic spines. All panels show Gray's Type 1 asymmetric synapses with electron dense thickenings at the postsynaptic terminal (arrows). Thickenings represent postsynaptic densities as defined ultrastructurally. Adapted from Gray [1959] Abbreviations: pre, presynaptic process; post, postsynaptic process; m, mitochondria; s, spine apparatus; sp, dendritic spine; den, dendrite

Figure 1.2 Organization of receptor-scaffold and macromolecular complexes in the postsyanptic density (PSD). (A) Excitatory postsynaptic clusters of glutamate receptors with their asociated scaffolding molecules, as mediated by PDZ or PDZ-like protein-interaction domains. Metabotropic glutamate receptors (mGluR), NMDA receptors (NMDAR), and AMPA receptors (AMPAR) bind to the PDZ domains of Homer, PSD-95, and GRIP, respectively. The unbound protein domains of Homer, PSD-95, and GRIP are available to bind other synaptic proteins, thus forming supramolecular signaling complexes. PSD domains are in red, S, SH3 domain; GK, guanylate kinase domain (from Sheng, 1997). (B) Schematic diagram of the laminar network of major supramolecular complexes immediately adjacent to the membrane and the supermolecular complex of the PSD nucleated by the Shank platform matrix. Contacts between proteins indicate an established interaction between them. Domain structure is shown only for PSD-95 (PDZ doamin, red; SH3 domain, dark green; GK domain, light blue) and GRIP1. Other scaffolding molcecules are shown in yellow, signaling enzymes are shown in light green, and actin binding proteins are shown in pink. CaMKII is shown as a dodecamer. Unnamed gray shapes denote PSD proteins that are not specifically illustrated, but are known to interact with with the particular PSD proteins shown. Abbreviations: AKAP150, A-kines anchoring protein 150 kDa; CAM, cell adhesion molecule; Fyn, a Src family tyrosine kinase; GKAP, guanylate kinase-associated protein; H, Homer; IRSp53, insulin receptor substrate 53 kDa; KCh, K+ channel; nNOS, neuronal nitric oxide synthase; RTK, receptor tyrosine kinase (e.g., ErbB4; SPAR, spine-associated RapGAP). Figure adapted from Sheng and Hoogenradd [2007].

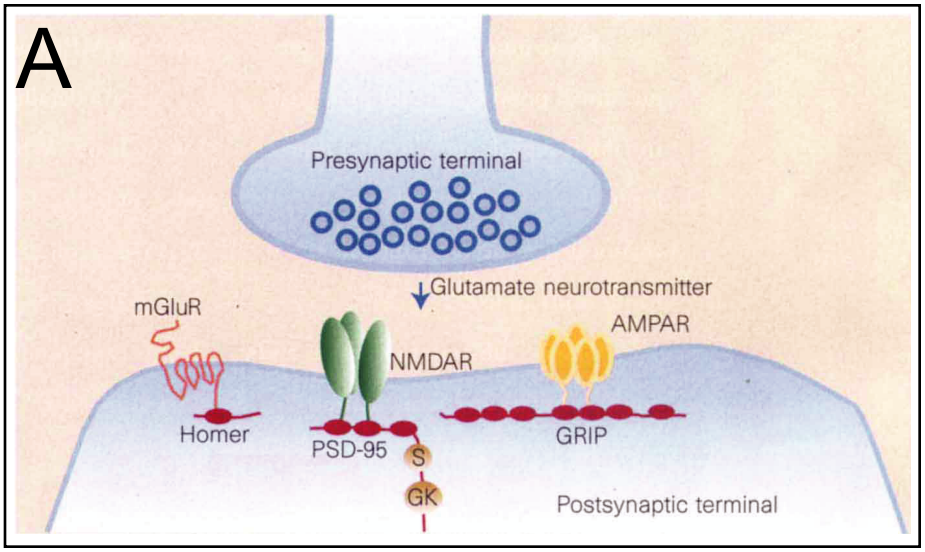
A
Presynaptic terminal
Glutamate neurotransmitter
mGluR
AMPAR
NMDAR
Homer
PSD-95
S
GK
GRIP
Postsynaptic terminal

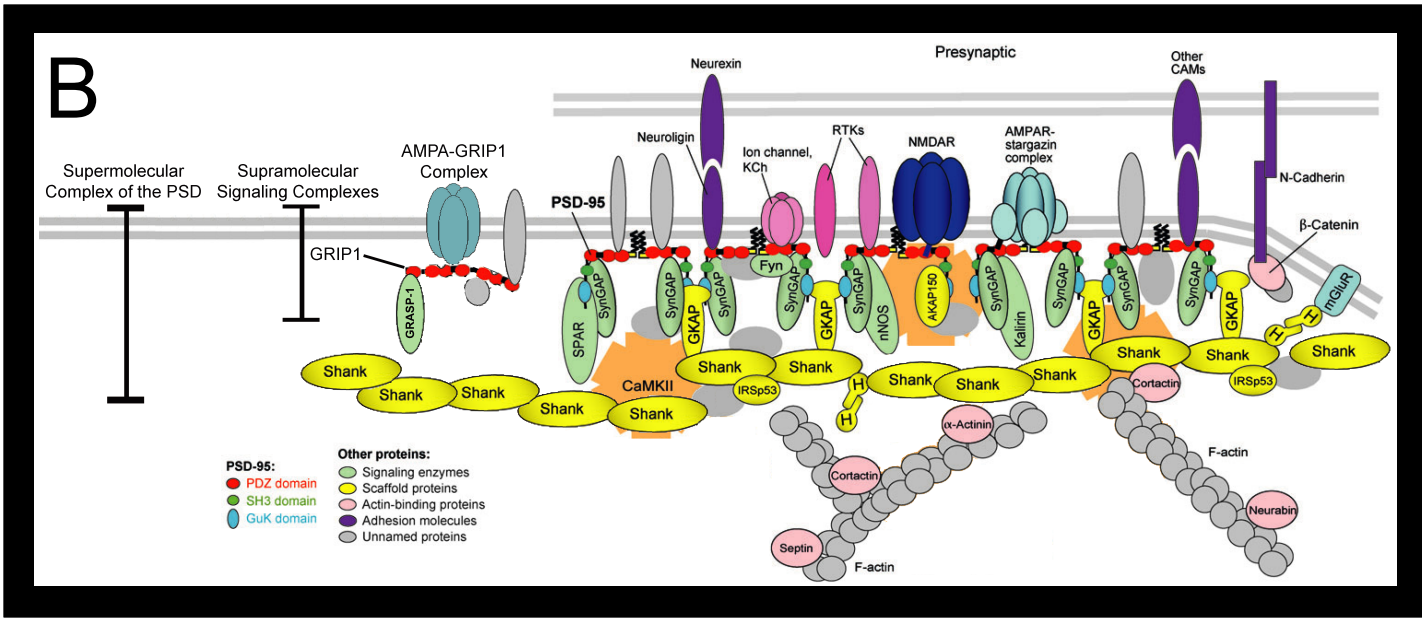
B
Supermolecular Complex of the PSD
Supramolecular Signaling Complexes
AMPA-GRIP1 Complex
GRIP1
GRASP-1
PSD-95
Neurexin
Neuroligin
Ion channel, KCh
RTKs
NMDAR
AMPAR-stargazin complex
Presynaptic
Other CAMs
N-Cadherin
β-Catenin
mGluR
Fyn
SynGAP
GKAP
SPAR
nNOS
AKAP150
Kalirin
Shank
CaMKII
IRSp53
Cortactin
α-Actinin
F-actin
Septin
Neurabin
PSD-95:
PDZ domain
SH3 domain
GuK domain
Other proteins:
Signaling enzymes
Scaffold proteins
Actin-binding proteins
Adhesion molecules
Unnamed proteins

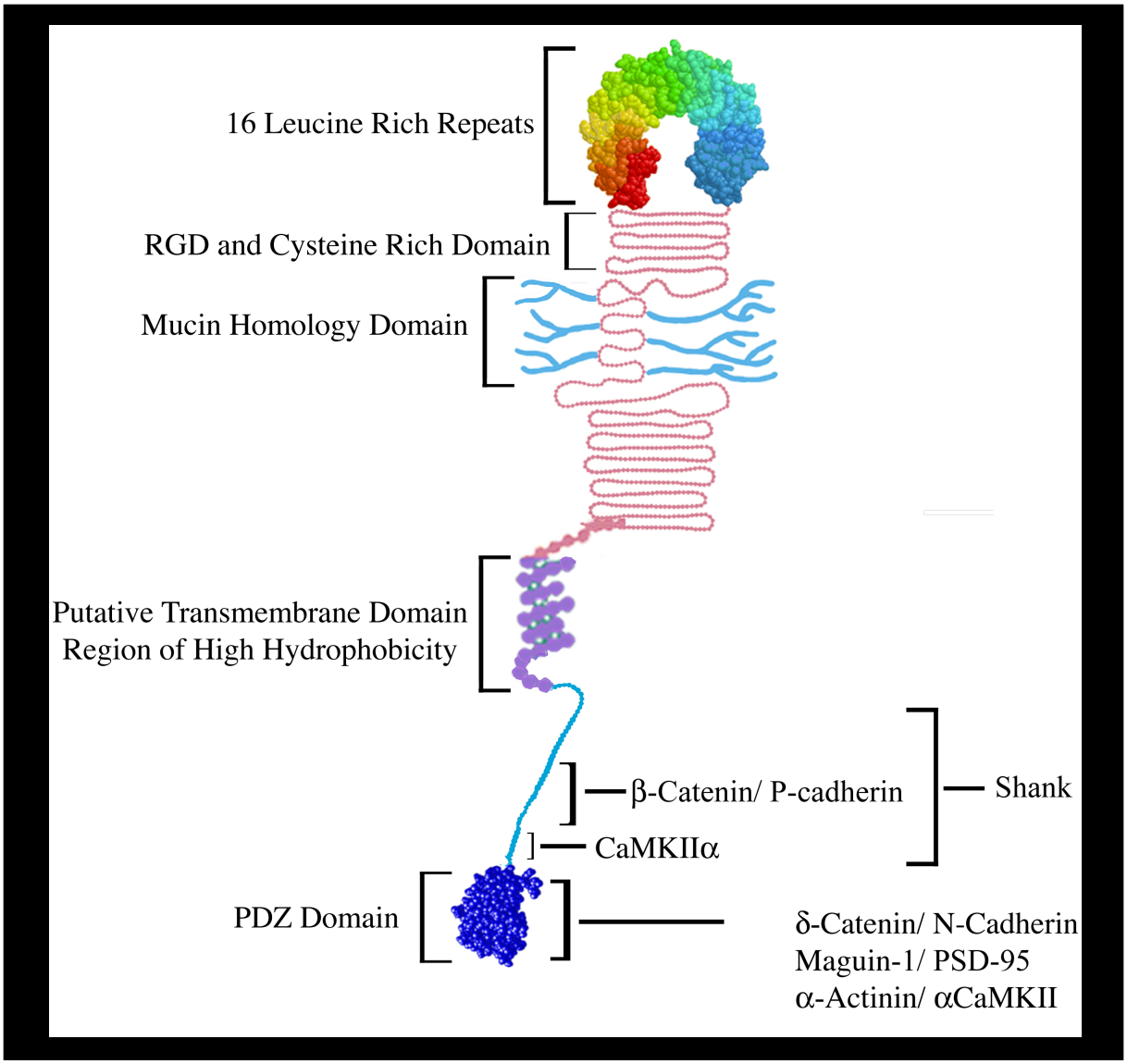

Figure 1.3 Densin protein domains and binding partners. The hypothetical structure of the Densin leucine rich repeat motif and the PDZ domain is based on homologous protein structures. The LRR structure is composed of 16 contiguous LRRs, and is immediately flanked on both sides by clusters of cysteine residues. The mucin-like repeats are thought to serve as sites for O-linked sugars (Apperson et al., 1996). The putative transmembrane domain was hypothesized due to the prediction of an amphipathic helix-like structure between amino acids 1223 to 1246. The region downstream from the putative transmembrane domain is known to bind Shank (Quitsch et al.,2005), CaMKII (Walikonis et al., 2001 and Strack, et al., 2000) and the β-catenin/ P-Cadherin complex in the kidney (Heikkila et al., 2007),. A PDZ domain is located at the C-terminal and is known to interact with the δ-catenin/ N-Cadherin complex (Inagaki et al., 2002), the α-Actinin/ αCaMKII ternary complex (Walikonis et al., 2001), and the Maguin-1/ PSD-95 complex (Ohtakara et al., 2002).

Figure 1.4 Immunocytochemical localization of Densin in 14-21 DIV hippocampal cultures (Apperson et al., 1996) and in situ hybridization of Densin in adult C57B/6J mouse (Allen Brain Map, Lein et al., 2007). (A- top panel) Double staining of Densin (red)/ Synapsin I (green; top panel) and Densin (red)/ PSD-95 (green; bottom panel). Overlay of dual channel confocal images (left) show that Densin (top panel, large arrowheads) and Synapsin I (top panel, small arrowheads) overlap. Small inset boxes on right show single channel images of Densin and Synapsin I. Overlay of dual channel images of Densin and PSD-95 show precise co-localization at punctal positions at spine tip structures along dendrites (arrowheads in inset box, bottom panel) as well as localization of Densin at the axon initial segment/ axon hillock (arrowhead in dual and single Densin channel images, bottom panel). Single channel images of Densin and PSD-95 are shown in bottom right panels. (B) In situ hybridization heat maps of Densin, NR2C and αCaMKII at saggital level 12-13 are shown. Densin gene expression is shown in comparison to NR2C (low gene expression in forebrain) and αCaMKII (high gene expression in forebrain). Densin is highly expressed in all regions except the cerebellum. In contrast, NR2C is highly expressed in the cerebellum, but not in the forebrain, while αCaMKII is highly expressed throught all brain regions. Heat map color scale indicates level of gene expression.

A

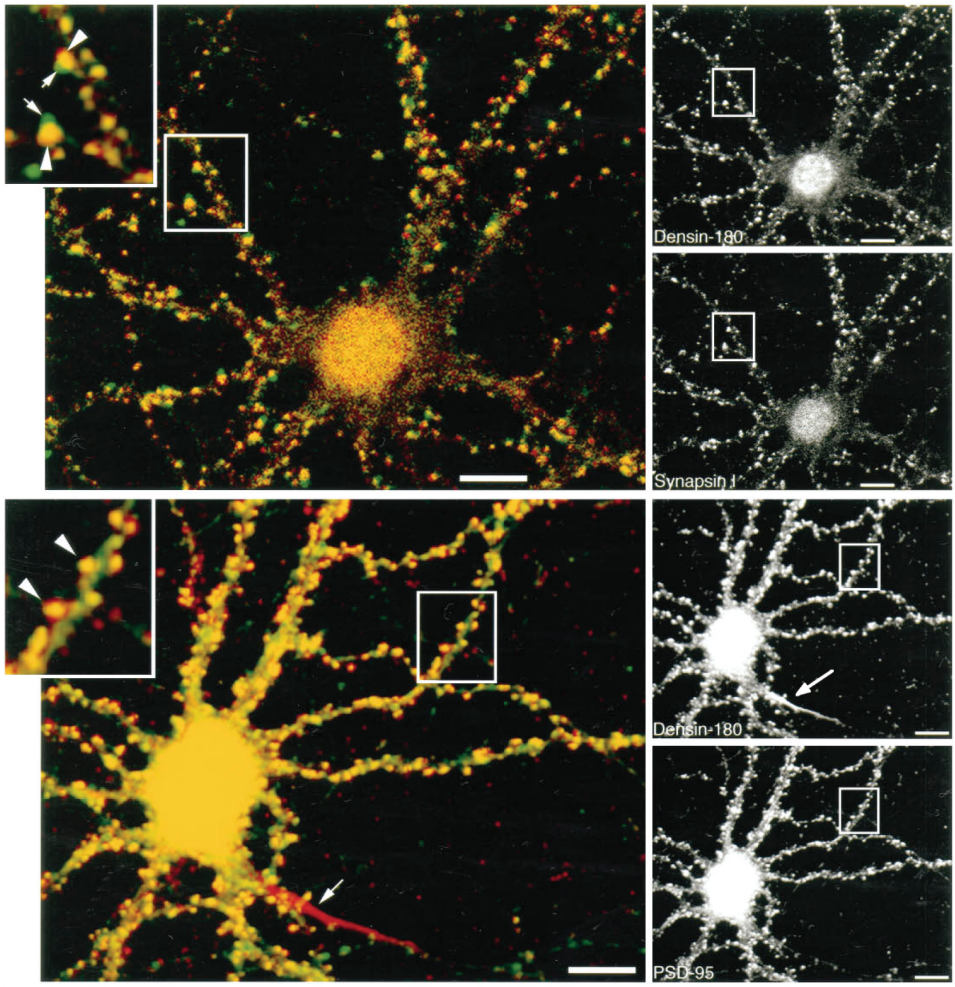
Densin-180
Synapsin I
Densin-180
PSD-95

B

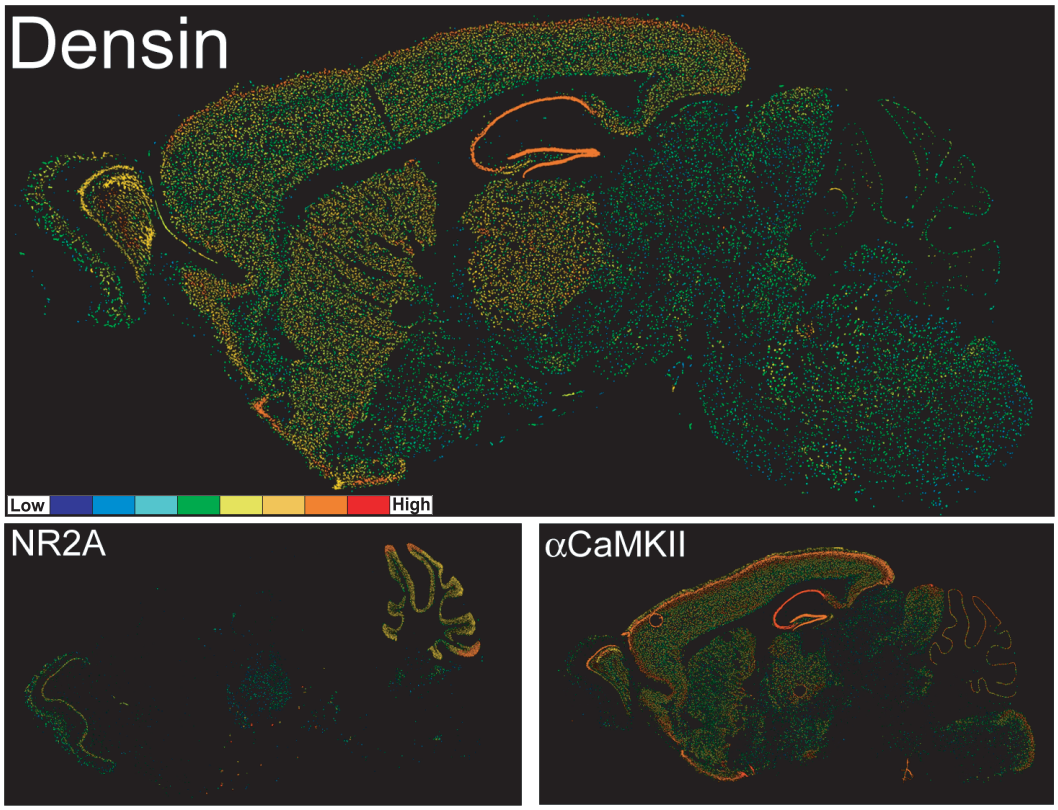
Densin
Low
High
NR2A
αCaMKII

Chapter 2: Design of Targeting Construct for Densin Deletion, Confirmation of Densin Knockout, and Initial Characterization of the Knockout Phenotype

Introduction

Derangements in synaptic transmission and plasticity are part of the pathology of numerous neurological and mental health diseases including epilepsy, schizophrenia, depression, and Alzheimer's disease. In excitatory synapses of the CNS, the postsynaptic reception, integration, and transduction of signals is mediated by the supermolecular complex of the postsynaptic density. Understanding the role that particular PSD proteins play in normal and pathological states will greatly enhance our knowledge of the underlying molecular mechanisms which contribute to overall mental health and well being.

A major step in the study of a protein's function in any biological system is the generation of a mutant phenotype that completely lacks expression of the protein. Numerous core proteins of the PSD have been studied in this manner, including PSD-95 [1], αCaMKII [2, 3], the GluR2 subunit of the AMPA receptor [4], SynGAP [5], δ-catenin [6], and Shank [7]. Knockouts have also been generated for all the subunits of the NMDA receptor, including the NR1 subunit [8, 9], NR2A subunit [10], NR2B subunit [11], NR2C subunit [12] and NR2D subunit [13]. Finally, transgenic animals have been generated with deletions in the cytoplasmic tails of the NR2A, NR2B, and

NR2C subunits of the NMDA receptor [14]. These mutant and transgenic animals have provided an immensely detailed understanding of their roles in synaptic transmission and plasticity. However, a more holistic understanding of how these core PSD proteins are functionally and structurally integrated into the supramolecular complex of the PSD still remains elusive.

As previously discussed, Densin is a core protein of the PSD and has been shown to complex with Maguin-1/ PSD-95, α-Actinin/ CaMKII, δ-catenin/ N-cadherin, Shank, β-catenin, and Nephrin. Given the facts that 1) PSD-95 and Shank are major scaffolding molecules for signaling complexes within the PSD, 2) CaMKII activity is of critical importance for integrating Ca^{2+} signaling in the PSD, 3) β-catenin, δ-catenin, N-cadherin, and nephrin are key players in mediating cell adhesion, spine morphology and dendritic arborization, and 4) α-Actinin plays a key role in actin cytoskeletal dynamics, Densin seems to sit at a major hub for cross-linking and integrating major signaling complexes within the PSD.

Here I describe the generation and initial characterization of a Densin knockout mutation in the mouse.

Material and Methods

2.1 Intron-Exon boundary structure and gene-targeting construct

Intron-Exon boundaries of Densin were determined by identifying all known cDNA and splice variants of Densin in the NCBI and Celera databases and mapping them onto the NCBI and Celera mouse genome databases.

A CITB mouse BAC library (Research Genetics) encoding genomic sequence of strain 129S1Sv (recently renamed 129S3Sv/ImJ) was screened with a cDNA probe encoding Densin Exon 3. CITB Mouse BAC Clone 456C10 hybridized with the probe for Exon 3. The BAC DNA insertion junctions were sequenced and aligned against the known genomic sequence of Densin. The presence of Exon 3 in the BAC clone was determined by PCR. A restriction map of the BAC clone was developed and a 9.9kb region, which included Exon 3 and its surrounding introns, was cloned into the pKO Scrambler 907 vector (Stratagene). The long arm of the Densin targeting construct contained a 7.8kb fragment including intron 2, Exon 3, and part of intron 3; the short arm contained a 2.1kb fragment of intron 3 (Fig 2.1). The first loxP site was inserted 4.8kb upstream of Exon 3. A hygromycin selection cassette, flanked on both sides by loxP sites (no. 2 and 3), was cloned into the short arm of the targeting sequence 1.1kb downstream from Exon 3 (Fig 2.1).

2.2 Generation of mouse embryonic stem cells for injection into blastocysts

The linearized targeting construct (25μg) was electroporated into $1x10^7$ cells/cuvette of mouse ES (CJ7) cells. Transfected ES cells were grown in the presence of hygromycin (200μg/ml) for 7-8 days to select for homologous recombinants. Two recombinant clones with both 5^1 and 3^1 construct integration were identified and confirmed by PCR. One clone (2G8) exhibited a normal karyotype and was expanded for the generation of Densin transgenic ES cells. Ninety-eight 129B6 blastocysts injected with ES cells from the 2G8 clone were implanted into seven pseudo-pregnant mothers.

Chimeric pups exhibiting a >90% agouti coat color were used for subsequent breeding. Preparation of ES cells for electroporation, injection, blastocyst implantation and breeding of chimeras were performed under the direction of Dr. Shirley Pease in the Transgenic Mouse Core Facility at Caltech (Pasadena, CA).

2.3 Knockout animal breeding strategy

Eight adult male chimeras were freely mated to C57BL6 *EIIaCre*$^{+/+}$ expressing female mice (Jackson Laboratory, ME) developed in the laboratory of H. Westphal (NIH, Bethesda. MD; Lakso et al., 1996). F1 generation offspring were screened for mosaic *Cre*-recombination patterns by PCR. F1 animals exhibiting genomic mosaicism were subsequently mated to wild-type C57BL6 mice (Fig 2.2). Segregation of the *EIIaCre* transgene and *Cre*-recombined alleles was monitored by PCR in the F2 generation. F2 generation *EIIaCre*$^{-/-}$, Densin$^{+/-}$ (total excision loxP1/3 recombination pattern) males were liberally mated to wild-type C57BL6 females to generate a large F3 population of Densin$^{+/-}$ animals for subsequent production of Densin$^{-/-}$ null mutants for experimentation.

2.4 Genotypic verification of knockout

Genomic DNA was isolated from mouse ear punch or tail samples and used for PCR. For Densin knockout genotyping a set of three primers was used: one recognizing a sequence 5^{1} of the first loxP site (LoxPrayUp; 5^{1}-GAGATGCTCTCAAGATAGACATG-3^{1}), one recognizing a sequence 3^{1} of the first loxP site (LoxPrayLow; 5^{1}-CTCCAATTCTGAAGCCAGTAG-3'), and one recognizing a sequence 3^{1} to the third loxP site (PostHygro2; 5^{1}-ACAGAACTGGCTTCTGTCCAC-

3[1]); the LoxPrayUp-LoxPrayLow and LoxPrayUp-PostHygro2 banding patterns recognize wild-type or knockout genotypes, respectively. The PCR protocol used for genotyping the Densin knockout line was as follows: 10 cycles of 95ºC/ 30sec denaturation, 58ºC/ 30sec annealing, 72ºC extension followed by 20 cycles of 95ºC/ 30sec denaturation, 56ºC/ 30sec annealing, 72ºC extension, followed by a final extension at 72ºC for 5 min. Correct banding patterns of a single 187bp fragment for *wt*, 187/ 257bp PCR fragments for heterozygous animals, and a single 257bp PCR fragment from knockout animals were observed (Fig 2.3A).

2.5 Forebrain homogenization and Immunoblot verification of knockout

Forebrains were isolated from five 6-8 week old Densin wt-*ko* pairs. Forebrains were individually homogenized (Potter-Elvehjem homogenizer) in 2.4ml buffer (4mM HEPES-NaOH pH 7.4, 0.32M sucrose, Roche Complete EDTA-free protease inhibitors, adjusted to pH 7.4 with 1N NaOH) at 900 rpm in Teflon-glass homogenizers. Homogenate was centrifuged for 10 min/ 1000 g in a Sorval SM24 rotor. Supernatant was flash frozen in liquid nitrogen and stored in 400 μl aliquots at -80ºC.

Aliquots of individual forebrain homogenates were assayed upon use for total protein concentration by the bicinchoninic acid method (Pierce, Rockford, IL) with bovine serum albumin (Thermo Fisher, Rockford, IL) as a standard, and analyzed on a Versa-Max microplate reader (Molecular Devices, Sunnyvale, CA). Equal amounts of forebrain protein (10 μg or 50 μg), adjusted for total volume, were dissolved in SDS-PAGE sample buffer, boiled at 90ºC for 5 min, and centrifuged for 2 min in an Eppendorf microcentrifuge.

Samples were fractionated by SDS-PAGE on 7.5 or 9% acrylamide gels and transferred to nitrocellulose membranes (Schleicher & Schuell) in transfer buffer (25mM Tris, 200mM glycine, 20% methanol). Membranes were blocked with 5% milk in TBS buffer (20mMTris, 150mM NaCl) for 1 hour at room temperature followed by overnight incubation with primary antibody in TBS + 0.1% Tween 20 blocking buffer at 4ºC. Primary antibodies were used at the following dilutions: Densin CT245 (1:2500), M2 (1:2500), and LRR (1:1000). All Densin antibodies are described by Apperson, et al., 1996. Membranes were washed three times with TBS + 0.1% Tween 20 blocking buffer at room temperature. Bound antibodies were detected with IRdye700- or IRdye800- (1:10,000) secondary antibodies (Rockland, Gilbertsville, PA). Membranes were then washed three times with TBS + 0.1% Tween 20, followed by two washes with TBS. Blots were visualized with the Odyssey Infrared Imaging System (Fig 2.3B; Li-Cor Bioscience, Lincoln, NE).

2.6 RNA seq confirmation of exon 3 deletion and expression

Ten adult males (five wt:ko sibling pairs), 11 weeks of age were killed by cervical dislocation. Forebrains were dissected from two wt:ko sibling pairs (four animals total) and hippocampal tissues was dissected from three wt:ko sibling pairs (six animals total). The forebrain and hippocampal tissue were not harvested on the same day, but all subsequent processing was the same.

Once the brain tissue was harvested, it was immediately flash frozen in liquid nitrogen. Brain tissue was weighed and placed in mirVana lysis buffer (Cat # AM1560, Ambion, Foster City, CA). The tissue was minced and then sequentially sheared by

passage through 20g and 25g needles. The samples were allowed to sit at room temperature for 5 minutes at which time, each was supplemented with 75µl MicroRNA homogenate additive (mirVana kit). Samples were shaken by hand for 15 seconds and subsequently incubated on ice for 10 minutes. Total RNA was extracted using phenol/ chloroform, isolated using mirVana Filter Cartridges as per the manufacturers recommendations, eluted with mirVana elution buffer, and supplemented with ScriptGuard (Epicentre Biotechnologies, Madison, WI). Sample concentrations were measured using the Nanodrop quantification system (Thermo Scientific, Waltham, MA).

Residual genomic DNA was enzymatically removed using Baseline Zero DNase (Epicentre Biotechnologies). RNA was re-extracted using phenol/ chloroform and precipitated O/N with ethanol. The RNA was dried, re-suspended in 50µl dH_2O supplemented with ScriptGuard, and its concentration measured using Nanodrop. RNA was subsequently stored at -80ºC.

Oligo(dT) selection from total RNA, cDNA preparation, sequencing and read mapping was performed as previously described [15]. Analysis of the expression level of the gene loci was performed with ERANGE software as previously described [15]. Unique RPKM (reads per kilobase of exon model per million mapped reads) counts were used for subsequent statistical analysis.

Results

2.7 Genomic organization of the Densin gene

The Densin gene was located on mouse chromosome 3 at position 161,551,730 to 161,910,689, with a length of 358,959 bp. The gene contains 27 exons. Two start

codons were identified within exon 3. The first start codon is formed by the last base pair of exon 2 and the first two base pairs of exon 3. The second start codon is +16 base pairs from the first. No other methionine start codons were identified. Exons 2, 7, 9, 17, 22, 23, and 24 are predicted to be alternatively spliced. A predicted homology site for a matrix attachment region/ scaffold attachment region (MAR/SAR) was identified at -2000bp from the start of the Densin gene. Such regions are known to flank transcriptionally active chromosome regions and may contain a concentration of transcription factor binding sites [16]. Contained within exon 22 is a cDNA sequence reported from a macaque brain cDNA library (gi:9967402).

2.8 Targeting construct and breeding

Following electroporation with the exon 3 targeting construct, two ES clones were identified to have undergone homologous recombination with one showing a healthy karyotype. The mutant ES clone was injected into 98 host blastocysts and subsequently implanted into seven pseudo-pregnant females. 40 pups (F0) were born of which 14 exhibited chimeric coat coloration. Three chimeras with greater than 90% agouti coat color were mated to C57B6 females expressing *cre*-recombinase under the EIIa promoter. 8 out of 19 pups that were littered (F1) exhibited germline transmission and genomic mosaicism as determined by PCR (data not shown). Three male mosaic pups were subsequently bred to C57B6 wild type females. Litters exhibited an assortment of monogenic genotypes. Pups that were heterozygous for the complete deletion of exon 3 and the hygromycin selection cassette were denoted knockout founder animals (Fig 2.2; F2 generation). Mice retaining the LoxP flanked exon 3 but showing deletion of the

hygromycin selection cassette were denoted conditional/ floxed founder animals (F2; Fig 2.2). Both sets of F2 heterozygous founder animals were liberally bred to wt C57B6 animals to generate a large F3 population that was subsequently interbred to produce full knockout animals for experimentation.

2.9 Verification of the homozygous ko mouse

The chromosomal deletion of exon 3 in knockout mice was verified by performing PCR on genomic DNA isolated from ear punches and tail clippings (Fig 2.3a). RNA Seq analysis demonstrated that the Densin transcript is stably expressed, but lacks exon 3 and the start codon necessary for protein translation (Fig 2.4a). Immunoblots with antibodies targeting the n-terminal LRR domain, the Mucin homology domain, and the c-terminal PDZ domain confirmed that no Densin protein was expressed (Fig 2.3b)

To examine if the homologous recombination of the targeting construct and deletion of exon 3 resulted in aberrant expression of genes flanking the Densin locus, we performed an RNA seq analysis on two wt:ko sibling pairs at 11 weeks of age. No significant changes in the transcript expression levels of the seven genes flanking the Densin locus were observed (Fig 2.4b). These data indicate that the homologous recombination of the targeting construct and deletion of exon 3 do not disrupt or alter the expression levels of those genes most proximal to the Densin locus. Consequently, the observed phenotypes in this animal will not be confounded by alterations in promoter/ enhancer regions resulting from the insertion of the targeting construct.

2.10 Homozygous Densin knockout mice show a runted phenotype

Crossing of Densin heterozygous mice results in progeny with a Mendelian distribution of 1.2 wt : 2.4 het : 1 ko (n=328). Thus, the Densin mutation does not result in embryonic lethality. Once born, knockout animals are viable and are able to compete for nutritional resources as demonstrated by the presence of an abdominal milk spot (image not shown). On P0, knockout animals are indistinguishable from their wildtype or heterozygous litter mates. However, by P4 knockout animals are significantly smaller. Of 74 knockout animals born, 51 showed runted phenotypes and 23 were of normal weight and size when compared to wt and heterozygous litter mates (data not shown). This data suggests that the runt phenotype is not fully penetrant.

At three weeks of age, knockout animals are still significantly smaller compared to their litter mates (weight= -44.95%, $p<0.01$; length= -15.48%, $p<0.01$). By the time of weaning (3-4 weeks of age) 20% of the knockouts had died (11 out of 51). By 11 weeks of age the size disparity between knockout and wild type animals significantly decreases, but was still statistically significant (weight= -11.86%, $p<0.05$; length= -4.92%, $p<0.05$) (Fig 2.5).

2.11 Densin knockout mice have seizures when injected with Nembutal

Twelve wt:ko sibling pairs were injected perinatally with 100μg/gram body weight of Nembutal. The animals were immediately placed into a small fishbowl ~40cm (l) x ~15cm (w) ~21cm (h), and their behavior recorded with a high speed video camera.

Animals were injected without prior knowledge of their genotype. The onset of seizures typically occurred within 1 min 15 seconds to 1 min 45 seconds. This delay is probably associated with the length of time it takes for the Nembutal to reach the brain. All animals injected exhibited a stiffening of their tail within 30-40 seconds after injection. Nine out of twenty four animals injected progressed into full-blown seizures characterized by violent, uncontrollable spastic convulsions of their entire body. When the genotype of the animals was revealed, we determined that all nine of the animals that had seizures were knockout animals. None of the wild type animals had seizures.

Just prior to the onset of the seizure, the animals exhibited staccato like movement and began to rear. While the seizures were occurring, all of the animals exhibited a flagellar-like motion in their tail. Furthermore, their front limbs seemed to become immobile. The tonic-colonic-like seizures lasted for 30 to 45 seconds, at which time the animals ceased to move. All animals were euthanized within 3 minutes of becoming inactive.

References

1. Migaud, M., et al., *Enhanced long-term potentiation and impaired learning in mice with mutant postsynaptic density-95 protein [see comments].* Nature, 1998. **396**(6710): p. 433-9.
2. Silva, A.J., et al., *Deficient hippocampal long-term potentiation in α-calcium-calmodulin kinase II mutant mice.* Science, 1992. **257**: p. 201-206.
3. Silva, A.J., et al., *Impaired spatial learning in α-calcium-calmodulin kinase II mutant mice.* Science, 1992. **257**: p. 206-211.
4. Kashiwabuchi, N., et al., *Impairment of motor coordination, Purkinje cell synapse formation, and cerebellar long-term depression in GluR delta 2 mutant mice.* Cell, 1995. **81**(2): p. 245-52.
5. Vazquez, L.E., et al., *SynGAP regulates spine formation.* J. Neurosci., 2004. **24**: p. 8796-8805.
6. Israely, I., et al., *Deletion of the neuron-specific protein delta-catenin leads to severe cognitive and synaptic dysfunction.* Curr Biol, 2004. **14**(18): p. 1657-63.
7. Hung, A.Y., et al., *Smaller dendritic spines, weaker synaptic transmission, but enhanced spatial learning in mice lacking Shank1.* J Neurosci, 2008. **28**(7): p. 1697-708.
8. Li, Y., et al., *Whisker-related neuronal patterns fail to develop in the trigeminal brainstem nuclei of NMDAR1 knockout mice.* Cell, 1994. **76**(3): p. 427-37.
9. Forrest, D., et al., *Targeted disruption of NMDA receptor 1 gene abolishes NMDA response and results in neonatal death.* Neuron, 1994. **13**(2): p. 325-38.
10. Sakimura, K., et al., *Reduced hippocampal LTP and spatial learning in mice lacking NMDA receptor ε1 subunit.* Nature, 1995. **373**: p. 151-155.
11. Kutsuwada, T., et al., *Impairment of suckling response, trigeminal neuronal pattern formation, and hippocampal LTD in NMDA receptor epsilon 2 subunit mutant mice.* Neuron, 1996. **16**(2): p. 333-44.
12. Ebralidze, A.K., et al., *Modification of NMDA receptor channels and synaptic transmission by targeted disruption of the NR2C gene.* J Neurosci, 1996. **16**(16): p. 5014-25.
13. Ikeda, K., et al., *Reduced spontaneous activity of mice defective in the epsilon 4 subunit of the NMDA receptor channel.* Brain Res Mol Brain Res, 1995. **33**(1): p. 61-71.
14. Sprengel, R., et al., *Importance of the intracellular domain of NR2 subunits for NMDA receptor function in vivo.* Cell, 1998. **92**(2): p. 279-89.
15. Mortazavi, A., et al., *Mapping and quantifying mammalian transcriptomes by RNA-Seq.* Nat Methods, 2008. **5**(7): p. 621-8.
16. Boulikas, T., *Nature of DNA sequences at the attachment regions of genes to the nuclear matrix.* J Cell Biochem, 1993. **52**(1): p. 14-22.

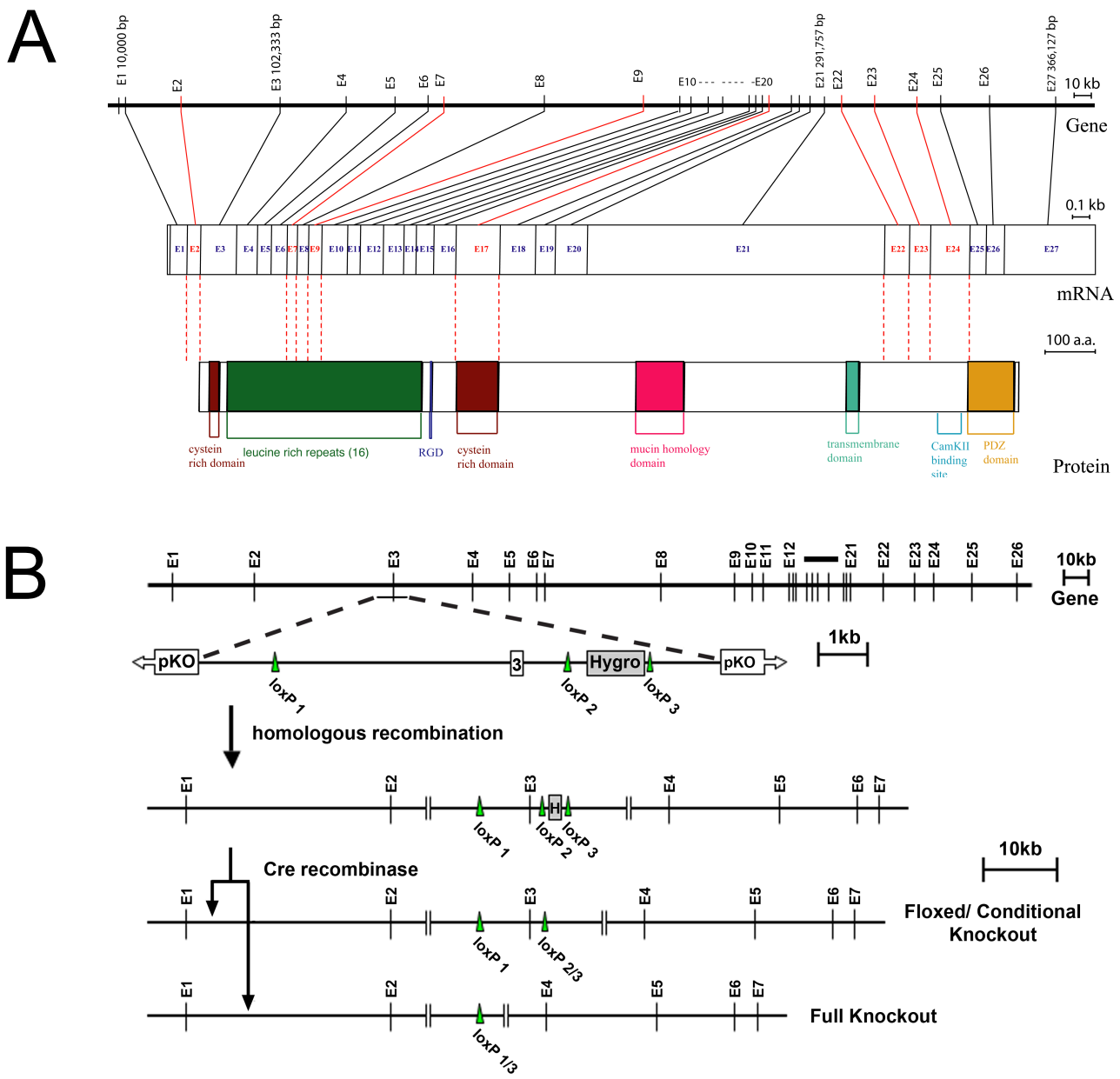

Figure 2.1 Structure of the Densin gene and design of the targeting construct. (a) The Densin gene contains 27 exons, spanning 358,959 nucleotides. Exons flanked by alternative splicing consensus sequences are marked red. cDNAs demonstrating alternative splicing of these exons have been characterized (Jiao et al., 2008). The translation start codon is contained in Exon 3, along with the first cysteine-rich domain, and the beginning of the LRR. The region encoded by exons 22, 23, and 24, and known to bind β-catenin (Heikkila et al., 2007), Shank (Quitsch et al., 2005), and CaMKII (Walikonis et al., 2001 and Strack, et al., 2000), can be alternatively spiced (Jiao et al., 2008 and Strack et al., 2000). The last two exons encode the PDZ domain. (b) The exon 3 targeting construct included a LoxP site inserted into intron 2 and a hygromycin selection cassette flanked by LoxP sites, inserted into intron 3. Expression of Cre-recombinase *in utero* results in either the deletion of the hygromycin selection cassette, resulting in a floxed exon 3/ conditional knockout, or in the deletion of both exon 3 and the hygromycin cassette, resulting in a full knockout.

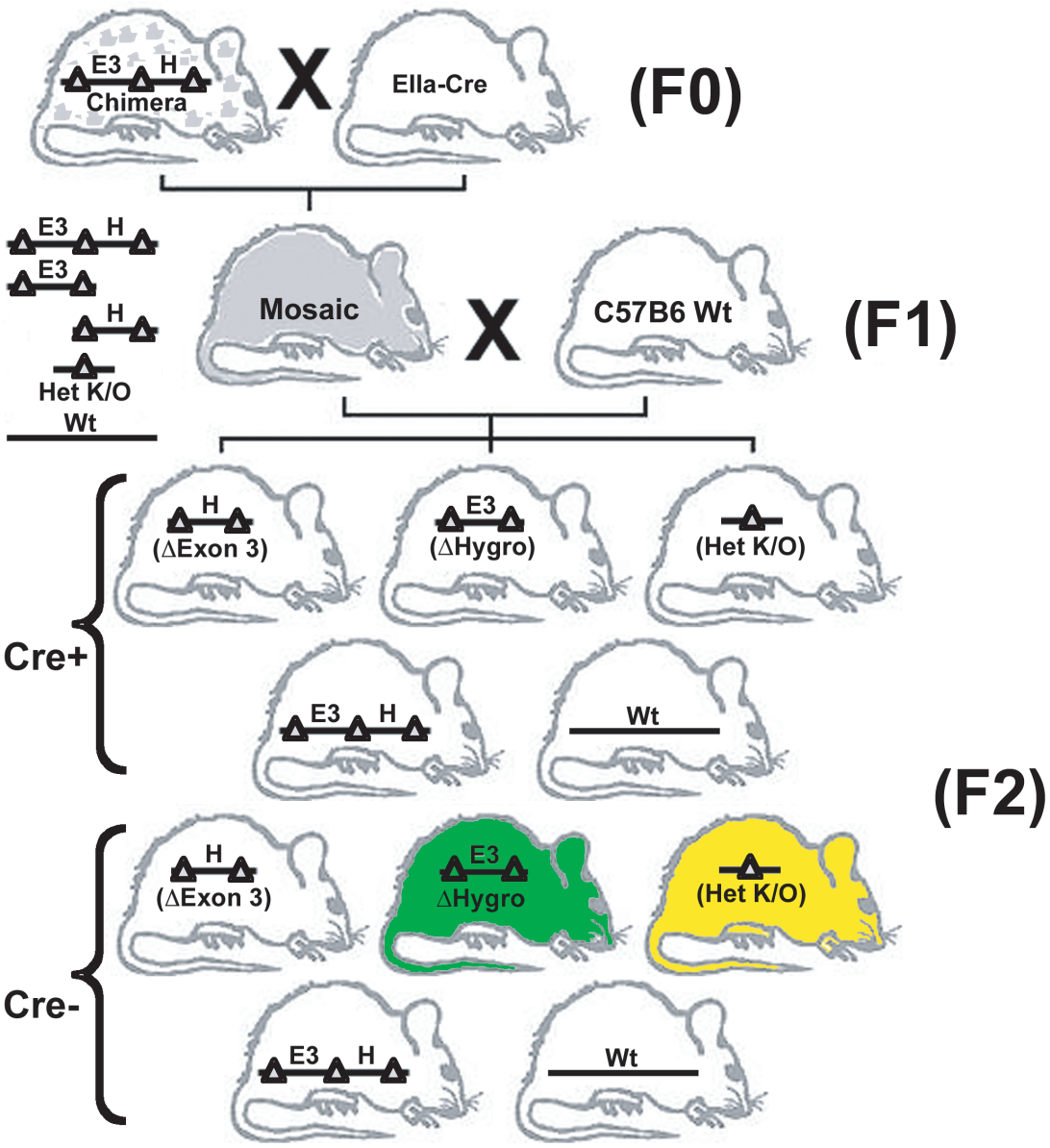

Figure 2.2: Cre- mediated germline mosaicism and breeding strategy for the generation of floxed conditional ko and full knockout animals. Chimeric males produced from implanted embryos are mated with Cre-recombinase expressing females. F1 generation males exhibiting genomic mosaicism are bred to wt C57B6 females to segregate Cre+ alleles from floxed and exon 3 deleted alleles. F2 generation ΔHygro (heterozygous floxed exon 3, green) and total Δ (heterozygous exon 3 deletion, yellow) founder animals are continuously bred to wt C57B5 animals. F3 generation exon 3 deleted heterozygous animals are interbred for subsequent experimentation.

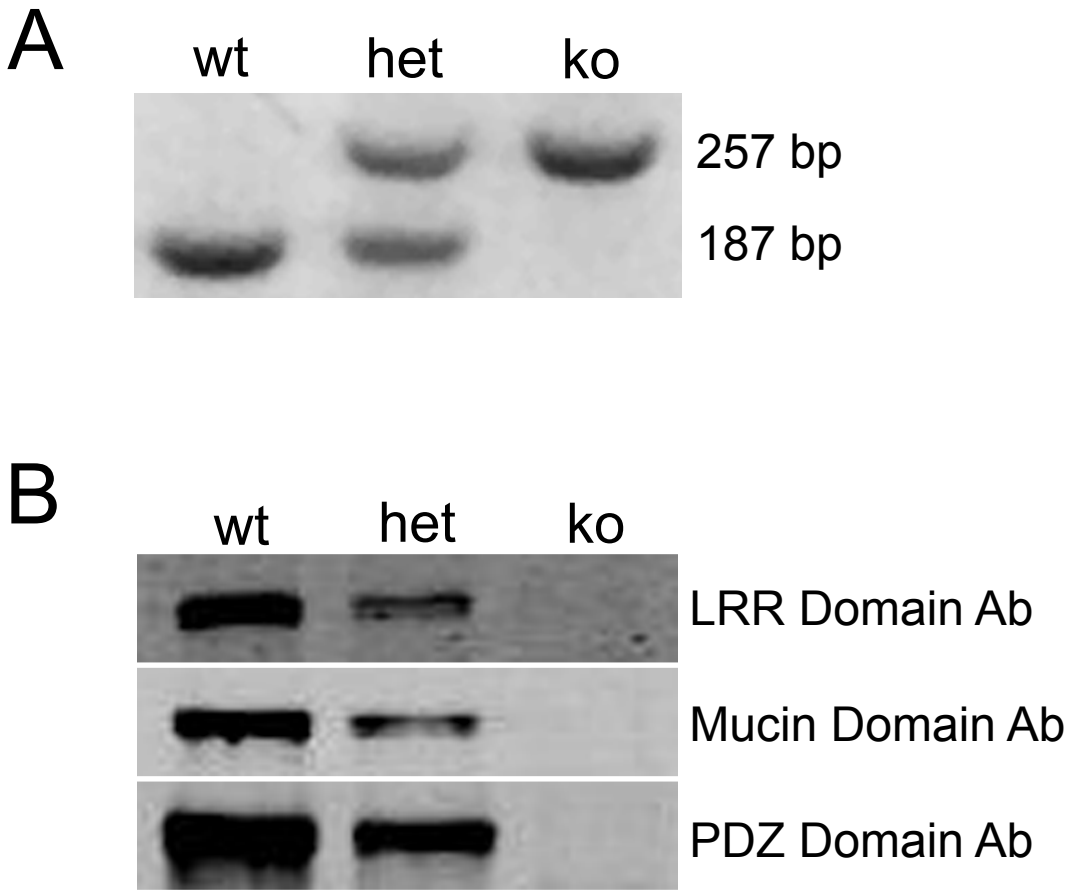

Figure 2.3 Genomic PCR and immunoblot confirmation of knockout. (a) Examples of PCR products from DNA of wildtype (wt), heterozygous (het), and knockout (ko) litter mates. (b) Immunoblot analysis of Densin protein expression in forebrain homogenates of 6-week-old animals. Antibodies to three distinct regions of Densin were used to detect expression levels of the protein.

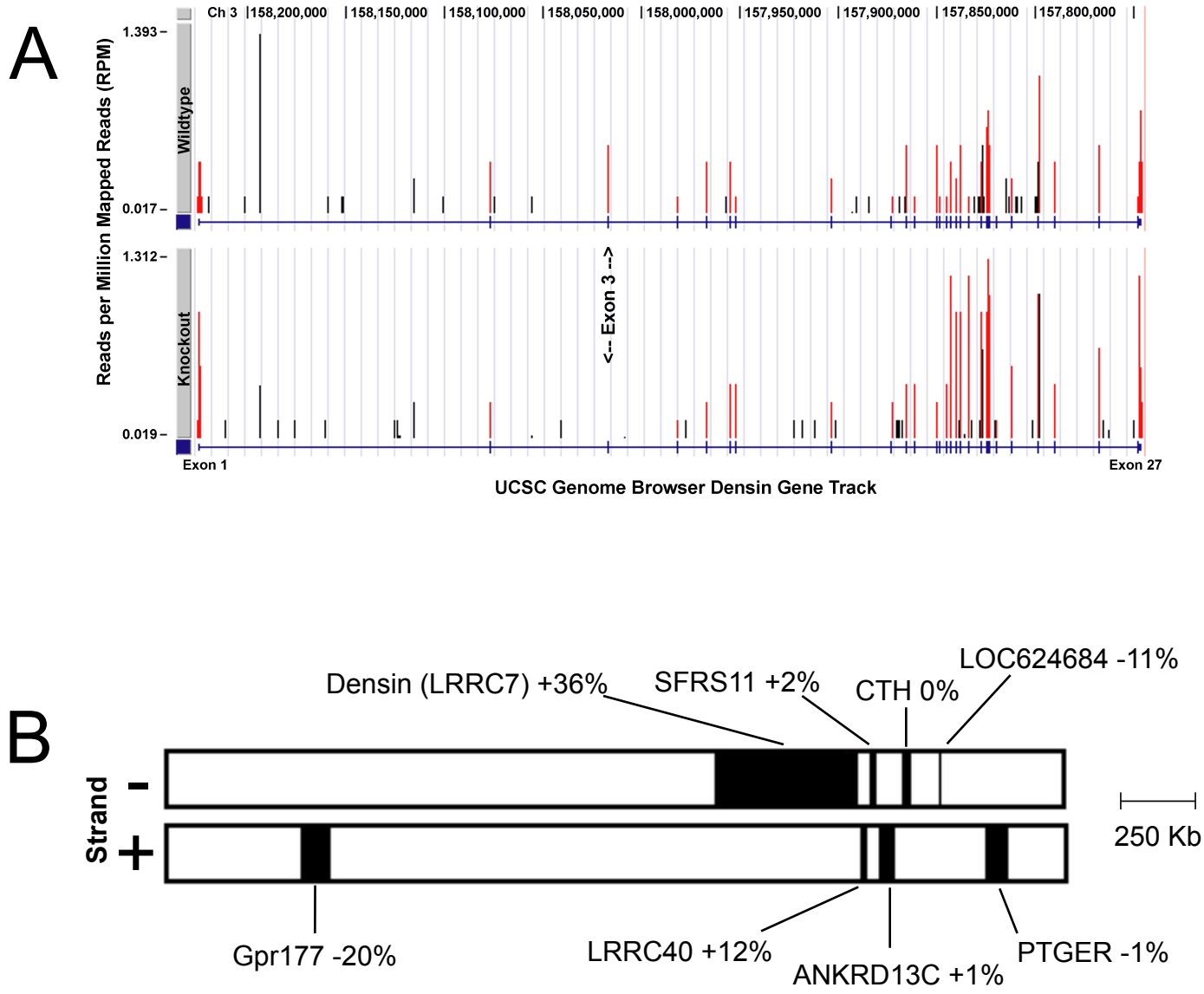

Figure 2.4 Validation of exon 3 deletion and confirmation of unaltered gene expression of genes flanking the Densin locus. (a) Comparison of wt and ko animal Densin transcripts. Exon positions (blue dashes along the horizontal axis) are predicted by the University of California, Santa Cruz, genome browser based on Refseq, Uniprot, GenBank, and comparative genomics databases (http://genome.ucsc.edu). Red bars denote RPKM counts mapped to that exon. Black bars represent the RPKM count mapped to positions outside known exon modles. Note the differences in scales for the y-axis. The deletion of exon 3 from the ko transcripts is highlighted. (b) Genes flanking the Densin locus show no significant changes in their level of gene transcription.

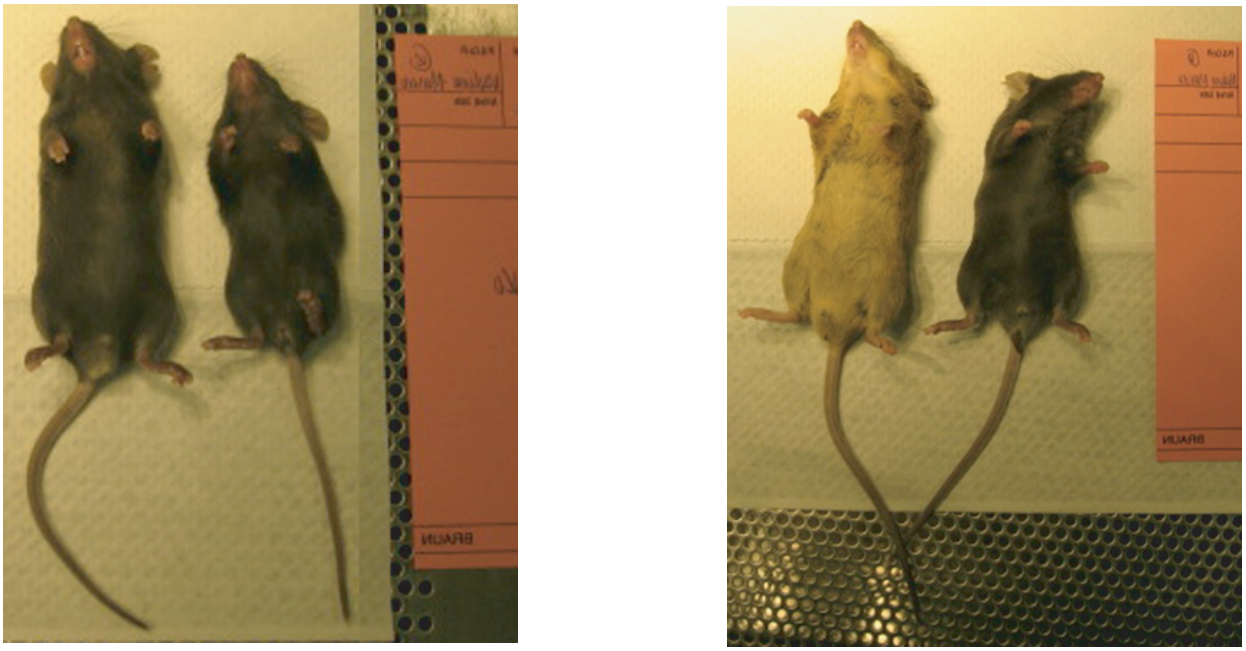

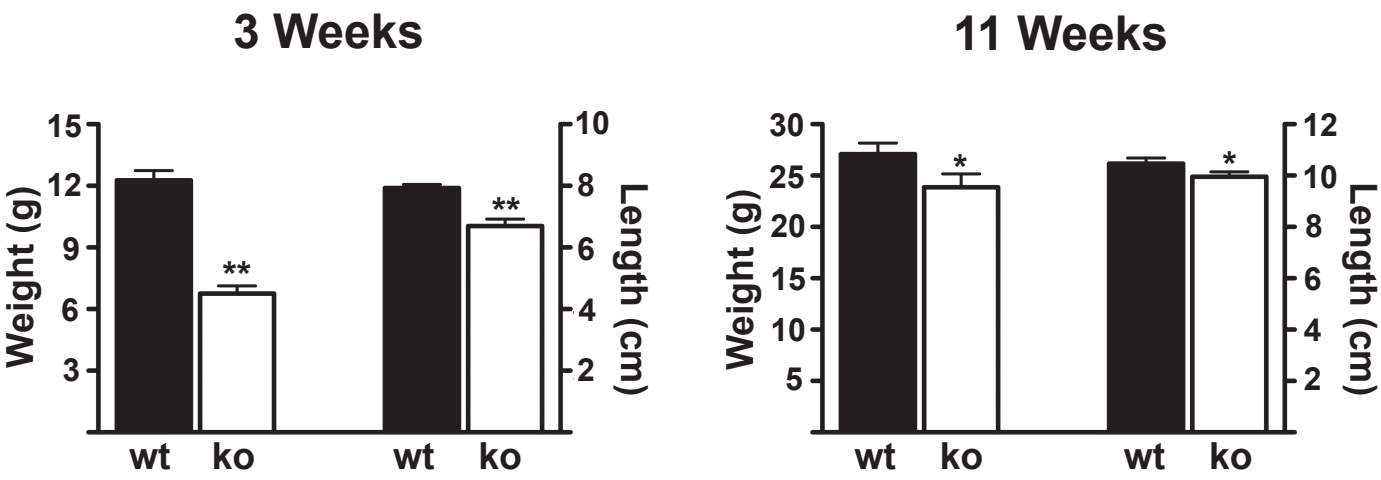

Figure 2.5 The Densin ko mutation causes a runt phenotype (image). At 3 weeks of age, knockout animals are significantly smaller than their wildtype litter mates (ko weight= -44.95%, $p<0.01$, ko length= -15.48%, $p<0.01$); no significant size variation is observed in heterozygous litter mates (data not shown). At 11 weeks of age, animals continue to exhibit a runted phenotype, though the size difference decreases (ko weight= -11.86%, $p<0.05$; ko length= -4.92%, $p<0.05$)

Chapter 3: Analysis of Dendritic Arborization and Spine Morphology

Introduction

Neurons are specialized computational compartments that integrate and regulate the propagation of information. The principle language used by neurons to communicate with each other is the action potential. Numerous biophysical and structural properties of neurons have evolved to modulate action potential integration and propagation. Cellular morphology is crucial to our understanding of information processing and communication styles, because neuronal shape is directly related to the computations performed by the cell [1]. Two key morphological characteristics of neurons are dendritic arbor structure and dendritic spine geometry. While spines [2] and dendritic branches [3] can both operate as computational compartments, how their shape, size, and structure affect their function and intrinsic properties is still poorly understood.

An astonishing diversity of dendritic arbor structures exists among neurons of different and similar classes (Fig 3.1). The shape, size, and complexity of dendritic trees can modulate action potential propagation [4] and influence the intrinsic firing pattern of a neuron [5]. Specifically, Mainen and Sejnowski demonstrated that firing patterns correlate strongly with the extent of arborization, and Vetter et al. [4] showed that action potential propagation is strongly influenced by 1) the number of branching points, 2) the rate of increase in dendritic membrane area, and 3) the relationship between the diameter of parent and daughter dendrites at branchpoints. Ultimately, both of these studies imply

that the level of dendritic complexity is a key metric for understanding a neuron's intrinsic properties.

Like dendritic arbor structure, a spine's morphology can impact its function. As previously discussed in chapter one, the shape and biochemical components of dendritic spines play an important role in synaptic plasticity. Spine structures can be quite diverse, but are typically categorized into four basic groups: mushroom, thin, stubby, and branched (Fig 3.1b); these categories may also reflect their functional history [6]. These categories are based on the ratio of two measurements, 1) spine neck length, and 2) head volume. Synaptic activity can alter spine shape, composition of the resident PSD, and signaling dynamics. The spine neck acts as a diffusion barrier, isolating spine heads from the parent dendritic shaft. This isolation results in a specialized biochemical compartment capable of influencing plasticity at the synapse [2]. Furthermore, though spine necks are not able to sufficiently restrict synaptic currents, neck resistance can establish a membrane potential microdomain within the spine head and specifically restrict Ca^{2+} concentrations [7-9].

The structure of dendritic arbors and spine necks may serve somewhat distinct functions, however their development and activity dynamically impact each other. In fact, the growth and development of dendritic arbors are concurrent in time and space with synaptic formation, with proteins of the postsynaptic density playing an integral role in both processes [10]. Given the likely role of Densin in synaptic plasticity, synaptogenesis, and signaling and adhesion complexes, I undertook a comparative study to measure changes in dendritic arborization and spine shape between wild type and knockout animals. Results from these studies are presented here.

Material and Methods

3.1 Infection of Primary Hippocampal Neurons and Analysis of Dendritic Arbors

Primary hippocampal cultures were prepared and maintained as described (Chapter 4.2). At 18-19 DIV cells were infected with a sindbis virus containing green fluorescent protein (GFP) as previously described [11]. 12-14 hours post-infection, cells were fixed on coverslips and mounted as described (Chapter 4.2).

Images were taken on a LSM 5 PASCAL/ Exciter confocal microscope maintained by the Caltech Biological Imaging Center. Images were acquired using a 40x/ 1.3 Plan-Apochromat oil objective. The pinhole aperture was set at 0.5 μm with a zoom of 1x and image size of 1024 x 1024.

Sholl analysis was performed using the NIH ImageJ Sholl Analysis Plugin (v1.0) downloaded from the Ghosh lab website (http://www-biology.ucsd.edu/labs/ghosh/software/). Background dendrites extending into the image view from neighboring neurons were manually deleted. The origin of the concentric radii was set at the midpoint of the longest axis of the soma. Analysis parameters were as follows: starting radius, 1 μm; ending radius, 75 μm; radius step size, 2 μm; radius span, 1 μm; span type, median. Statistics were performed using the Prism statistical package (GraphPad, San Diego, CA).

3.2 Mouse Strains and Imaging of Spines

Homozygous green fluorescent protein (GFP) line-M transgenic mice [12] in a C57BL6 background (a kind gift from Dr. Joshua Sanes, Harvard University, Cambridge, MA) were crossed with F2 generation Densin$^{+/-}$ animals to produce GFP$^{+/-}$ / Densin$^{+/-}$ animals. GFP$^{+/-}$ / Densin$^{+/-}$ animals were subsequently crossed to produce GFP expression in a Densin null mutant background. Genomic DNA was isolated from mouse ear punch or tail samples and used for PCR. Genotyping protocols for GFP line-M were previously described [12].

Four GFP positive Densin$^{+/+}$ and Densin$^{-/-}$ 8-10 week old age-matched pairs were perfused transcardially as previously described [13]. 50μm coronoal sections were cut with a vibratome and mounted with Prolong Gold antifade reagent. Slides were individually coded by a member of the Kennedy lab and randomly ordered for image acquisition. Images were acquired on a LSM 5 PASCAL/ Exciter confocal microscope with a 100x 1.4 NA lense and 2x optical zoom. Images of dendrites (from 20 sections per animal) were reconstituted from stacks of 40 0.4 μm optical sections and preprocessed with blind iterative deconvolution software (Autodeblur) Autoquant. Spine morphology was analyzed using 3DMA spine analysis software developed in the laboratory of Brent Lindquist (Stony Brook University, Stony Brook, NY) (Koh et al., 2002). By using a geometric approach, the 3DMA software automatically detects and quantifies the three-dimensional structure of dendritic spines from stacks of high-resolution confocal microscopic images. The software then assigns the detected spines to one of three morphological categories (thin, stubby, or mushroom) based on the ratio of

neck length to head volume [14]. The investigator was blind to genotype during image acquisition and analysis of spine morphology.

3.3 Statistics

Raw data are presented as averages +/- standard error of the mean (SEM), with *n* indicating the number of experiments. Data sets that report percentage changes from control values are expressed as geometric means (GM) to avoid a statistical phenomenon in which the averages of ratios tend to overestimate differences. The GM was calculated as the *n*th root of the product of the percentage changes from the control values. The standard error of the geometric mean (SEGM) was calculated by multiplying the GM by the SE of the arithmetic mean of the logarithms of the percentage changes from the control values.

Statistical analyses of two groups were measured using Student's t tests (two-tailed). One-sample t tests (two-tailed) were used to determine whether data sets that were normalized to matched control values were significantly different from 100%. Statistical analyses of data containing more than two groups were performed using the one-way ANOVA test, followed by Tukey–Kramer analysis, to account for multiple comparisons. The Kolmogorov–Smirnov method was used to assess whether data sets had Gaussian distributions, as required for t tests and ANOVA analyses. In cases where the data were not Gaussian, nonparametric tests were used as stated.

Results

3.4 Dendritic Arborization

Analysis of dendritic arbor structure in Densin ko mice revealed an effect of deletion of Densin on branching of proximal dendrites and on overall dendritic branch complexity. Qualitative observations suggested that the primary dendritic trunks emanating from the soma are thicker in Densin$^{-/-}$ hippocampal neurons. Furthermore, somal apexes from which the dendritic trunk and branches sprout are broad and flattened relative to wt neurons.

Quantitative analysis of the structure of dendritic arbors using the Sholl method revealed a statistically significant increase in the number of proximal dendrites within 10 μm of the soma (wt= 53.57 +/-1.74, ko= 103 +/-1.49; $p<0.0001$). However, the Densin ko neurons show an overall decrease in the number of dendritic branches and complexity as determined by the average number of total dendritic intersections (wt= 360.86 +/-2.15, ko= 252.82 +/-1.36; $p<0.0001$). The findings indicate that the ability to initiate branch points and extend dendrites is altered in Densin ko neurons.

3.5 CA1 Dendritic Spine Structure

The results of Quitsch et al. [15] in cultured neurons demonstrated that overexpression of Densin in primary hippocampal cultures resulted in the elaboration of the dendritic arbor structure. Furthermore, they showed that presynaptic clusters for synaptophysin formed along the elaborated dendritic branches, suggesting that Densin plays a role in synaptogenesis. This would suggest that neurons of Densin knockout animals might have a decreased spine density. To test this hypothesis, we crossed

Densin$^{-/-}$ animals with GFP+ line-M transgenic mice. These mice express GFP sparsely in a golgi-like pattern in CA1 pyramidal neurons [12]. We acquired confocal images of fluorescent basal dendrites of CA1 pyramidal neurons in littermates, with the investigator being blind to the genotype of the animal. Three-dimensional images of the dendrites were deconvolved from z-stacks, and spine morphology was analyzed as described in Section 3.2 and 3.3.

We found that adult hippocampal neurons from Densin$^{-/-}$ mice had a 13% increase in spine density compared to wild type neurons (Fig 3.3). Furthermore, the volume of spines heads decreased 11% in Densin$^{-/-}$ mice (Fig 3.3). Though a trend towards an increase in spine length was observed, the difference was not statistically significant. These results show that Densin plays a role in spine morphology and density.

References

1. Spruston, N., *Pyramidal neurons: dendritic structure and synaptic integration.* Nat Rev Neurosci, 2008. **9**(3): p. 206-21.
2. Sabatini, B.L., M. Maravall, and K. Svoboda, *Ca^{2+} signaling in dendritic spines.* Curr Opin Neurobiol, 2001. **11**(3): p. 349-56.
3. Polsky, A., B.W. Mel, and J. Schiller, *Computational subunits in thin dendrites of pyramidal cells.* Nat Neurosci, 2004. **7**(6): p. 621-7.
4. Vetter, P., A. Roth, and M. Hausser, *Propagation of action potentials in dendrites depends on dendritic morphology.* J Neurophysiol, 2001. **85**(2): p. 926-37.
5. Mainen, Z.F. and T.J. Sejnowski, *Influence of dendritic structure on firing pattern in model neocortical neurons.* Nature, 1996. **382**(6589): p. 363-6.
6. Bourne, J.N. and K.M. Harris, *Balancing structure and function at hippocampal dendritic spines.* Annu Rev Neurosci, 2008. **31**: p. 47-67.
7. Yasuda, R., et al., *Imaging calcium concentration dynamics in small neuronal compartments.* Sci STKE, 2004. **2004**(219): p. pl5.
8. Wilson, C.J., *Passive cable properties of dendritic spines and spiny neurons.* J Neurosci, 1984. **4**(1): p. 281-97.
9. Noguchi, J., et al., *Spine-neck geometry determines NMDA receptor-dependent Ca2+ signaling in dendrites.* Neuron, 2005. **46**(4): p. 609-22.
10. Cline, H. and K. Haas, *The regulation of dendritic arbor development and plasticity by glutamatergic synaptic input: a review of the synaptotrophic hypothesis.* J Physiol, 2008. **586**(6): p. 1509-17.
11. Vazquez, L.E., et al., *SynGAP regulates spine formation.* J. Neurosci., 2004. **24**: p. 8796-8805.
12. Feng, G., et al., *Imaging neuronal subsets in transgenic mice expressing multiple spectral variants of GFP.* Neuron, 2000. **28**(1): p. 41-51.
13. Carlisle, H.J., et al., *SynGAP regulates steady-state and activity-dependent phosphorylation of cofilin.* J. Neurosci., 2008. **28**: p. 13649-13683.
14. Koh, I.Y., et al., *An image analysis algorithm for dendritic spines.* Neural Comput, 2002. **14**(6): p. 1283-310.
15. Quitsch, A., et al., *Postsynaptic shank antagonizes dendrite branching induced by the leucine-rich repeat protein Densin-180.* J Neurosci, 2005. **25**(2): p. 479-87.

Figure 3.1 The morphologies of dendrites and spines affect their function. (A) Diversity of arbor structures between and within neuron classes dynamically affect their integration and propagation of action potentials, and ultimately their firing patterns. Top, dendritic morphologies of nonpyramidal cells. Left to right, fast spiking basket cell, late-spiking neurogliaform, non-fast spiking somatostatin Martinotti cell, non-fast spiking cholecystokinin (CCK) large basket cell, non-fast spiking small basket cell, and non-fast spiking double bouquet cell (adapted from Kawaguchi et al., 2006). Bottom, structures of pyramidal neurons from different cortical layers. Left to right, neurons of layer II/ III, layer V, CA3, CA1, subiculum (adapted from Spruston, 2008). (B) Structural diversity in spine size and shape. A 3-dimentional reconstruction of a dendritic shaft (gray) and protruding spines (red, thin spine; green, stubby; blue, mushroom; yellow, branched). Postsynaptic densities can also vary in shape and size (purple).

A

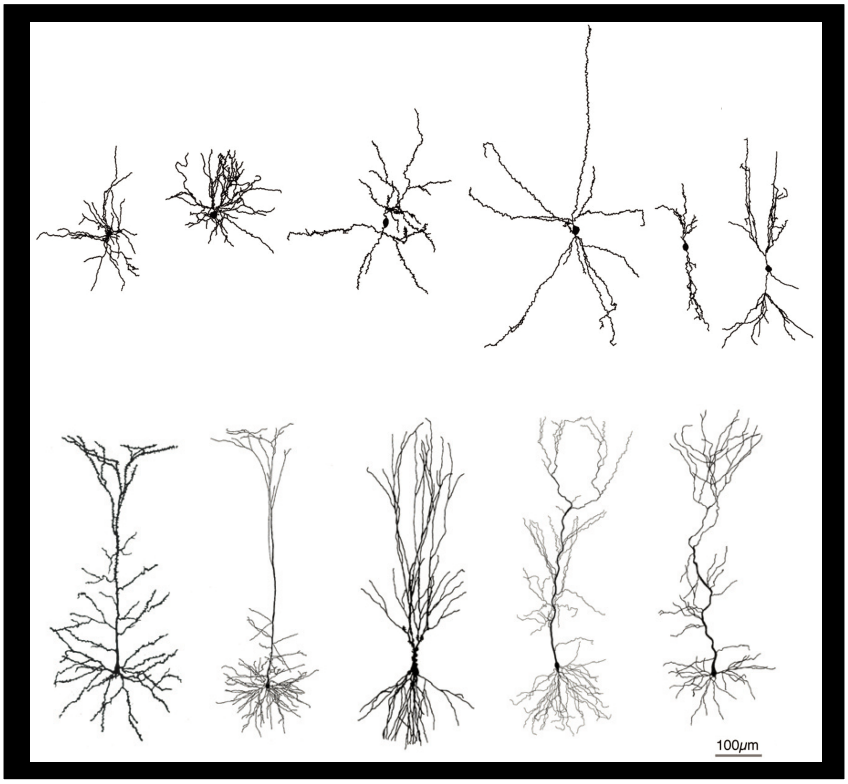
100μm

B

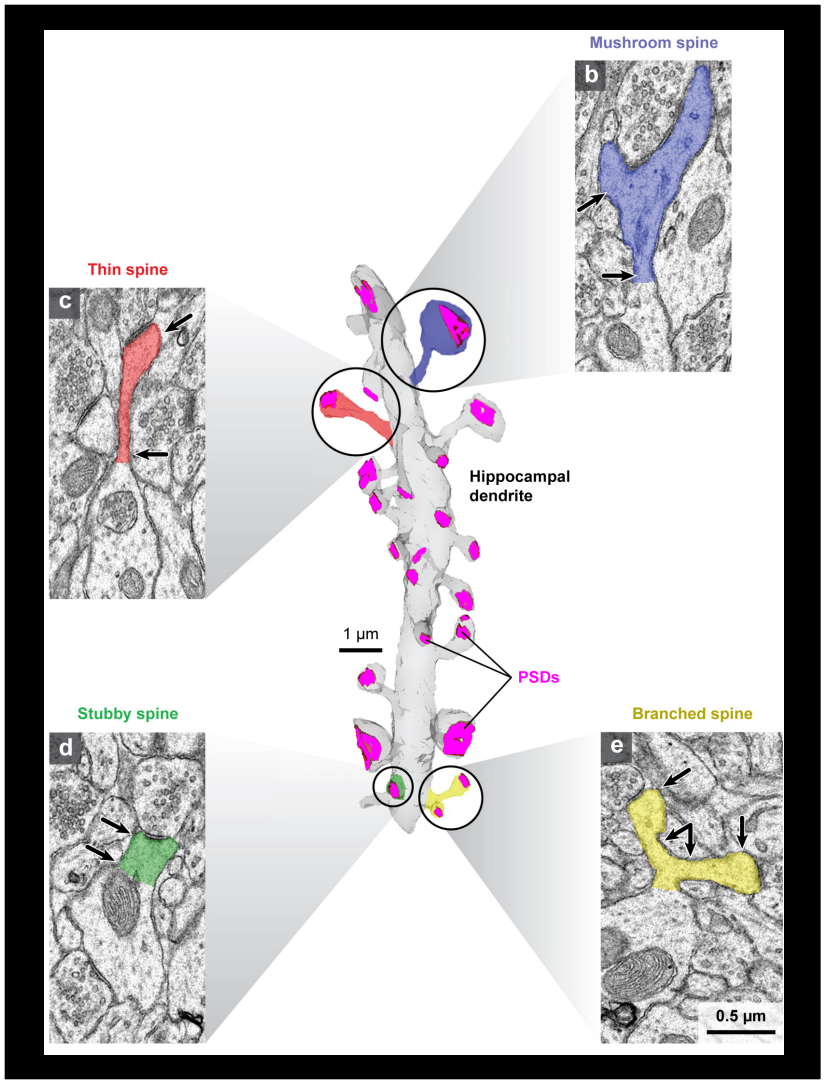
Mushroom spine
b
Thin spine
c
Hippocampal dendrite
1 μm
PSDs
Stubby spine
d
Branched spine
e
0.5 μm

Figure 3.2 Cultured Densin ko neurons have thicker dendritic trunks and an increase in the number of proximal dendritic branches. (A) 18 DIV primary hippocampal cultures infected with sindbis-GFP. Primary apical and basal dendritic trunks (arrows) are thicker in ko neurons. Images represent the phenotypic range observed. Images are compressed z-stacks of three .5 μm consecutive optical sections. (B) Sholl analysis of cultured wild type (black) and ko (red) hippocampal neurons demonstrates an increased number of proximal dendritic branches within 10 μm of the soma as determined by the average of number of intersecting dendrites (wt= 53.57 +/-1.74, ko= 103 +/-1.49; $p<0.0001$). However, Densin ko neurons exhibit a decreased level of dendritic complexity as determined by the average number of total dendritic intersections (wt= 360.86 +/-2.15, ko= 252.82 +/-1.36; $p<0.0001$). The number of dendrities crossing concentric circles of increasing radii centered about the soma was counted. Ten neurons from each of three sets of wt/ ko primary hippocampal cultures were analyzed. The x-axis indicates distance from the origin in μm; the y-axis indicates the number of dendritic intersections. Error bars indicate SEM.

A

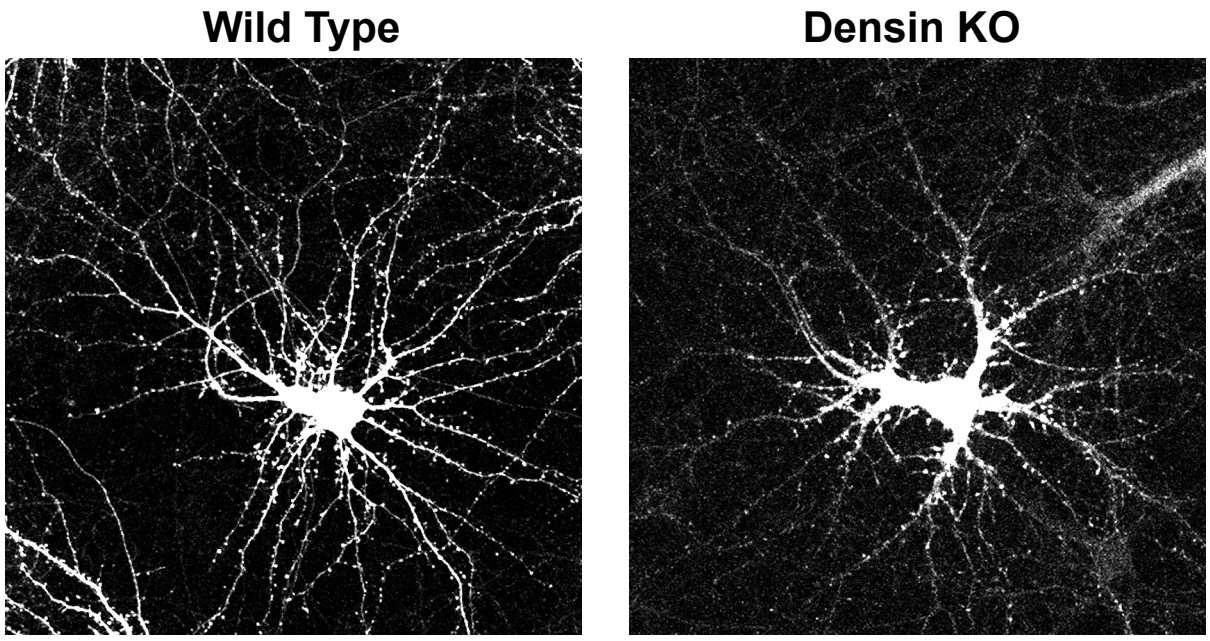
Wild Type
Densin KO

B

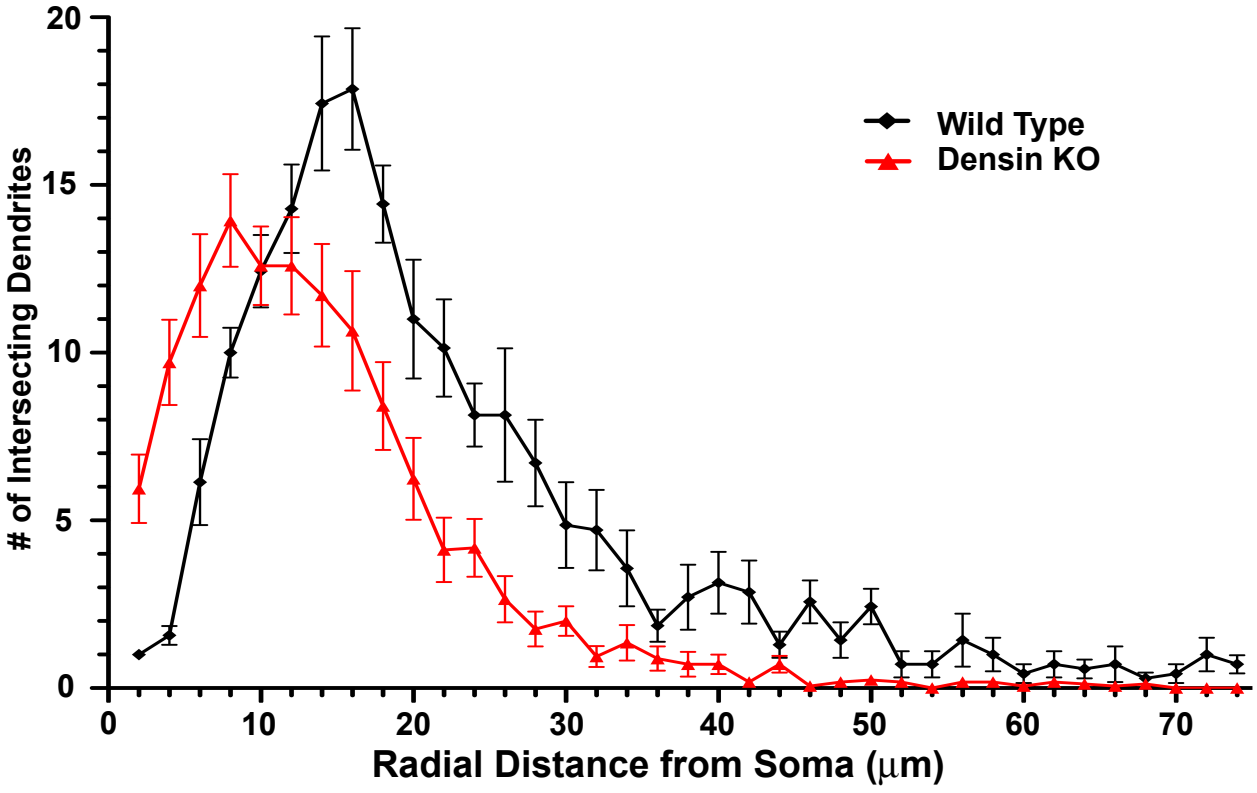
Wild Type
Densin KO
# of Intersecting Dendrites
Radial Distance from Soma (μm)
0
5
10
15
20
0
10
20
30
40
50
60
70

Figure 3.3 Homozygous deletion of Densin increases spine density and decreases spine volume on adult hippocampal CA1 neurons *in vivo*. A) Example dendrites are shown for GFP+/ Densin$^{+/+}$ and GFP+/ Densin$^{-/-}$ mice. B) The data show a significant increase in the absolute density of spines per micrometer of dendrite on Densin$^{-/-}$ hippocampal neurons compared to wildtype (wt= 1.93 +/-0.07 spines/ μm dendrite; Densin$^{-/-}$= 2.19 +/- 0.07 spines/ μm dendrite; $p<0.01$). The data also show a significant decrease in the volume of spine heads on dendrites of Densin$^{-/-}$ hippocampal neurons compared to wild type (wt= 0.067 +/- 0.002 μm^3; Densin$^{-/-}$= 0.061 +/- 0.002 μm^3; $p<0.01$). Finally, the data show no significant change in the length of spines in Densin$^{-/-}$ hippocampal neurons compared to wild type (wt= 0.59 +/-0.01 μm; Densin$^{-/-}$= 0.61 +/-0.01μm; $p>0.05$).

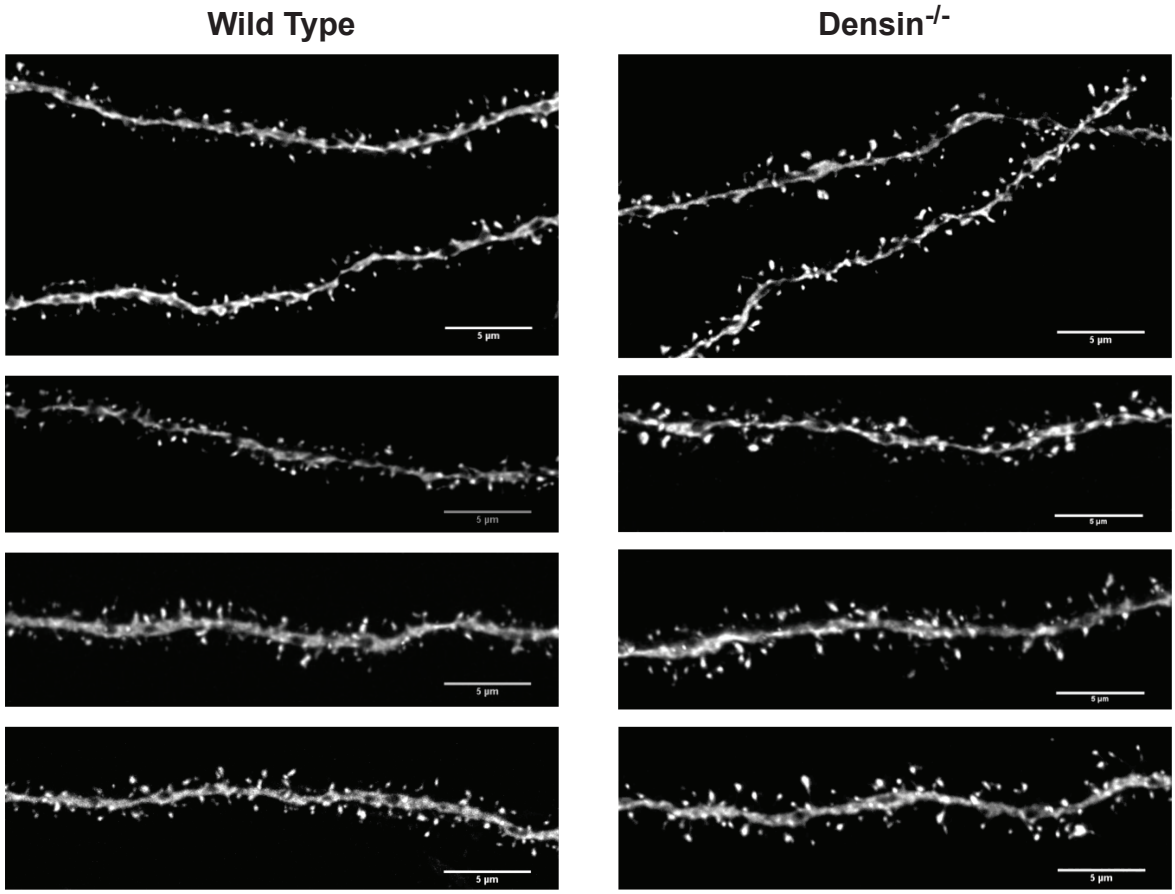
Wild Type
Densin-/-
5 µm

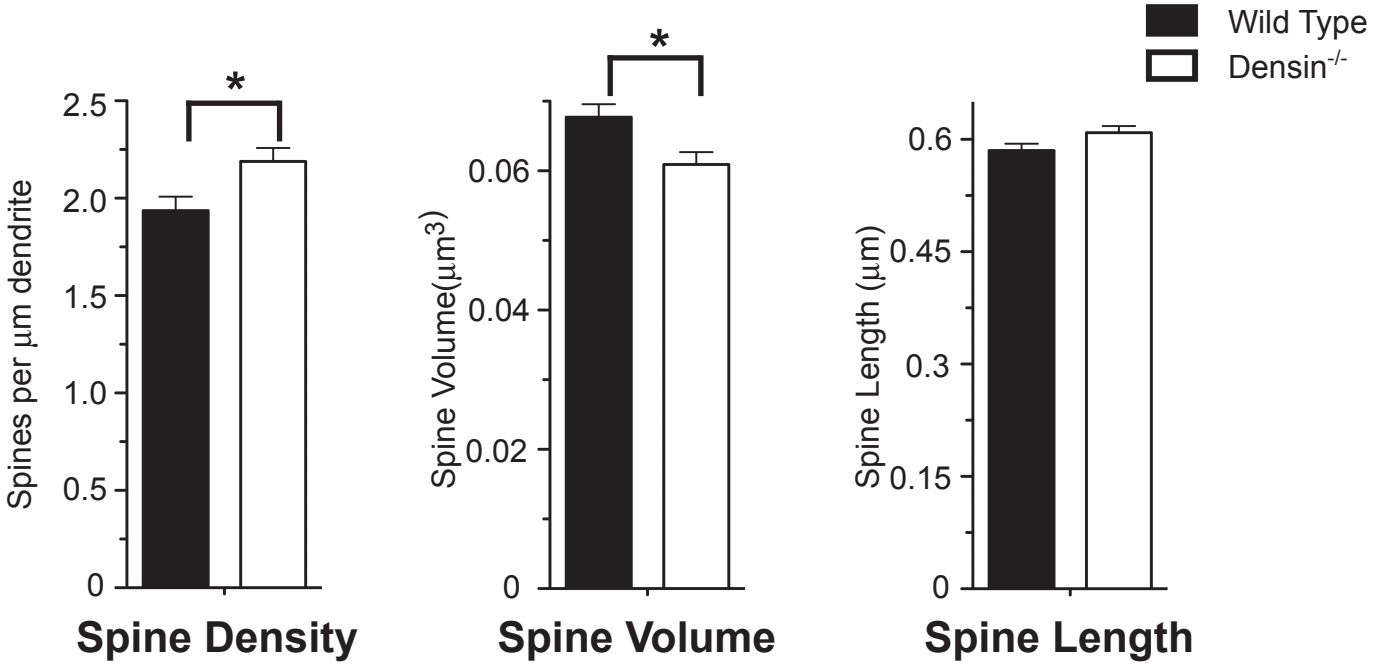
Wild Type
Densin-/-
Spines per µm dendrite
2.5
2.0
1.5
1.0
0.5
0
*
Spine Density
Spine Volume(µm3)
0.06
0.04
0.02
0
*
Spine Volume
Spine Length (µm)
0.6
0.45
0.3
0.15
0
Spine Length

Chapter 4: The Role of Densin in the Postsynaptic Density and Docking of CaMKII

Introduction

Because proteins of the PSD apparatus work as an integrated whole, their differential spatial and temporal interactions are integral to the nature and strength of a postsynaptic response to impinging signals. Furthermore, the subcellular targeting and dynamic alterations in the localization of signaling and regulatory proteins may produce diversity in signaling complexes and increased specificity for target substrates [1]. The behavior of CaMKII enriched in the PSD reflects this dynamic spatial and temporal activity.

CaMKII is a Ser/ Thr kinase that is central to the coordination and execution of signal transduction of Ca^{2+} signals [2]. CaMKII is a dodecameric holoenzyme that is assembled in stochastic combinations from two homologous catalytic subunits, alpha and beta [3, 4]. These isoforms appear to differentially affect synaptic and dendritic morphology. In particular, αCaMKII is important for regulating synaptic strength and stabilization of dendritic arbors [5]. βCaMKII seems to have a greater effect on the degree of dendritic arborization, as well as the formation and number of synapses [6]. These differences may reflect the different developmental time courses of their expression. In addition to the markedly different roles in neuronal plasticity, the α and β subunits also impart differential subcellular distribution and translocation dynamics in response to NMDA receptor stimulation[7-9].

CaMKII is highly concentrated in the PSD [10, 11] suggesting that one or more docking sites within the PSD likely mediate its postsynaptic accumulation. Recent work indicates that the cytocolic tails of the NR2A and NR2B subunits of the NMDA receptor bind to CaMKII, thus serving as docking sites within the PSD [12-14]. Hell and co-workers found that both phosphorylated and unphosphorylated CaMKII can bind to these NMDA receptor subunits (Leonard, et al., 1999). However, activation of CaMKII, via NMDA receptor stimulation, greatly increases its affinity for the NMDA receptor.

In addition to their role in binding CaMKII, the c-terminal tails of the NR2A and NR2B subunits are also required for proper localization of functional NMDA receptor to the synapse [15]. The carboxyl terminal tails of the NR2 subunits contain protein binding sequences required for their interaction with MAGUK family proteins (PSD-95, SAP102, PSD-93 and SAP97) [15-17]. This interaction facilitates their localization to the synapse. Deletion of the NR2A or NR2B c-terminal tails results in the near total loss of synaptic NMDA localization [15, 18-21]. Furthermore, the loss of the NR2B c-terminus results in neonatal death, phenocopying the full length knockout of the NR2B subunit [18, 21, 22] and deletion of the NR1 subunit [23, 24].

Given the potential importance of the NMDA receptor's NR2 subunits for nucleating CaMKII at the PSD, our lab acquired two knockin mutant mouse lines created in the Seeburg lab; $NR2A^{\Delta c/\Delta c}$ and $NR2B^{\Delta c/\Delta c}$. Both of these mouse lines contain deletions of their carboxyl terminal cytoplamsic tails [18]. These two mouse strains were crossed to produce animals heterozygous for both $NR2A^{\Delta c/\Delta c}$ and $NR2B^{\Delta c/\Delta c}$. Progeny heterozygous for both mutations were interbred to generate $NR2A^{\Delta c/\Delta c}$ x $NR2B^{\Delta c/\Delta c}$ primary neuronal cultures. These "double-tailless" neuronal cultures were subsequently

used to study the effects of the loss of cytoplasmic tails on CaMKII localization to the PSD.

In addition to the NMDA receptor, we hypothesized that Densin may act as a second docking site for CaMKII in the PSD. Biochemical studies performed in the Kennedy lab found that Densin can bind CaMKII in its intracellular domain [25]. Similar to the interaction of CaMKII with the NR2 tails, binding of the kinase to Densin does not require autophosphorylation. However, activation by autophosphorylation increases the affinity of CaMKII for Densin ~100 fold [25].

In the following series of experiments, we set out to test the hypothesis that Densin and the NMDA receptor are the primary docking sites for CaMKII in the PSD. we proposed to do this by analyzing changes in co-localization of CaMKII with PSD-95 in dissociated hippocampal cultures via immunofluorescent image analysis. We hypothesize that the loss of the NR2 tails will result in a decrease of CaMKII localization at the PSD. Consequently, we first analyze colocalization of CaMKII with PSD-95 in $NR2A^{\Delta c/\Delta c}$ x $NR2B^{\Delta c/\Delta c}$ primary hippocampal cultures. Loss of the NR1 subunit causes the NR2 subunits to be retained in the endoplasmic reticulum, resulting in the loss of NMDA receptor at the synapse [26]. Consequently, we hypothesize that primary neuronal cultures made from NR1 knockout embryos should phenocopy the $NR2A^{\Delta c/\Delta c}$ x $NR2B^{\Delta c/\Delta c}$ primary neuronal cultures. we then analyzed the colocalization of CaMKII with PSD-95 in the Densin knockout mouse. Finally, we cross the Densin and NR1 knockout lines to generate $Densin^{-/-}$ x $NR1^{-/-}$ primary hippocampal cultures to investigate CaMKII colocalization with PSD-95 when both Densin and the NMDA receptor are removed from the PSD.

Material and Methods

4.1 Mouse strains

$NR2A^{\Delta c/\Delta c}$ animals were maintained as a homozygous mutant line while the $NR2B^{\Delta c/\Delta c}$ animals were maintained as heterozygous individuals because mice homozygous for the $NR2B^{-/-}$ mutation are embryo lethal; both $NR2A^{\Delta c/\Delta c}$ and $NR2B^{\Delta c/\Delta c}$ mutants were generous gifts from Peter Seeburg. $NR2A^{\Delta c/\Delta c}$ homozygous mice where crossed with $NR2B^{+/\Delta c}$ heterozygous mice to create $NR2A^{+/\Delta c}$ x $NR2B^{+/\Delta c}$ heterozygous animals. These animals where then crossed to generate $NR2A^{\Delta c/\Delta c}$ x $NR2B^{\Delta c/\Delta c}$ embryos for cell culture experiments.

Densin knockout animals were maintained as a heterozygotes. NR1 mutants, a generous gift from Peter Seeburg, were maintained as heterozygotes. $NR1^{+/-}$ mutants were crossed with F2 generation $Densin^{+/-}$ animals to produce $NR1^{+/-}$ x $Densin^{+/-}$ heterozygotes. $NR1^{+/-}$ x $Densin^{+/-}$ animals (F3) were subsequently crossed to produce $NR1^{-/-}$ x $Densin^{-/-}$ double knockout embryos for cell culture experiments.

Genomic DNA was isolated from mouse ear punch samples and used for PCR based genotyping.

4.2 Primary neuronal cultures and immunocytochemistry

Hippocampi from 16-day-old embryos (wildtype, $NR2A^{\Delta c/\Delta c}$ x $NR2B^{\Delta c/\Delta c}$, $NR1^{-/-}$, $Densin^{-/-}$, and $Densin^{-/-}$ x $NR1^{-/-}$), were dissected and dissociated with trypsin and mechanical trituration. Cells were plated onto glass coverslips coated with Poly-D,L-

Lysine (Sigma, St. Louis, MO). Cultures were maintained in neurobasal media (Invitrogen, Carlsbad, CA) and supplemented with B27, glutamate, and Glutamax-I (Invitrogen). Genotypes of cell cultures were determined with genomic DNA isolated from embryonic tissue.

After 18-21 days *in vitro*, cover slips coated with cells were rinsed in ice-cold PBS and placed briefly in ice-cold methanol. The methanol was replaced with -20ºC methanol and incubated at -20ºC for 10-15 min. Cells were rinsed and incubated in h-PBS (450mM NaCl and 20mM phosphate buffer, pH 7.4) for 15 min and blocked with 5% normal goat serum and 0.05% Triton X-100 in h-PBS for 1 hour at 4ºC. Fixed cultures were then placed in preblock buffer for one hour. Fixed cultures were then incubated overnight with primary antibodies; rabbit anti-PSD-95 (D27E11, 1:200; Cell Signaling, Beverly, MA) and mouse anti-αCaMKII (6G9, 1:1000; ABR, Golden, CO). Coverslips were washed three times (15 min per wash) in blocking buffer followed by incubation with goat anti-mouse conjugated to Alexa 568 and goat anti-rabbit conjugated to Alexa 488 secondary antibodies (Molecular Probes) at room temperature for 1 hour. Coverslips were then washed once in blocking buffer for 15min and twice in PBS for 15 min. Coverslips were then post-fixed in 2% paraformaldehyde in PBS for 10 min followed by two washes in PBS for 10 min each. Finally, coverslips were mounted on microscope slides with a drop of Prolong antifade reagent (Invitrogen) and allowed to dry overnight.

4.3 Fluorescent microscopy and image analysis

All immunofluorescent images were acquired on a Zeiss Axiovert 200M (Thornwood, NY) fluorescent microscope equipped with a 63x/1.4 oil objective and a high-resolution CCD camera (Axiocam MRm) controlled by Zeiss AxioVision 3.1 imaging software. Image exposure time was independently determined for each experiment by setting the exposure length to sub-maximal pixel brightness based on wildtype images. All images from the same experiment were acquired under identical settings.

Image analysis was conducted with the NIH ImageJ software program. PSD-95 was used as the marker for the PSD region. Threshold for PSD-95 immunostaining was set to allow all recognizable PSD-95 puncta to be included in the creation of the mask. The PSD-95 mask was then overlayed onto the CaMKII image. All CaMKII puncta that colocalized with the PSD-95 mask were measured for intensity. 15-20 neurons were analyzed per embryo. Each genotype was analyzed at least three different times from litters dissected from three different pregnant females. Mutant animals were always compared to wild type litter mates.

Values for brightness of CaMKII puncta normalized to wild type littermates were analyzed with the Prism statistical package (Graphpad, San Diego, CA) and normalized to wt. The one-sample *t* test (two-tailed) was used to determine whether the brightness of CaMKII puncta in mutant neurons was significantly different from that of wild type neurons. Data are presented as averages +/- standard error of the mean (SEM) with correlating p-value. All images are presented without alterations to brightness or contrast.

4.4 Quantitative immunoblot

Preparations of forebrain homogenates for immunobloting were performed as previously described (Section 2.5). Blots of five wt/ko sibling pairs were probed, in triplicate, for the following proteins: aCaMKII (6G9, 1:2500), synGAP (PA1-046, 1:1000), PSD-93 (PA1-043, 1:300), and PSD-95 (7E3, 1:2000; ABR, Golden, CO); GluR1 (1:500) and GluR2/3 (06-307, 1:200) from Upstate Biotechnology, Lake Placid, NY; α-Actinin (EA-53, 1:3000) and Actin (1:5000) from Sigma, St. Louis, MO; NR1 (1516, 1:700; Chemicon, Temecula, CA); β-Catenin (1:4000), NR2A (Uma, 1:2500), (NR2B Xandria, 1:2500), δ-Catenin/ NPRAP (1:300,) and Citron (CT261, 1:1000) developed in house; and Erbin, 1:1000 (a generous gift from Lin Mei, Medical College of Georgia, Augusta, GA). Blots were visualized with the Odyssey Infrared Imaging System (Li-Cor Bioscience, Lincoln, NE). Quantification of integrated IR fluorescence intensity was performed with the Li-Cor Odyssey analysis software. Statistical analysis was performed using the Prism software package. A one-sample *t* test (two-tailed) was used to determine whether fluorescence intensity of protein bands from knockout animals was significantly different from that of wild type litter mates. Data are presented as average +/- (SEM) with correlating p-value.

Results

4.5 Docking of CaMKII in the PSD

To investigate whether the loss of the NMDA receptor and Densin would affect the localization and accumulation of CaMKII in the PSD we measured the intensity of

CaMKII puncta colocalizing with PSD-95 in dissociated hippocampal neurons cultured from individual E16 mouse embryos.

In mature NR2A$^{\Delta c/\Delta c}$ x NR2B$^{\Delta c/\Delta c}$ mutant cultures (18 DIC), the CaMKII puncta colocalizing with PSD-95 are significantly less intense than wild type (-18.7% +/-1.2, $p<0.0001$; Fig 4.1). Similarly, cell cultures from NR1$^{-/-}$ embryos show a statistically significant decrease in the intensity of CaMKII puncta colocalizing with PSD-95 (-17.7% +/- 1.9, $p<0.0001$; Fig 4.1). When comparing the intensity of CaMKII puncta between the NR2A$^{\Delta c/\Delta c}$ x NR2B$^{\Delta c/\Delta c}$ and NR1$^{-/-}$ mutant cultures, no significant change is observed, suggesting that the NR2A$^{\Delta c/\Delta c}$ x NR2B$^{\Delta c/\Delta c}$ and NR1$^{-/-}$ mutants are indeed phenocopies.

In the Densin knockout we also see a significant decrease in the intensity of CaMKII puncta colocalizing with PSD-95 (-23.9% +/-3.7, $p<0.0005$; Fig 4.2). However, this result is confounded by our quantitative immunoblot studies that show a global decrease in αCaMKII protein expression (-18.12% +/-2.7, $p<0.01$; Fig 4.5). This result suggests that the loss of CaMKII colocalization with PSD-95 in the cell culture experiments may be due to the global decrease in CaMKII expression.

Densin$^{-/-}$ x NR1$^{-/-}$ cultures exhibited a still larger decrease in the intensity of CaMKII puncta colocalizing with PSD-95 (-57.1% +/-1.16, $p<0.0001$; Fig 4.3). Moreover, the Densin$^{-/-}$ x NR1$^{-/-}$ cultures exhibit a greater loss in intensity of CaMKII colocalizing with PSD-95 than the sum of the losses in single knockout cultures (-57.1% vs. -42.1%, respectively; Fig 4.4. These data may suggest that the NMDA receptor and Densin can compensate for each other in their effects on localization of CaMKII in the PSD. If this is true then their ability to maintain a pool of CaMKII in the PSD is synergistic. However, the decrease in CaMKII puncta intensity can also be the result of a

global decrease in CaMKII expression. This can result from a loss of activity dependent αCaMKII protein expression.

4.6 Decrease in the concentration of core PSD proteins in the Densin knockout

To determine if the loss of Densin affected the composition of the PSD we measured the level of several other core PSD proteins by quantitative immunoblot.

We found that the amounts of NR1 and NR2A subunits of the NMDA receptor significantly decreased (-22.0% +/- 4.3, $p<0.05$; -36.4% +/- 4.3 $P<0.01$, respectively) compared to wild type (Fig 4.5). Given that we found no significant decrease in the NR2B subunit, these data suggest that the composition of the NMDA receptor in the forebrain is shifted towards NR1-NR2B receptors in the Densin knockout mouse. Furthermore, we found a change in the ratio of expression of AMPA subunits. Specifically, the GluR2 subunit decreased by 24.24% +/- 1.9 ($p<0.01$) and GluR1 show no statistically significant change.

Erbin, a member of the LAP protein family of which Densin is also a member, is a PSD protein that has high sequence homology with Densin. We wondered whether its expression might increase as a compensatory response to the loss of Densin. In contrast, the level of Erbin decreased substantially by 45.1% +/- 3.7 ($p<0.0001$; Fig 4.5). Its level was the most significantly affected of any of the proteins investigated.

PSD-95, a major scaffolding molecule of the PSD, decreased by 33.31% +/-1.6 ($p<0.001$) in the forebrain homogenates (Fig 4.5). PSD-95 is known to interact with Densin through the dimerization of Maguin-1 (Ohtakara et al., 2002). Furthermore, PSD-

95 is known to bind directly to or mediate interactions with all of the PSD proteins whose expression levels are significantly decreased. Thus, our results suggest that the loss of Densin may destabilize a PSD complex that is organized by PSD-95.

Finally, we found that αCaMKII was significantly decreases by 18.12% +/-2.7 ($p<0.01$). This global decrease may result from a loss of activity dependent translation or degradation.

Core PSD proteins that did not exhibit significant changes in their level of expression were α-Actinin, NR2B, SynGAP, PSD-93, δ-catenin, β-catenin, Citron, and the GluR1 subunit (data not shown).

References

1. Meyer, T. and K. Shen, *In and out of the postsynaptic region: signalling proteins on the move.* Trends Cell Biol, 2000. **10**(6): p. 238-44.
2. Kennedy, M.B., et al., *Structure and regulation of type II calcium/calmodulin-dependent protein kinase in central nervous system neurons.* Cold Spring Harb. Symp. Quant. Biol., 1990. **55**: p. 101-110.
3. Bennett, M.K., N.E. Erondu, and M.B. Kennedy, *Purification and characterization of a calmodulin-dependent protein kinase that is highly concentrated in brain.* J. Biol. Chem., 1983. **258**: p. 12735-12744.
4. Kolodziej, S.J., et al., *Three-dimensional reconstructions of Calcium/Calmodulin-dependent (CaM) kinase II alpha and truncated CaM kinase II alpha reveal a unique organization for its structural core and functional domains.* J Biol Chem, 2000. **275**(19): p. 14354-9.
5. Wu, G.Y. and H.T. Cline, *Stabilization of dendritic arbor structure in vivo by CaMKII.* Science, 1998. **279**(5348): p. 222-6.
6. Fink, C.C., et al., *Selective regulation of neurite extension and synapse formation by the beta but not the alpha isoform of CaMKII.* Neuron, 2003. **39**(2): p. 283-97.
7. Shen, K. and T. Meyer, *Dynamic control of CaMKII translocation and localization in hippocampal neurons by NMDA receptor stimulation.* Science, 1999. **284**(5411): p. 162-6.
8. Shen, K., et al., *Molecular memory by reversible translocation of calcium/calmodulin-dependent protein kinase II.* Nat Neurosci, 2000. **3**(9): p. 881-6.
9. Shen, K., et al., *CaMKIIbeta functions as an F-actin targeting module that localizes CaMKIIalpha/beta heterooligomers to dendritic spines.* Neuron, 1998. **21**(3): p. 593-606.
10. Kennedy, M.B., *Signal-processing machines at the postsynaptic density.* Science, 2000. **290**: p. 750-754.
11. Kennedy, M.B., M.K. Bennett, and N.E. Erondu, *Biochemical and immunochemical evidence that the "major postsynaptic density protein" is a subunit of a calmodulin-dependent protein kinase.* Proc. Natl. Acad. Sci. U.S.A., 1983. **80**: p. 7357-7361.
12. Strack, S. and R.J. Colbran, *Autophosphorylation-dependent targeting of calcium/calmodulin- dependent protein kinase II by the NR2B subunit of the N-methyl- D-aspartate receptor.* J Biol Chem, 1998. **273**(33): p. 20689-92.
13. Leonard, A.S., et al., *Calcium/calmodulin-dependent protein kinase II is associated with the N- methyl-D-aspartate receptor.* Proc Natl Acad Sci U S A, 1999. **96**(6): p. 3239-44.
14. Omkumar, R.V., et al., *Identification of a phosphorylation site for calcium/calmodulin-dependent protein kinase II in the NR2B subunit of the N-methyl-D-aspartate receptor.* J. Biol. Chem., 1996. **271**: p. 31670-31678.
15. Wenthold, R.J., et al., *Trafficking of NMDA receptors.* Annu Rev Pharmacol Toxicol, 2003. **43**: p. 335-58.

16. Kornau, H.-C., et al., *Domain interaction between NMDA receptor subunits and the postsynaptic density protein PSD-95.* Science, 1995. **269**: p. 1737-1740.
17. Kornau, H.-C., P.H. Seeburg, and M.B. Kennedy, *Interaction of ion channels and receptors with PDZ domain proteins.* Curr. Opin. Neurobiol., 1997. **7**: p. 368-373.
18. Sprengel, R., et al., *Importance of the intracellular domain of NR2 subunits for NMDA receptor function in vivo.* Cell, 1998. **92**(2): p. 279-89.
19. Abe, M., et al., *NMDA receptor GluRepsilon/NR2 subunits are essential for postsynaptic localization and protein stability of GluRzeta1/NR1 subunit.* J Neurosci, 2004. **24**(33): p. 7292-304.
20. Steigerwald, F., et al., *C-Terminal truncation of NR2A subunits impairs synaptic but not extrasynaptic localization of NMDA receptors.* J Neurosci, 2000. **20**(12): p. 4573-81.
21. Mori, H., et al., *Role of the carboxy-terminal region of the GluR epsilon2 subunit in synaptic localization of the NMDA receptor channel.* Neuron, 1998. **21**(3): p. 571-80.
22. Kutsuwada, T., et al., *Impairment of suckling response, trigeminal neuronal pattern formation, and hippocampal LTD in NMDA receptor epsilon 2 subunit mutant mice.* Neuron, 1996. **16**(2): p. 333-44.
23. Forrest, D., et al., *Targeted disruption of NMDA receptor 1 gene abolishes NMDA response and results in neonatal death.* Neuron, 1994. **13**(2): p. 325-38.
24. Li, Y., et al., *Whisker-related neuronal patterns fail to develop in the trigeminal brainstem nuclei of NMDAR1 knockout mice.* Cell, 1994. **76**(3): p. 427-37.
25. Walikonis, R.S., et al., *Densin-180 forms a ternary complex with the α-subunit of CaMKII and α-actinin.* J. Neurosci., 2001. **21**: p. 423-433.
26. Fukaya, M., et al., *Retention of NMDA receptor NR2 subunits in the lumen of endoplasmic reticulum in targeted NR1 knockout mice.* Proc Natl Acad Sci U S A, 2003. **100**(8): p. 4855-60.

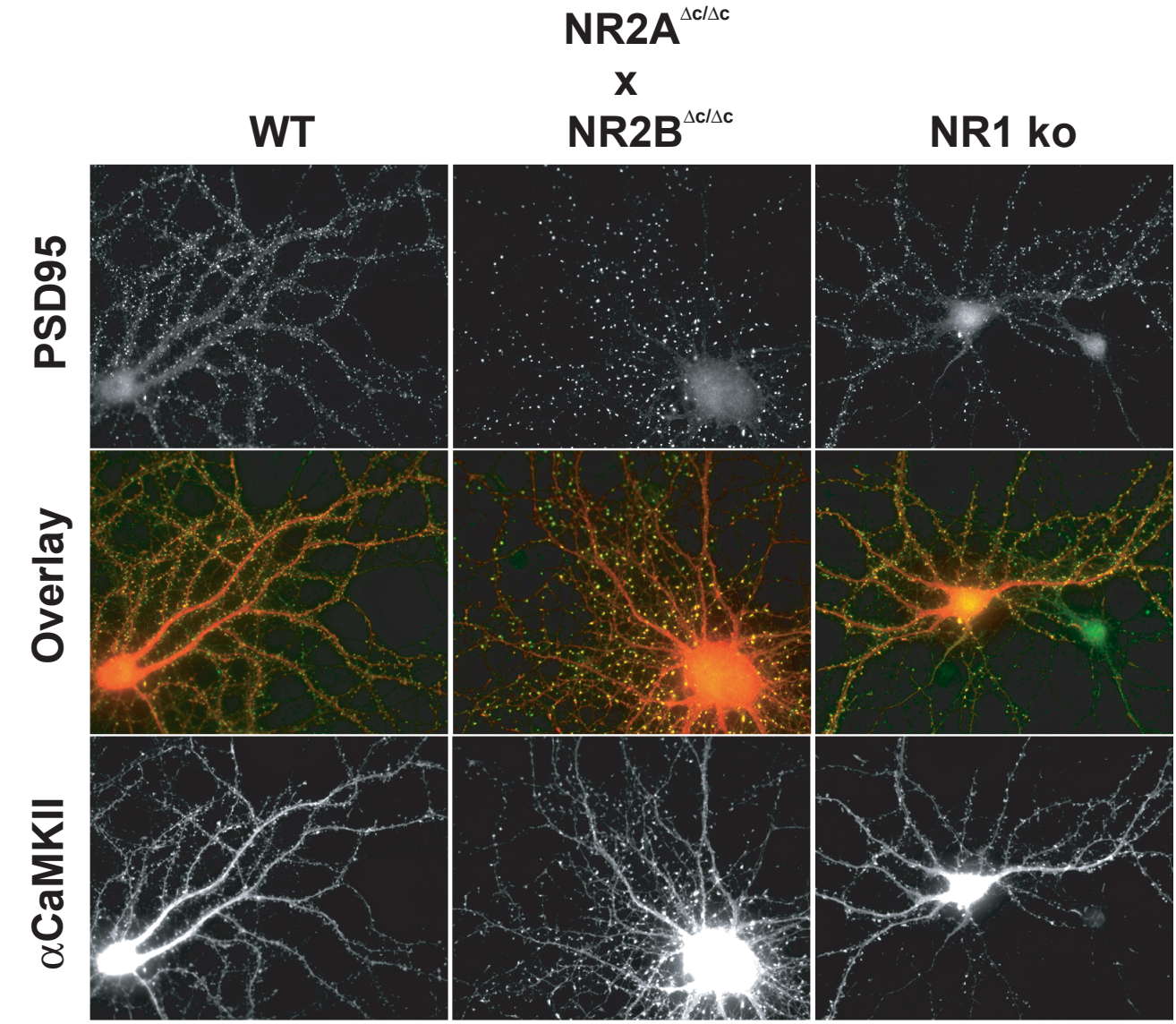

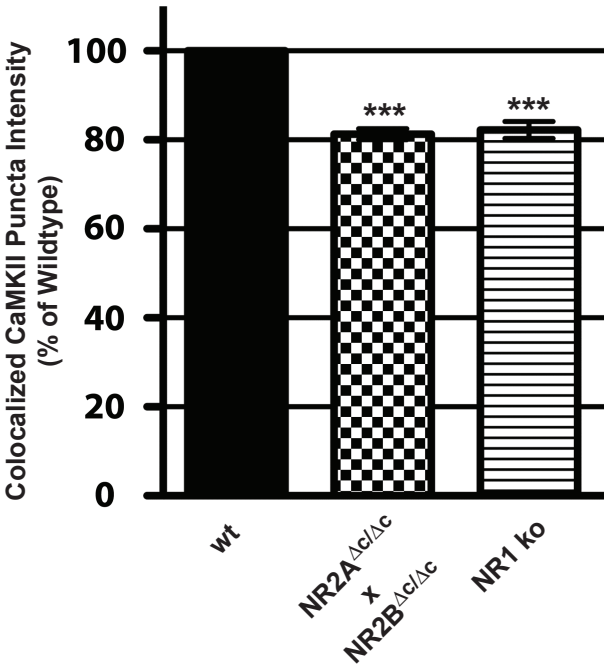

Figure 4.1 Loss of the NMDA receptor results in a decrease of CaMKII co-localizing with PSD95 at the tips of spines. Representative images are from 18 DIC primary hippocampal cultures co-stained for αCaMKII and PSD-95. CaMKII puncta colocalizing with PSD-95 in NR2A$^{\Delta c/\Delta c}$ x NR2B$^{\Delta c/\Delta c}$ mutant cultures decrease by -18.7% +/- 1.2 ($p<0.0001$). CaMKII puncta colocalizing with PSD-95 in NR1$^{-/-}$ knockout cultures decrease by -17.7% +/- 1.9 ($p<0.0001$).

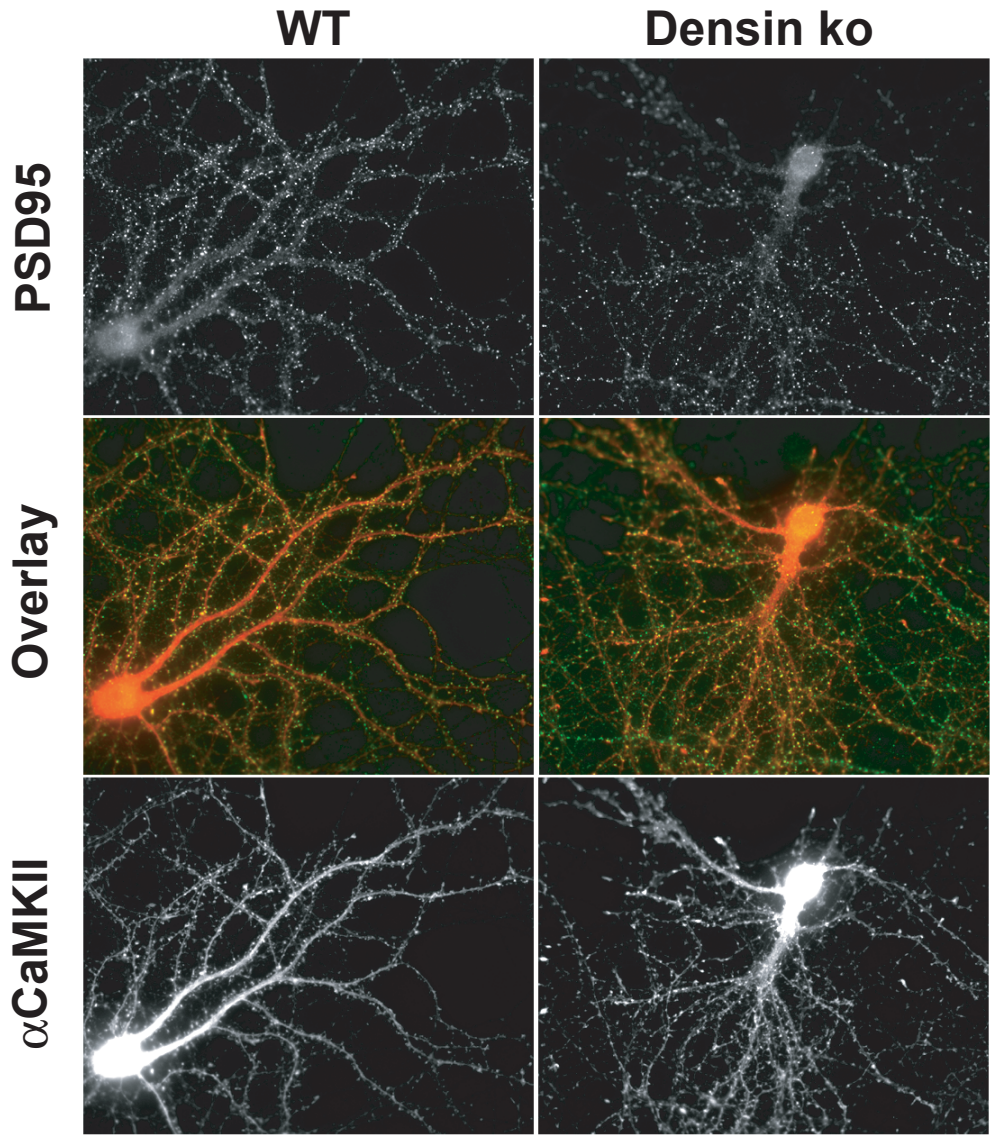

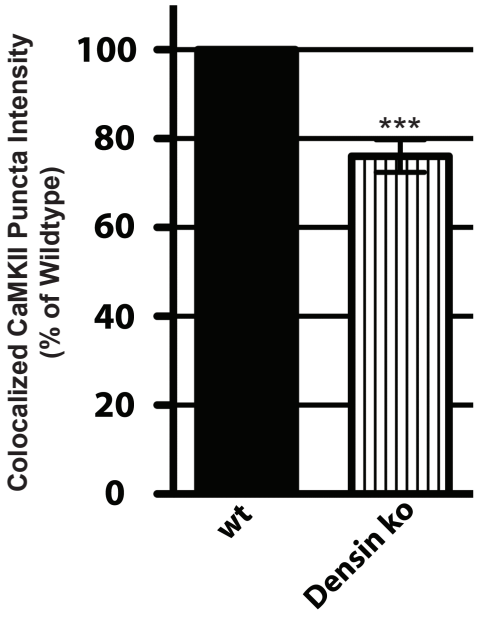

Figure 4.2 Loss of Densin results in a decrease of CaMKII (red channel) colocalizing with PSD95 (green channel) at the tips of spines in 18 DIC primary hippocampal cultures (-23.9% +/- 3.7; $p<0.0005$).

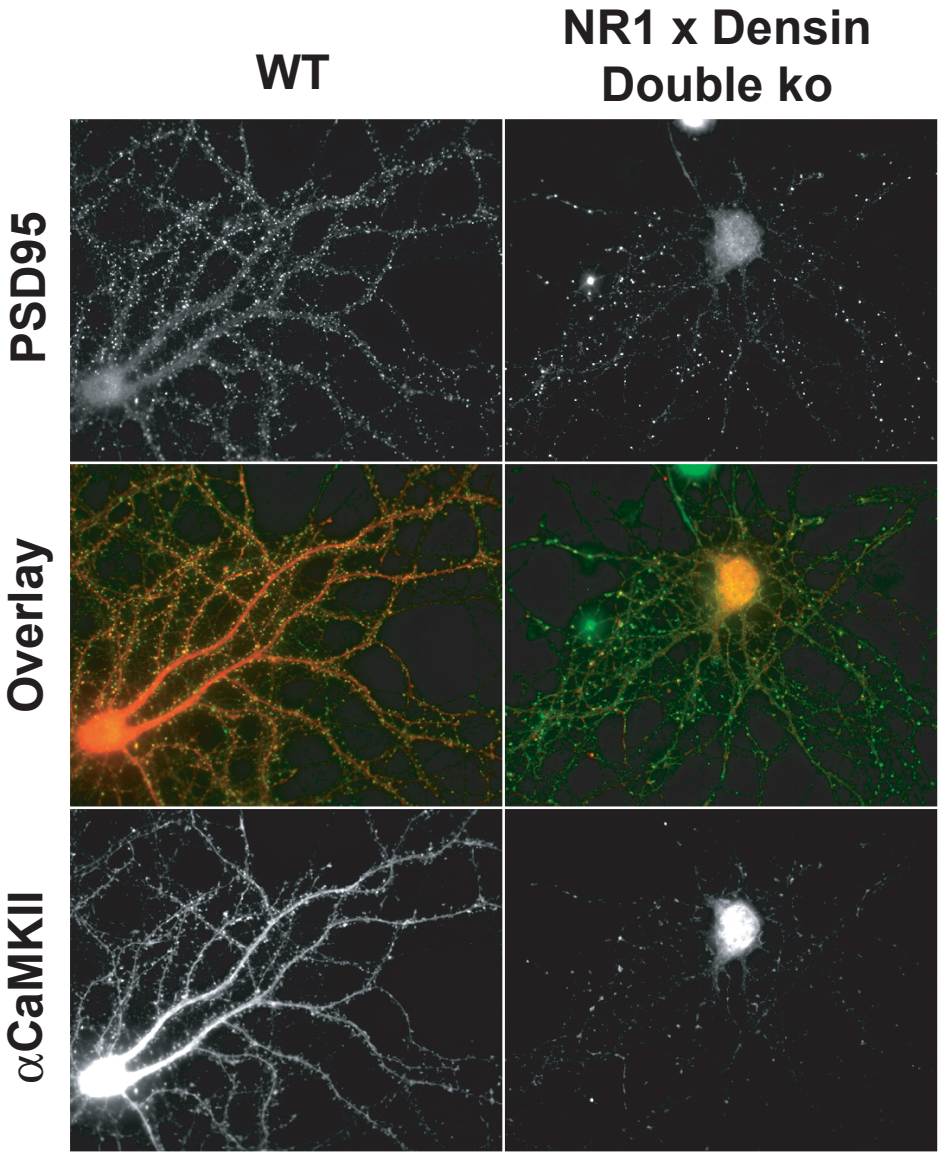

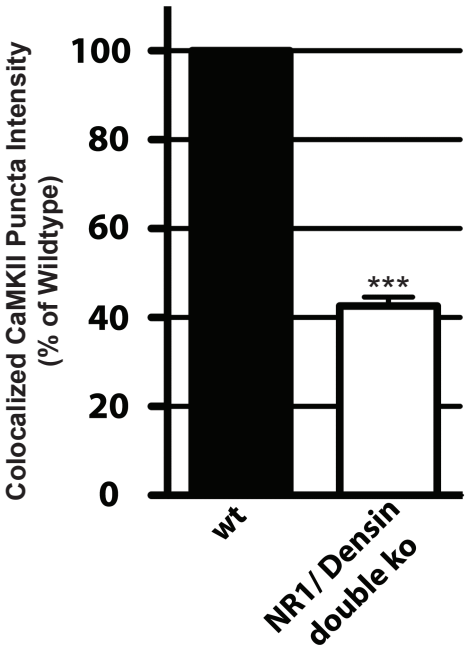

Figure 4.3 Loss of both Densin and NR1 results in a synergisitc decrease in CaMKII puncta intensity. The intensity of CaMKII punta colocalizing with PSD-95 shows a -57.1% +/- 1.16 ($p<0.0001$) decrease relative to wild type cultures.

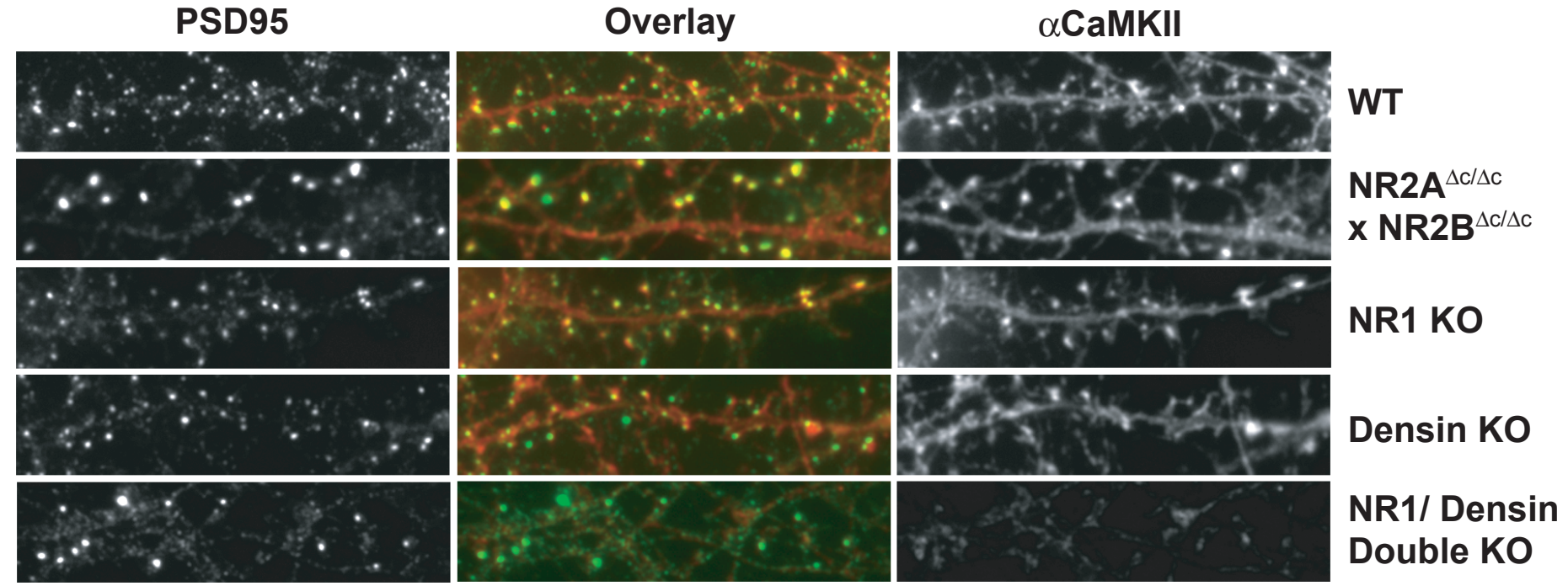

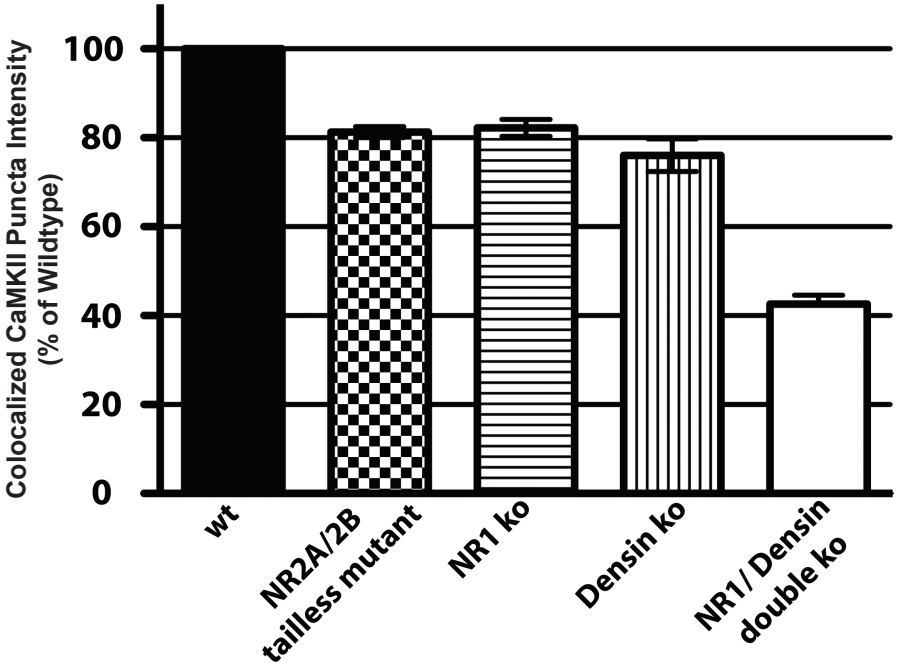

Figure 4.4 Representative images of dendritic branches from Figures 4.1, 4.2, and 4.3. The images shown here represent primary hippocampal cultures made from sibling embryos from a single pregnant female. NR2A$^{\Delta c/\Delta c}$ x NR2B$^{\Delta c/\Delta c}$ cultures were compared to their own wild type litter mates.

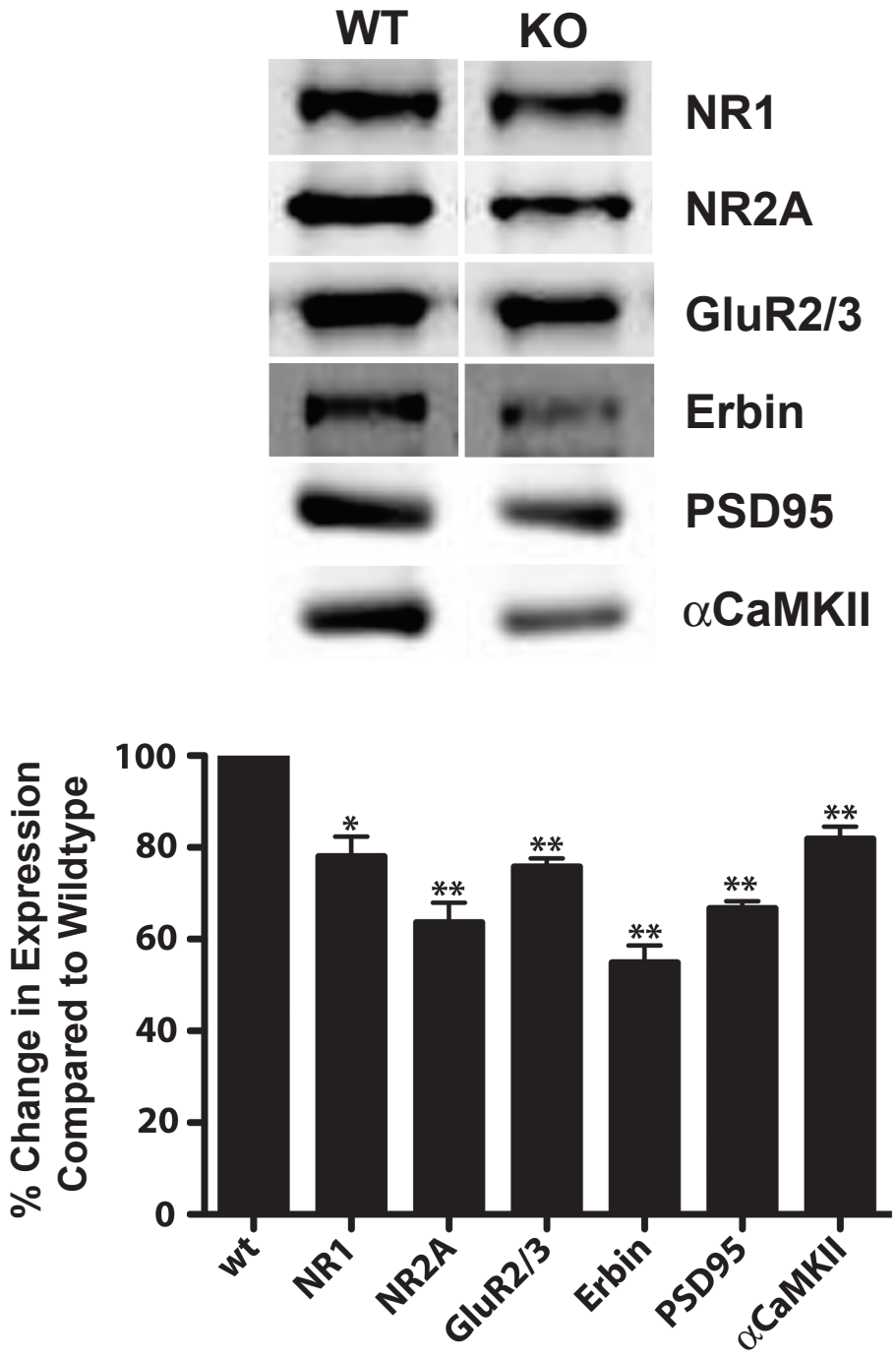

Figure 4.5 Loss of Densin results in an altered composition of the postsynaptic density complex. Quantitative immunoblotting of forebrain homogenates was performed to determine the change in the expression of core PSD proteins. Representative blots are shown for core PSD proteins with statistically significant changes. Not shown are immunoblots for proteins that showed no difference (α-Actinin, NR2B, SynGAP, PSD-93, δ-Catenin, Citron, β-Catenin, and GluR1). No protein assayed exhibited an increase in expression level. * $p<0.05$; ** $p<0.01$

Chapter 5: Global Analysis of the Effect of Densin Knockout on Gene Transcription in the Brain

Introduction

High throughput methods for analyzing transcriptional changes in response to deletion or mutation of a gene has provided modern biologists with a powerful tool for identifying candidate genes involved in observed phenotypes. Methods such as sequencing of expressed sequence tags (ESTs), microarray analysis, whole-genome tiling arrays, and other high throughput platforms have provided a wealth of insight into many biological processes. However, they have not been without limitations, chief among them are a need for prior knowledge of the sequences being investigated, poor discrimination of highly similar sequences, poor reproducibility of results across laboratories and platforms, and the semi-quantitative nature of the signals, especially of low abundance species [1, 2]. RNA-seq, a new, ultra-high throughput sequencing method for quantifying and annotating transcriptomes aims to alleviate many of these technical limitations. However, one major limitation still exists, we don't know how best to analyze these large datasets to distill biologically relevant information that can inform future experimentation.

In this chapter I present some preliminary findings from the first application of RNA seq technology to characterize changes in gene transcription from a gene knockout mutation.

Material and Methods

5.1 Construction of forebrain and hippocampal RNA seq libraries

The generation of forebrain and hippocampal RNA seq libraries was previously described (Chapter 2.6)

5.2 Analysis of RNA seq data sets

A simple analysis scheme was used to identify the transcripts that differed between brains of wild type and Densin knockout mice. Analysis was based on the RPKM counts generated from the "unique read" output. Only transcripts in which one of the RPKM values was >1 was considered. The percent difference in RPKM counts was calculated for all transcripts of a wt:ko sibling pair. For further analysis, the direction of change (increase or decrease) had to be the same for both sets of sibling pairs.

The top 150 transcripts were then compared between the forebrain and hippocampus. Transcripts that were on both lists were further analyzed.

Gene ontology information was obtained by submitting my list of most affected transcripts to the web-based Ingenuity Pathway Analysis (IPA) bioinformatics software program (Ingenuity Systems, Redwood City, CA). I then identified the transcripts that seemed most relevant to the phenotypes observed in the Densin knockout mouse.

Results

5.3 The Densin knockout animal does not exhibit gross changes in transcriptional activity

The RPKM counts were compared for each transcript to determine if there was any global changes in transcription. The degree of relationship between the wild type and knockout sibling pairs was determined by calculating the correlation value (Fig 5.1). Wild type and knockout forebrain transcript levels are highly correlated and significant; r^2 values of 0.9963 (pair 1; Fig 5.1a) and 0.9928 (pair 2; data not shown); $p<0.0001$ for both pairs. Hippocampal transcript levels are also highly correlated between the wild type and knockout; r^2 values of 0.9727 (pair 1; Fig 5.1b) and 0.9963 (pair 2), $p<0.0001$ for both pairs. This means that most transcript levels do not change between the wild type and knockout animals. Such a high correlation suggest that the loss of Densin does not result in large scale changes in transcriptional activity.

5.4 Transcription levels do not change for PSD proteins with decreased levels of protein in the knockout

Relatively small changes in the forebrain were detected for all six of the PSD proteins whose protein levels were significantly decreased in the forebrain of knockout mice (Fig 5.2). In the hippocampus, of these six proteins only the transcript level for Erbin showed a large change, +22.6%. These results suggest that the decrease in protein levels are not due to changes in gene transcription.

5.5 Immediate early gene transcripts show large changes in the Densin knockout mice

The transcript levels of eight immediate early genes (Arc, Egr1-4, Fos, Fos-b, and Junb) are decreased in the forebrain (Fig 5.3). Interestingly, seven of these transcripts show a concomitant increase in the hippocampus. Four of these IEGs (Egr1/ zif268, Egr2, Egr3, and Arc) have symmetrically changed transcript levels.

Transcript	% Change Forebrain	% Change Hippocampus
Egr1/ Zif268	-25.68103818	24.57384221
Egr2	-53.74	52.59259259
Npas4	-46.10	7.581967213
Fos	-41.25	18.49529781
Junb	-35.39	61.3592233
Egr4	-34.08	47.10312862
Fosb	-29.38	38.53727145
Egr3	-27.27	26.63920357
Arc	-46.55	47.56240576

Such results suggest that Densin may play a different mechanistic role in the hippocampus compared to the forebrain.

5.6 Comparison of transcript levels of PSD protein genes in the forebrain and hippocampus

76 transcripts were analyzed for their relative enrichment in the hippocampus verses the forebrain of wild type animals (Table 5.1). Enrichment was defined as a two-fold (100%) or more increase in hippocampal expression compared to the forebrain. A similar table was generated for changes in the relative enrichment of transcripts in the

hippocampus of Densin knockout mice. Transcripts were manually grouped into functional families based on published reports.

In wild type mice, transcripts for Pak6 and Ras-GRF 2 are highly enriched in the hippocampus, exhibiting an enrichment of +476% and +671% of forebrain levels, respectively. The transcript of Pak3, another cytoskeletal remodeling protein, is also enriched in the hippocampus. Transcripts for glutamate receptor subunits NR2A, NR2B, GluR1 and GluR2, and the high voltage-dependent R-type α1E Ca^{2+} channel are also enriched in the hippocampus relative to the forebrain. Finally, Maguin-1, an adaptor protein that links Densin to PSD-95, and likely to the NMDA receptor complex, shows a marked hippocampal enrichment (+129%). Transcripts enriched in the forebrain relative to the hippocampus are Rac3, PKCδ, Hras1, LIM Kinase 1, and the inward rectifying K^+ channel Kcnj4.

One interesting find concerns the transcript levels of GKAP. GKAP is a major adaptor protein linking the PSD-95/ NMDA receptor complex to the Shank sub-matrix. In the wild type animal GKAP is not expressed in the hippocampus. This result is supported by in situ hybridization reported in the Allen Brain Map (Fig 5.4). Interestingly, the GKAP transcript is turned on in the hippocampus of the knockout animal.

5.7 Candidate genes for the seizure phenotype

Npas4 and Gabra2 (GABA-A α2) show two of the largest absolute changes in the forebrain (Fig 5.5); neither exhibit large changes in the hippocampus (Npas4, +7.6%, GABA(A) α2). In the forebrain, Npas4 decreases by 46%, while $GABA_A$ α2 increases

by 80.8%. These are appealing candidate transcripts for the seizure phenotype because $GABA_A$ α2 is one of four $GABA_A$ receptor subunits that can mediate the action of benzodiazepine drugs [3, 4], and Npas4 directly regulates the development of inhibitory synapses [5].

References

1. Wang, Z., M. Gerstein, and M. Snyder, *RNA-Seq: a revolutionary tool for transcriptomics.* Nat Rev Genet, 2009. **10**(1): p. 57-63.
2. Shendure, J., *The beginning of the end for microarrays?* Nat Methods, 2008. **5**(7): p. 585-7.
3. Rudolph, U., et al., *Benzodiazepine actions mediated by specific gamma-aminobutyric acid(A) receptor subtypes.* Nature, 1999. **401**(6755): p. 796-800.
4. Low, K., et al., *Molecular and neuronal substrate for the selective attenuation of anxiety.* Science, 2000. **290**(5489): p. 131-4.
5. Lin, Y., et al., *Activity-dependent regulation of inhibitory synapse development by Npas4.* Nature, 2008. **455**(7217): p. 1198-204.

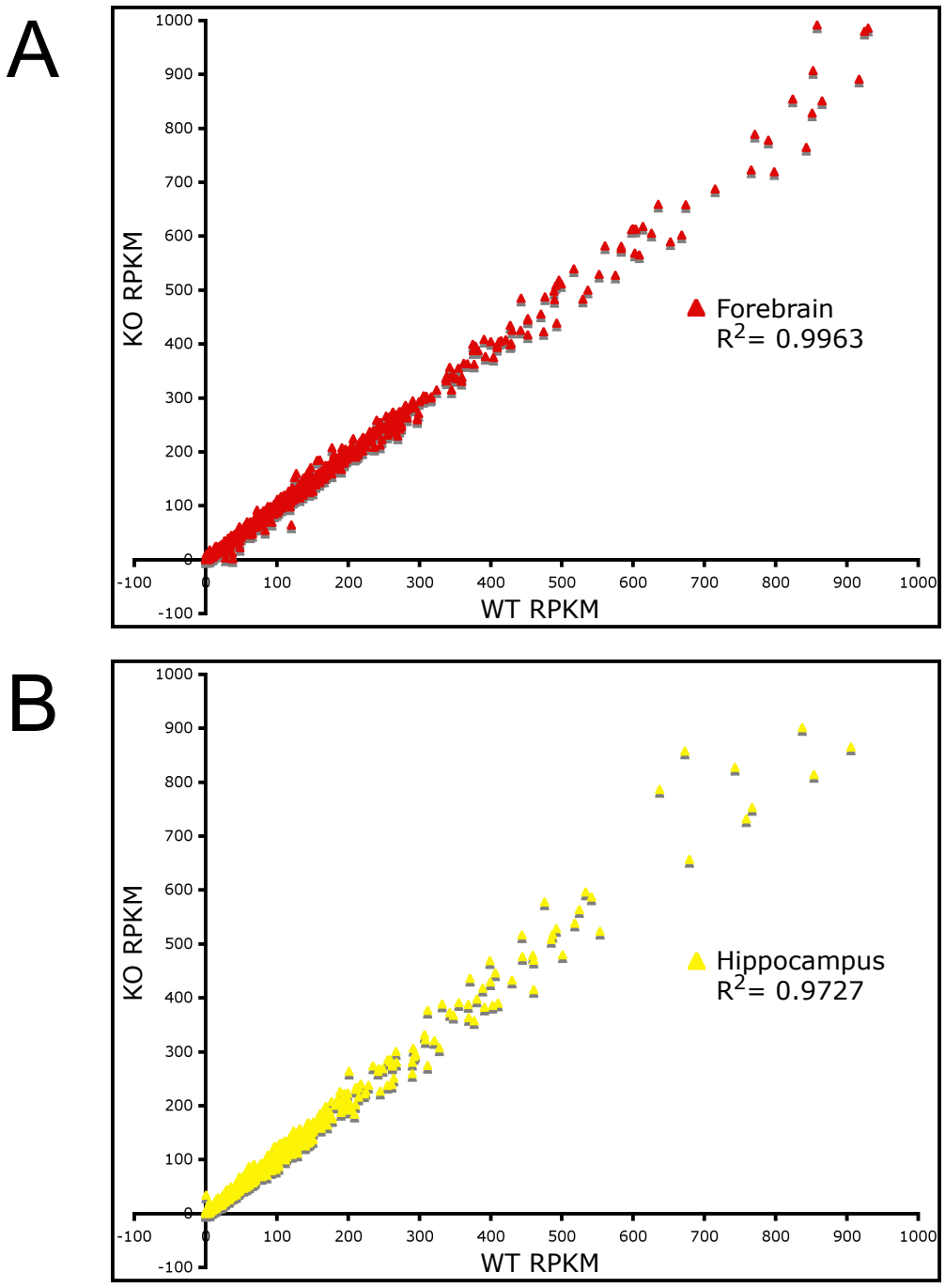

Figure 5.1 Comparison of wild type and ko transcriptional activity (as measured in reads per kilobase of exon per million mapped reads; RPKM) demonstrates that the loss of Densin does not result in gross changes in gene expression in either the forebrain or hippocampus. (A) Comparison of RPKM values from RNA seq libraries generated from sibling pair wt and ko animal forebrain tissue (red) demonstrate a positive linear correlation (R^2= 0.9963, p<0.0001). (B) Comparison of RPKM values from RNA seq libraries generated from sibling pair wt and ko animal hippocampal tissue (yellow) demonstrate a positive linear correlation (R^2= 0.9727, p<0.0001). Intra-genotype comparisons (wt vs. wt or ko vs. ko) of forebrain or hippocampus tissue RNA seq libraries (R^2 >0.97, p<0.0001 for all libraries compared; data not shown) demonstrates reproducibility, linearity, and sensitivity of the RNA seq method.

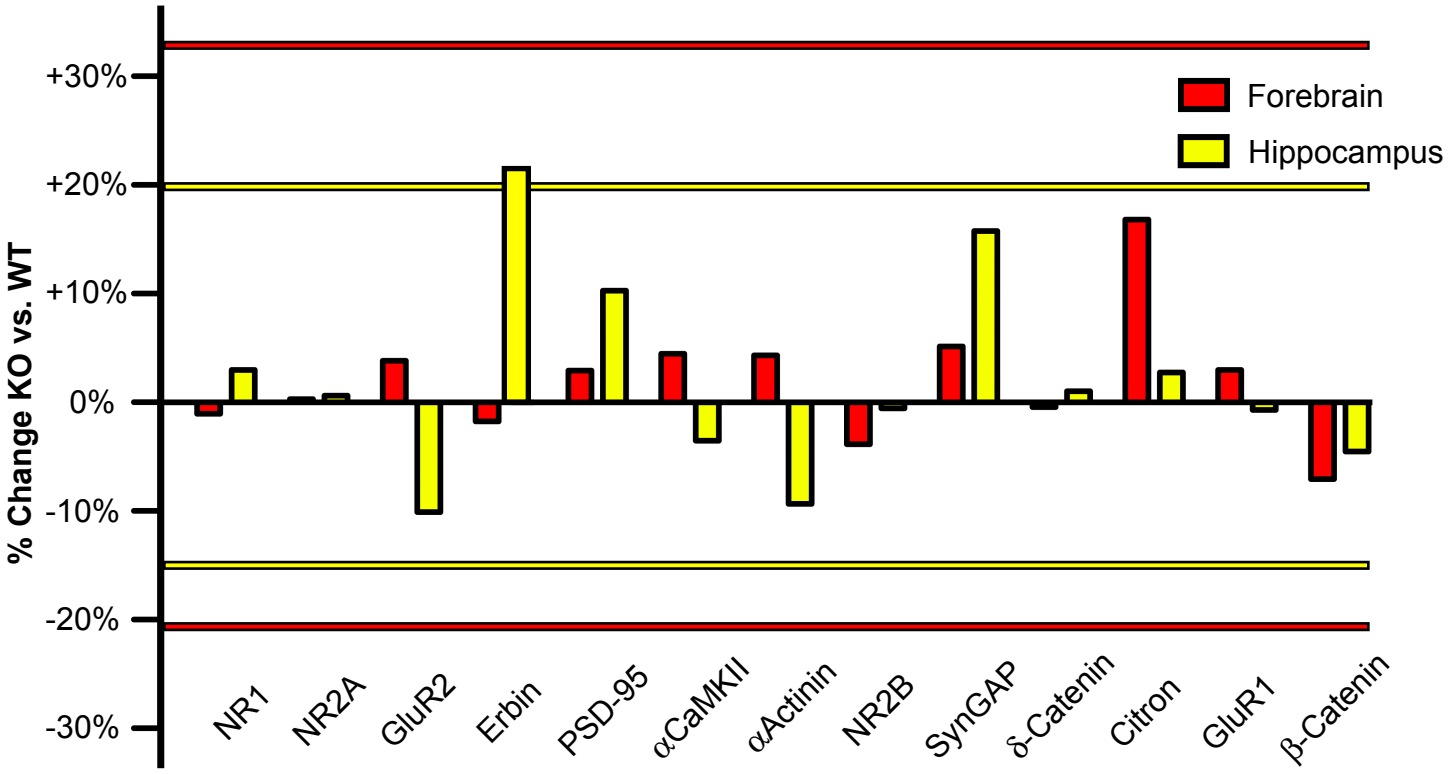

Figure 5.2 Decreased changes in gene transcription are not the likely cause of the decreased protein expression levels observed for the PSD proteins studied by immunoblot (Fig 4.5). Relatively small changes in the ko animal forebrain or hippocampus are observed for transcript levels of the PSD proteins studies by quantitative immunoblots. Erbin is the only PSD transcript that shows a relatively large increase in its level of expression (+22.6%). Bars represent average percent change between wild type and knockout RPKM values (red, forebrain; yellow, hippocampus) . Yellow horizontal lines represent the 5% (-16.97%) and 95% (19.72%) percentile ranges for changes in the hippocampal. Red horizontal lines represent the 5% (-21.56%) and 95% (32.42%) percentile ranges for changes in the forebrain.

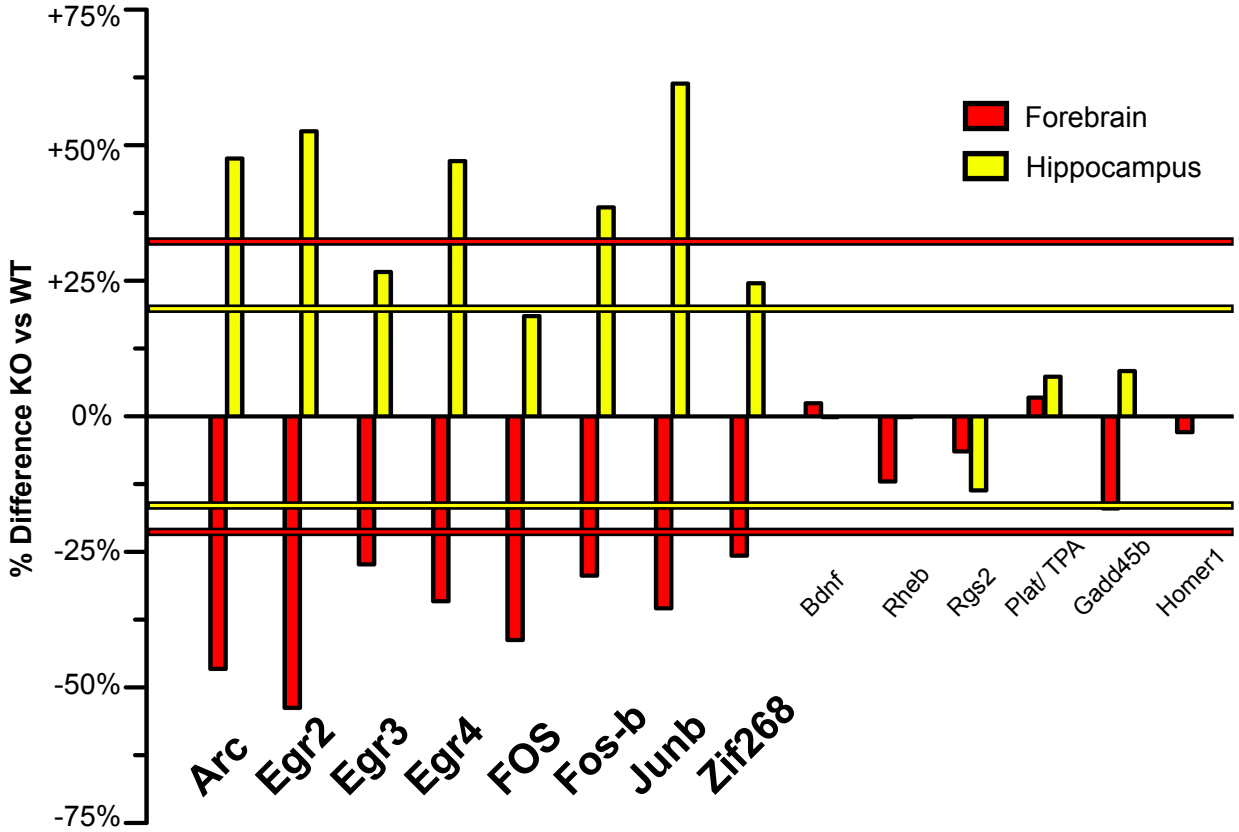

Figure 5.3 A subset of Immediate Early Gene (IEG) transcripts (large, bold text) show altered expression levels in both the forebrain and the hippocampus of Densin knockout mice. Expression of Arc, Egr1-4 (Egr1 = Zif268), Fos, Fos-b, and Junb decrease in the forebrain (red). Expression of Arc, Egr1-4, Fos-b and Junb increase in the hippocampus (yellow). Half of the IEGs show highly similar symmetric changes in opposite directions (Arc, -46.5% fb, +47.5% hip; Egr3, -27.3% fb, +26.6% hip; Egr2, -53.7% fb, +52.6% hip; Zif268, -25.7% fb, +24.6% hip). IEGs in small type are shown as a comparison. Bars represent average percent change between wild type and knockout RPKM values (red, forebrain; yellow, hippocampus) . Yellow horizontal lines represent the 5% (-16.97%) and 95% (19.72%) percentile ranges for changes in the hippocampal. Red horizontal lines represent the 5% (-21.56%) and 95% (32.42%) percentile ranges for changes in the forebrain.

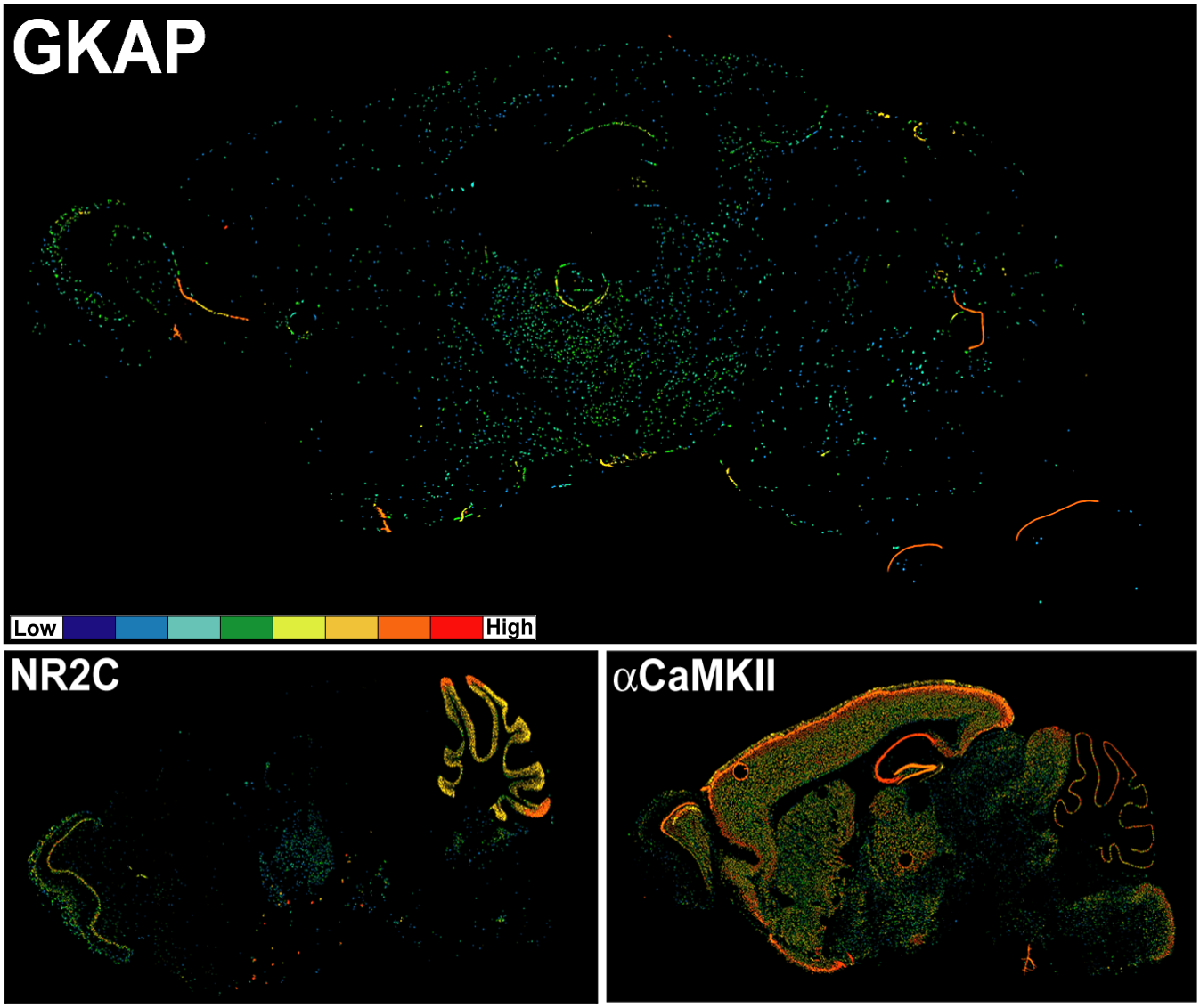

Figure 5.4 In situ hybridization heat maps of GKAP, NR2C and αCaMKII at saggital level 12-13 are shown. GKAP gene expression is low in all regions of the brain and is shown in comparison to NR2C (low gene expression in forebrain) and αCaMKII (high gene expression in forebrain). GKAP expression results are supported by RNA seq analysis which shows low expression in the forebrain and no expression in the hippocampus. Heat map color scale indicates level of gene expression.

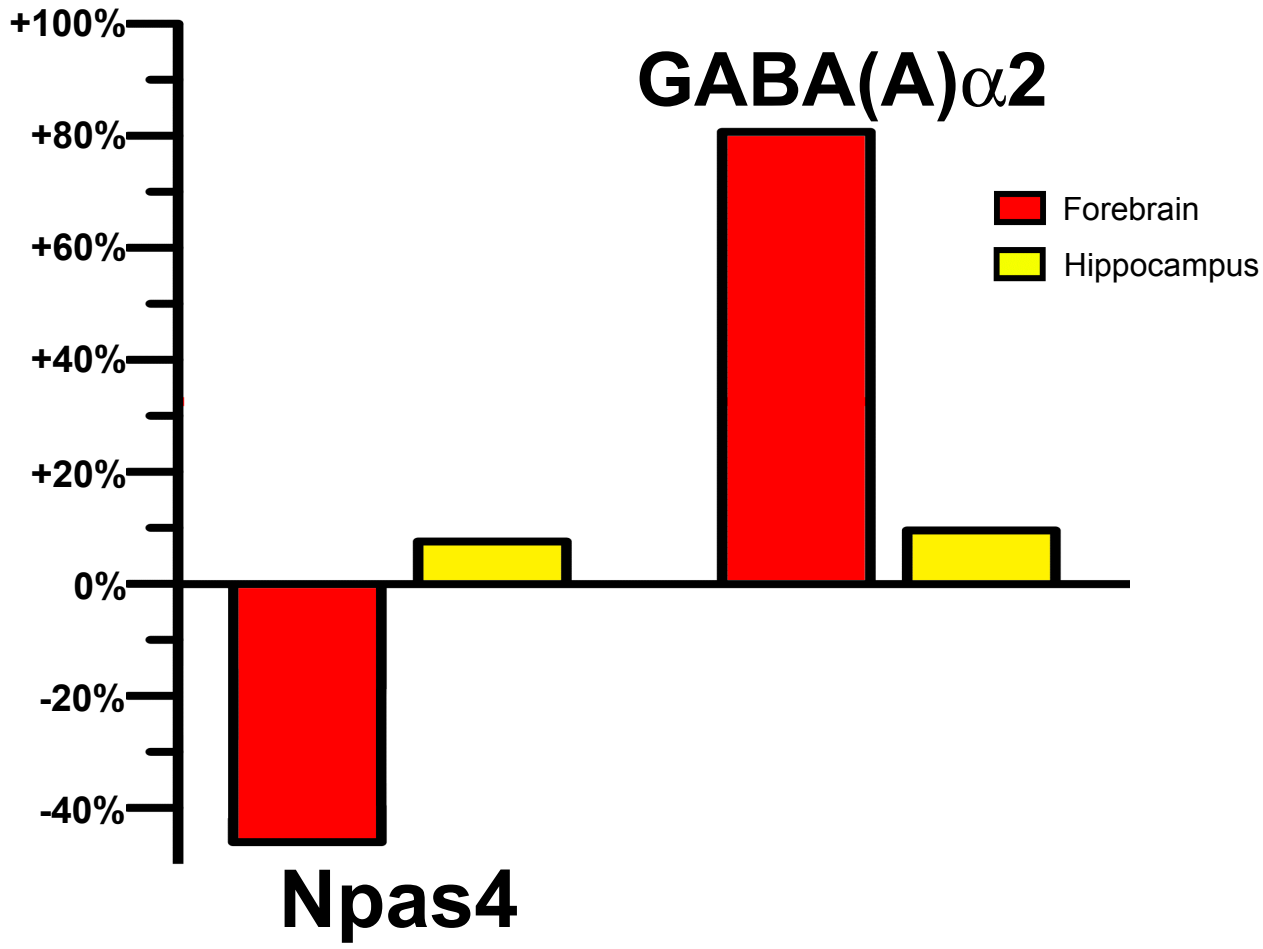

Figure 5.5 Npas4 and GABA(A)α2 are candidate genes whose expression could influence the seizure phenotype. Forebrain expression (red bars) of Npas4 and the GABA(A)α2 subunit are significantly altered in the Densin knockout mouse. The Npas4 transcript decreases by 46.1% and the GABA(A)α2 transcript increases by 80.8%. Neither exhibit large changes in the hippocampus (yellow bars; Npas4, +7.6%; GABA(A)α2, +9.5%).

	Wild type			Knockout		
	Forebrain (RPKM)	Hipp. (RPKM)	% Change (Hipp./ Forebrain)	Forebrain (RPKM)	Hipp. (RPKM)	% Change (Hipp./ Forebrain)
Glutamate Receptors						
NR1	162	125	-23%	161	129	-20%
NR2A	3	9	169%	3	9	170%
NR2B	7	13	104%	6	13	111%
NR2C	14	10	-30%	14	10	-26%
NR2D	7	4	-42%	7	5	-36%
GluR1	70	178	153%	72	177	144%
GluR2	45	94	110%	47	85	82%
GluR3	24	41	0%	24	37	0%
GluR4	15	11	-24%	17	10	-39%
Stargazin	21	18	-14%	21	21	2%
mGluR1	13	12	-10%	13	12	-12%
mGluR2	23	22	-7%	28	24	-15%
mGluR3	19	13	-32%	20	11	-46%
mGluR4	14	5	-61%	15	5	-67%
mGluR5	19	30	57%	20	28	39%
mGluR7	13	13	4%	13	14	3%
Scaffold Proteins						
Shank-1	35	64	81%	37	73	101%
Shank-2	15	24	53%	15	26	69%
Shank-3	39	34	-13%	39	36	-6%
Homer1	15	15	1%	15	15	6%
Homer2	9	13	42%	9	13	53%
GKAP	4	0	-91%	4	5	20%
GRIP-1	4	4	5%	5	5	3%
SAP-97	26	22	-14%	24	20	-17%
SAP-102	38	45	17%	37	42	13%
Chapsyn-110	46	41	0%	47	43	0%
PSD95	262	212	-19%	270	234	-13%
Gephyrin	23	19	0%	23	18	0%
Maguin-1	20	45	129%	23	42	83%
Signalling						
Calmodulin 1	790	679	-14%	778	657	-16%
Calmodulin 2	553	411	-26%	529	390	-26%
Calmodulin 3	1087	743	-32%	1060	827	-22%
SynGAP	55	55	0%	58	64	10%
Rac1	78	73	-6%	76	72	-5%
Rac2	1	1	-17%	1	0	-39%
Rac3	23	11	-50%	23	13	-43%
Kinases/ Phosphatases						
αCaMKII	496	759	53%	518	732	41%
βCaMKII	258	293	14%	264	292	10%
δCaMKII	15	10	-38%	14	8	-44%
γCaMKII	69	48	-31%	68	47	-32%
PKCα	19	33	70%	22	34	58%
PKCβ	84	117	39%	90	111	24%
PKCδ	34	16	-53%	33	13	-61%
Citron	10	9	-5%	12	10	-16%
CDK5	49	34	-30%	49	37	-25%
Adhesion Proteins						
δ-catenin	42	37	-11%	41	37	-10%
β-catenin	182	149	-18%	169	142	-16%
N-Cadherin	18	19	7%	18	18	-1%

	Wild type			Knockout		
	Forebrain (RPKM)	Hipp. (RPKM)	% Change (Hipp./ Forebrain)	Forebrain (RPKM)	Hipp. (RPKM)	% Change (Hipp./ Forebrain)
Densin	7	10	53%	9	12	29%
Regulatory and Cytoskeletal Associated Proteins						
Kalirin	34	42	25%	38	44	15%
α-actinin	8	5	-45%	9	4	-52%
Cofillin-1	163	89	-45%	149	96	-36%
Cofilin-2	18	18	-1%	17	15	-12%
Hras1	197	90	-54%	195	105	-46%
N-ras	7	9	26%	7	9	30%
Pak1	147	100	-32%	141	102	-28%
Pak2	9	11	25%	9	12	30%
Pak3	7	17	126%	8	15	80%
Pak6	3	16	476%	3	18	537%
Ras-GRF 2	15	117	671%	14	111	685%
LIM Kinase 1	26	13	-51%	25	14	-43%
LIM Kinase 2	14	11	-21%	15	12	-21%
RhoV	6	3	-39%	7	4	-45%
Rap1, GAP1	92	45	-51%	97	50	-48%
γ-Actin	0	0	0%	0	0	0%
Drebrin	92	83	-9%	93	100	8%
Cortactin	27	30	10%	26	32	21%
Ion Channels						
Calcium Channels						
P/Q-type Ca Channel	19	19	2%	20	21	6%
Voltage-dependent N-type α1B	8	11	37%	9	11	26%
Voltage-dependent L-type α1C	7	9	37%	6	9	33%
Voltage-dependent L-type- α1D	4	5	22%	4	5	21%
Voltage-dependent R-type α1E	10	24	145%	10	23	131%
Voltage-dependent T-type α1G	12	8	-32%	13	8	-38%
Potassium Channels						
Inward Rectifying K+ Channel	89	32	-64%	95	33	-66%
Ca^{2+} activated K^+ Channel 3	3	2	-24%	3	2	-31%
Ca^{2+} activated K^+ Channel 4	0	0	0%	0	0	0%
Immediate Early Genes						
Homer1	15	15	0%	15	15	0%
Egr1/ Zif268	93	33	-64%	69	41	-40%
Bdnf	6	7	34%	6	7	30%
Rheb	58	45	-23%	51	45	-12%
Rgs2	32	17	-46%	30	15	-50%
Plat/ TPA	15	12	-17%	15	13	-13%
Ptgs2	3	5	38%	2	4	71%
Egr2	7	1	-90%	3	1	-67%
Npas4	11	2	-77%	6	3	-54%
Fos	33	5	-85%	19	6	-71%
Junb	84	18	-79%	54	29	-46%
Egr4	26	9	-66%	17	13	-25%
Fosb	8	4	-53%	5	5	-8%
Gadd45b	16	8	-49%	13	9	-34%
Egr3	48	29	-39%	35	37	5%

Chapter 6: Discussion and Conclusions

CaMKII and PSD-95 colocalization studies

The spatial and temporal localization of signaling molecules are crucial for the form and endurance of synaptic plasticity [1-3]. Though the postsynaptic density acts as an integrated macromolecular machine, the spatial and temporal dynamics of individual PSD proteins are integral to the nature and strength of a postsynaptic response to impinging signals. Ca^{2+}/ calmodulin-dependent protein kinase II (CaMKII) is a major component of the PSD and is a crucial regulator of neuronal and behavioral plasticity [4-8]. Ca^{2+} signaling at the postsynaptic membrane occurs upon stimulation of the NMDA receptor and the subsequent activation of CaMKII. Consequently, the location of CaMKII relative to activated NMDA receptors is crucial to its subsequent signal transduction.

Numerous proteins of the PSD are known to bind and interact with CaMKII [9]. However, strategic interactions that specifically position CaMKII for optimal activation by Ca^{2+} influx and the subsequent phosphorylation of proteins important for LTP are particularly crucial. The binding of CaMKII with NR2A and NR2B subunits of the NMDA receptor is one such strategic interaction [1, 10-13]. We have hypothesized that Densin is another [14, 15].

Both the NR1 and NR2 subunits are required to form functional NMDA receptors at the synapse [16-18]. Deletion of synaptic NMDA receptors can thus be achieved by deletion of the c-terminal tails of the NR2 subunits [19, 20] or by deletion of the NR1 subunit [21]. I have shown that in NR2A x NR2B double tailless mutant animals,

CaMKII colocalization with PSD-95 is significantly reduced. Similarly, in NR1 knockout mice, CaMKII colocalization with PSD-95 decreases by the same amount. The loss of CaMKII colocalization with PSD-95 in both the NR1 and NR2A/ NR2B double tailless mice supports the notion that these genetic mutations are functionally equivalent with respect to their effect on localization of the NMDA receptors to synapses. Moreover, these studies support the role of the NMDA receptor as a PSD docking site for CaMKII.

I next investigated the localization of CaMKII at the tips of spines in Densin knockout mice. In the absence of Densin, CaMKII colocalization with PSD-95 is significantly decreased, supporting our hypothesis that Densin can act as a docking site for CaMKII at the PSD. Interestingly, the loss of CaMKII colocalization with PSD-95 in Densin knockout animals was equivalent to the loss of CaMKII colocalization with PSD-95 in both the NR2 double tailless and NR1 knockout mice. These results suggest that Densin and the NMDA receptor dock an equivalent sized pool of CaMKII in the PSD.

Finally, we investigated the effects of removing both the NMDA receptor and Densin on the localization of CaMKII. This was achieved by crossing mice heterozygous for both Densin and NR1. Our results showed a 60% decrease in the colocalization of CaMKII with PSD-95. Single knockouts of either Densin or NR1 resulted in only 23.9% and 18.7% decreases in CaMKII colocalization with PSD-95. The loss of ~60% CaMKII colocalization with PSD-95 suggests that the loss of both Densin and the NMDA receptor results in a synergistic decrease of CaMKII colocalization with PSD-95. A caveat to this interpretation is the fact that the levels of CaMKII is globally decreased in our primary hippocampal cultures. Consequently, the loss of CaMKII colocalization with PSD-95

may simply reflect the decrease in global CaMKII levels. Further investigation will be required to more fully interpret these observations.

A "compensatory" hypothesis would predict that in the Densin knockout mouse, more CaMKII would be bound to the tails of the NMDA receptor. I would propose testing this hypothesis by stimulating synaptic NMDA receptors in hippocampal slices from Densin knockout mice with bicuculline. If my hypothesis is correct, I should be able to detect an increase in CaMKII autophosphorylation and in phosphorylation of the NMDA receptor compared to wildtype. Such a result would provide support for a "compensatory" hypothesis.

I have shown that in the absence of the NMDA receptor, CaMKII can still be docked in the PSD. Previous work by Shen and co-workers [2, 22] has shown that CaMKII dynamically translocates upon synaptic stimulation with NMDA. Given that both the NMDA receptor and Densin can bind inactive CaMKII and that autophosphorylation of CaMKII increases its interaction with both proteins [14, 15], understanding the biological significance of this differential localization should be an exciting future line of investigation.

Quantitative Immunoblot Studies

Results from my quantitative immunoblot studies show that PSD-95, the NR1 and NR2A subunits of the NMDA receptor, Erbin and αCaMKII are all significantly decreased in the forebrain of knockout mice. I hypothesized that these decreases were the result of: 1) a decrease in gene transcription, 2) a decrease in the translation of these particular proteins, and/ or 3) an increase in their degradation. I investigated the first

hypothesis in collaboration with Barbara Wold's lab by utilizing RNA seq- a new, high-throughput sequencing method that allowed me to analyze transcriptional changes in all genes expressed in the forebrain and hippocampus in knockout mice [23].

Transcript levels for PSD-95, NR1, NR2A, Erbin, and αCaMKII did not decrease in a manner concomitant with the observed changes in their protein levels. Consequently, the decrease in protein levels may be due to changes in protein translation or protein degradation. It is possible that Densin selectively interacts with PSD-95 complexes that contain a specific composition of proteins, including NR1, NR2A, Erbin, and CaMKII. If this is the case, then the loss of Densin may result in the destabilization of these particular complexes, and potentially an increase in protein degradation.

Changes in Spine Density and Morphology

Changes in spine density are most often associated with homeostatic mechanisms aimed at regulating global synaptic input [24-26]. Furthermore, spine shape is correlated with the relative strength and maturity of a synapse [27, 28]. For example mushroom spines have larger, more complex PSDs [28]. Thin spines are associated with structural flexibility and smaller PSDs [29, 30]. Finally, stubby spines have been hypothesized to be a type of intermediate step between filapodial outgrowths and mature spines [31]. However, the clearest correlation between a spine, its functional strength and its degree of maturity is the size of its head [27, 28, 32-34].

In our analysis of dendritic spines from the CA1 area of the hippocampus of Densin knockout mice, we found a statistically significant increase in spine density (+13%) and a statistically significant decrease in spine volume (-11%); a trend towards

an increase in spine length (+4%) was observed, but not statistically significant. The increase in spine density along with a concomitant decrease in the size of the spine heads suggest that the loss of Densin likely affects synaptic input. However, the phenotypic changes observed may also suggest that the loss of Densin results in a stunted ability to form fully mature spines. Finally, as discussed later, the Densin knockout mice exhibited seizures when they were anesthetized with Nembutal and exhibited seizures. Given that seizures are known to affect spine dynamics and morphology, our results may be confounded by the seizures that these animals had prior to their perfusion . Additional work will be required to better understand the source of the observed spine phenotypes.

Dendritic Arborization

In culture, Densin knockout neurons exhibit broad and flattened dendritic trunks, and an overall decrease in the number of dendritic branches. These results are consistent with work demonstrating that Densin overexpression leads to an increase in dendritic branching [35]. Furthermore, results from my quantitative immunoblot studies shows that there is a significant decrease in the protein level of Erbin. Recent work by Reichardt and co-workers demonstrated that miRNA mediated knockdown of Erbin severely impairs dendritic morphogenesis [36]. They also showed that the loss of Erbin resulted in a mislocalization of δ-catenin.

δ-Catenin is part of a synaptic cell adhesion complex that includes N-cadherin [37]. Cadherin-catenin adhesion complexes have been shown to play important roles in synaptic plasticity, synaptogenesis and dendritic arborization [36, 38, 39]. Densin is known to directly bind δ-Catenin in the brain [40], a finding also observed in our lab

(Mary Kennedy, personal communication). δ-catenin is hypothesized to affect dendritic morphology through its regulation of the F-actin cytoskeleton via the Rho family of GTPases and cortactin activities [41]. Consequently, the mislocalization of δ-catenin results in aberrant dendritic structure through its regulation of the F-actin structure. The arborization changes seen in the Densin knockout mouse may thus be the direct result of a loss of δ-catenin localization or of the loss of Erbin.

RNA-Seq Analysis and Identification of Candidate Transcripts Potentially Involved in the Seizure Phenotype

An immediate early gene (IEG) is defined as a gene whose transcript expression is increased rapidly and transiently in a protein synthesis-independent manner in response to extracellular stimuli [42]. Numerous experimental paradigms have been used to induce the expression of IEG including serum stimulation of fibroblasts, maximal electroconvulsive seizures (MECS), LTP paradigms, behavioral experiences in novel environments, drug and hormone challenge [43-48]. IEG have been catergorized into two functional classes: 1) regulatory transcription factors (RTF) which control the transcription of downstream genes; and 2) effector IEGs, which directly influence cellular functions [46, 47]. Examples of RTFs whose transcript increase is response to neural activity in the forebrain are c-fos, c-jun, zif268/ Egr1, and examples of effectors are homer1a, Arc, Bdnf, and Cox-2. By virtue of their transcriptional regulatory activities, RTFs are well positioned to affect global changes in response to neuronal activation, while effector IEGs are likely to immediately impact neuron specific events. Lanahan

and Worley suggest that the IEG response in neurons is likely limited to 30-40 genes, of which perhaps 10-15 are transcription factors [47].

Our analysis of the effect of Densin knockout on transcription in forebrain and hippocampal tissue uncovered a striking effect on a subset of immediate early genes- Arc, Egr1/ zif268, Egr2-4, c-fos, fos-b, and junb. Specifically, in the forebrain we discovered that these eight transcripts were strongly decreased. Interestingly, this same group of eight transcripts showed a striking increase in their transcript levels in the hippocampus. Furthermore, seven of the eight IEGs affected are all classified as regulatory transcription factors; Arc is classified as an effector. It is not yet clear why these eight IEGs would be affected by the loss of Densin or why they would have such striking differences in their level of transcript expression between the forebrain and the hippocampus. Furthermore, why IEGs with the classification as RTF would be over-represented is also unclear. Continued investigations into the primary literature may unearth a particular type of IEG induction paradigm that may more readily induce RTF as opposed to effector IEGs. If such a paradigm has been found, it may give us insight into the particular mechanisms affected by Densin.

Recent work by Greenberg and co-workers (Lin *et. al,* 2008) showed that Npas4 is an activity-dependent transcription factor, and that levels of Npas4 determine the number of functional GABAergic synapses that are formed via the induction of a program of gene transcription. Given that neurological disorders such as schizophrenia and epilepsy are known to be associated with an imbalance between excitatory and inhibitory synapses (Mohler, 2006; Wassef et al., 2003), our results suggest that the decreased expression of the Npas4 transcripts may contribute to the seizure phenotype.

Though the sedative properties of Nembutal are mediated by the $GABA_A\alpha1$ subunit (Rudolph et al., 1999), the $GABA_A\alpha2$ transcript (which increases by 81% in the forebrain of knockout mice) can specifically bind Nembutal and is the primary subunit that mediates the anxiolytic action to barbiturates (Low et al., 2000). The other $GABA_A$ receptors that bind and mediate the action of benzodiazepines are the $\alpha3$ and $\alpha5$ subunits. Little to no change in forebrain or hippocampal gene expression is seen for the $\alpha1$ (+1.4% fb; -14% hip), $\alpha3$ (-2.8% fb; +9% hip) or $\alpha5$ (+13.4% fb; -0.99% hip) subunits. Given that Nembutal is a GABA agonist, it should be sedating; this obviously is not the case for the Densin knockout animal. One possibility for the induction of seizures upon Nembutal administration may lay in the network properties effected by tonic inhibition. Tonic inhibition occurs when extrasynaptic $GABA_A$ receptors are activated by ambient GABA, thus prolonging inhibitory post-synaptic currents (Isaacson *et al*, 1993; Rossi and Hamann, 1998). By adjusting the excitability of neurons, tonic inhibition can regulate the oscillatory properties of neuronal networks (Towers et al., 2004). GABA is mainly associated with inhibition in adult animals. However, alterations in the oscillatory properties of networks can affect the balance between excitatory and inhibitory activity. The loss of Densin and the subsequent effect on Npas4 and $GABA_A\alpha2$, may result in an aberrant disinhibition of a network when the normal response would be inhibitory. It is not yet clear what roles Npas4 or $GABA_A\alpha2$ play in the seizures generated by Nembutal injections. However, if their protein levels are indeed affected, the balance between inhibitory-excitatory networks may result.

Finally, both Densin and $GABA_A\alpha2$ can localize in the axon initial segment (AIS) [49-51]. It is reasonable to hypothesize that Densin may affect the localization of

$GABA_A\alpha2$ at the AIS. Consequently, in the absence of Densin, $GABA_A\alpha2$ may be mislocalized. Immunostaining experiments could shed light on this hypothesis.

Final Thoughts

One always hopes that the development of a knockout animal will not only provide support for proposed hypotheses, but will also yield information on how the system as a whole operates, thus leaving the researcher with many more questions than answers. Furthermore, one also hopes that the knockout animal will exhibit some exciting and unforeseen phenotype that will generate questions never even suggested based on current knowledge. On all these hopes, the Densin knockout animal has delivered.

Work conducted for my thesis is admittedly descriptive, but such is the nature of an initial characterization of a knockout mouse. Consequently, there is a wealth of experimental opportunities to be had. For example, in the course of making the full knockout animal, I also created a floxed/ conditional knockout. This conditional knockout strain has yet to be utilized for any experimental investigations. Many of the phenotypes I have identified (i.e., changes in spine morphology or dendritic arborization) or even the results from the RNA seq analysis certainly represent a system that has reached a new homeostatic set point. The conditional knockout can certainly be used to investigate the acute loss of Densin from neurons.

Another area ripe for further investigations is the affect that the deletion of Densin has on inhibitory networks. Does Densin play a role at the axon hillock? What protein(s) or complex(es) does Densin interact with at the AIS? Does Densin directly interact with

$GABA_A\alpha2$ containing receptors? Are transcriptional changes in Npas4 and $GABA_A\alpha2$ reflected at the protein level? If so, what effect does this have in relation to the sensitivity to Nembutal. Understanding the underlying mechanisms related to the loss of Densin and the susceptibility to seizures is of direct medical relevance. Furthermore, given that I have family members who suffer from epilepsy, I am well aware of the increased risk of complications from general anesthesia that epileptics face. Consequently, my interests are both scientific and personal.

Obviously, the continued investigations into the role of Densin within the PSD is central to the long-term interests of the Kennedy lab. Toward this end, we are currently engaged in a collaboration with Tom O'Dell's lab at UCLA to characterize any changes in the cellular physiology of the Densin knockout.

Currently, Holly Beale, another graduate student in the Kennedy lab, is moving forward on analyzing the data generated from the RNA seq collaboration with the Wold lab. This work has already identified candidate genes for some of the observed phenotypes and generated testable hypotheses. Furthermore, I would be remiss if I did not express excitement over being involved in the first ever use of this technology to investigate the transcriptional changes in a knockout mouse.

Given the host of cellular and molecular phenotypes exhibited by the Densin knockout mouse, it is highly likely that the Densin knockout mouse will also exhibit behavioral deficits. Tinh Luong, another graduate student in the Kennedy lab, has recently entered into a collaboration with Paul Patterson's lab to characterize behavioral deficits that impact learning and memory, motor coordination, or other aberrant behaviors.

One area or research outside the scope of the Kennedy lab, but interesting none-the-less, is the role of Densin in the kidney and pancreas. Densin is a component of the slit diaphragm complex of the kidney [52, 53] and autoimmune antibodies against Densin have been found in patients with type 1 diabetes [54] . Furthermore, the RNA seq analysis revealed that a host of kidney-, pancreas-, and diabetes-related transcripts were significantly changed in the Densin knockout. A future collaboration with a kidney biology laboratory could have immediate implications for understanding the molecular mechanisms and pathways in which Densin plays a role. Furthermore, the Densin knockout mouse can potentially help uncover disease mechanisms as they relate to diabetes.

References

1. Bayer, K.U., et al., *Interaction with the NMDA receptor locks CaMKII in an active conformation.* Nature, 2001. **411**(6839): p. 801-5.
2. Shen, K., et al., *Molecular memory by reversible translocation of calcium/calmodulin-dependent protein kinase II.* Nat Neurosci, 2000. **3**(9): p. 881-6.
3. Merrill, M.A., et al., *Activity-driven postsynaptic translocation of CaMKII.* Trends Pharmacol Sci, 2005. **26**(12): p. 645-53.
4. Elgersma, Y., et al., *Inhibitory autophosphorylation of CaMKII controls PSD association, plasticity, and learning.* Neuron, 2002. **36**(3): p. 493-505.
5. Silva, A.J., et al., *Impaired spatial learning in α-calcium-calmodulin kinase II mutant mice.* Science, 1992. **257**: p. 206-211.
6. Kennedy, M.B., *Regulation of synaptic transmission in the central nervous system: long-term potentiation.* Cell, 1989. **59**: p. 777-787.
7. Silva, A.J., et al., *Deficient hippocampal long-term potentiation in α-calcium-calmodulin kinase II mutant mice.* Science, 1992. **257**: p. 201-206.
8. Giese, K.P., et al., *Autophosphorylation at Thr286 of the alpha calcium-calmodulin kinase II in LTP and learning.* Science, 1998. **279**(5352): p. 870-3.
9. Griffith, L.C., C.S. Lu, and X.X. Sun, *CaMKII, an enzyme on the move: regulation of temporospatial localization.* Mol Interv, 2003. **3**(7): p. 386-403.
10. Leonard, A.S., et al., *Regulation of calcium/calmodulin-dependent protein kinase II docking to N-methyl-D-aspartate receptors by calcium/calmodulin and alpha-actinin.* J Biol Chem, 2002. **277**(50): p. 48441-8.
11. Tsui, J. and R.C. Malenka, *Substrate localization creates specificity in calcium/calmodulin-dependent protein kinase II signaling at synapses.* J Biol Chem, 2006. **281**(19): p. 13794-804.
12. Gardoni, F., et al., *Calcium/calmodulin-dependent protein kinase II is associated with NR2A/B subunits of NMDA receptor in postsynaptic densities.* J Neurochem, 1998. **71**(4): p. 1733-41.
13. Gardoni, F., et al., *Hippocampal synaptic plasticity involves competition between Ca2+/calmodulin-dependent protein kinase II and postsynaptic density 95 for binding to the NR2A subunit of the NMDA receptor.* J Neurosci, 2001. **21**(5): p. 1501-9.
14. Walikonis, R.S., et al., *Densin-180 forms a ternary complex with the α-subunit of CaMKII and α-actinin.* J. Neurosci., 2001. **21**: p. 423-433.
15. Strack, S., et al., *Association of calcium/calmodulin-dependent kinase II with developmentally regulated splice variants of the postsynaptic density protein densin-180.* J. Biol. Chem., 2000. **275**: p. 25061-4.
16. Dingledine, R., et al., *The glutamate receptor ion channels.* Pharmacol Rev, 1999. **51**(1): p. 7-61.
17. Meguro, H., et al., *Functional characterization of a heteromeric NMDA receptor channel expressed from cloned cDNAs.* Nature, 1992. **357**: p. 70-74.

18. Monyer, H., et al., *Heteromeric NMDA receptors: Molecular and functional distinction of subtypes.* Science, 1992. **256**: p. 1217-1221.
19. Barria, A. and R. Malinow, *NMDA receptor subunit composition controls synaptic plasticity by regulating binding to CaMKII.* Neuron, 2005. **48**(2): p. 289-301.
20. McIlhinney, R.A., et al., *Cell surface expression of the human N-methyl-D-aspartate receptor subunit 1a requires the co-expression of the NR2A subunit in transfected cells.* Neuroscience, 1996. **70**(4): p. 989-97.
21. Fukaya, M., et al., *Retention of NMDA receptor NR2 subunits in the lumen of endoplasmic reticulum in targeted NR1 knockout mice.* Proc Natl Acad Sci U S A, 2003. **100**(8): p. 4855-60.
22. Shen, K. and T. Meyer, *Dynamic control of CaMKII translocation and localization in hippocampal neurons by NMDA receptor stimulation.* Science, 1999. **284**(5411): p. 162-6.
23. Mortazavi, A., et al., *Mapping and quantifying mammalian transcriptomes by RNA-Seq.* Nat Methods, 2008. **5**(7): p. 621-8.
24. Kirov, S.A. and K.M. Harris, *Dendrites are more spiny on mature hippocampal neurons when synapses are inactivated.* Nat Neurosci, 1999. **2**(10): p. 878-83.
25. Kirov, S.A., C.A. Goddard, and K.M. Harris, *Age-dependence in the homeostatic upregulation of hippocampal dendritic spine number during blocked synaptic transmission.* Neuropharmacology, 2004. **47**(5): p. 640-8.
26. Burrone, J. and V.N. Murthy, *Synaptic gain control and homeostasis.* Curr Opin Neurobiol, 2003. **13**(5): p. 560-7.
27. Bourne, J. and K.M. Harris, *Do thin spines learn to be mushroom spines that remember?* Curr Opin Neurobiol, 2007. **17**(3): p. 381-6.
28. Harris, K.M., F.E. Jensen, and B. Tsao, *Three-dimensional structure of dendritic spines and synapses in rat hippocampus (CA1) at postnatal day 15 and adult ages: implications for the maturation of synaptic physiology and long-term potentiation.* J. Neurosci., 1992. **12**: p. 2685-2705.
29. Holtmaat, A.J., et al., *Transient and persistent dendritic spines in the neocortex in vivo.* Neuron, 2005. **45**(2): p. 279-91.
30. Zuo, Y., et al., *Development of long-term dendritic spine stability in diverse regions of cerebral cortex.* Neuron, 2005. **46**(2): p. 181-9.
31. Harris, K.M., *Structure, development, and plasticity of dendritic spines.* Curr Opin Neurobiol, 1999. **9**(3): p. 343-8.
32. Ganeshina, O., et al., *Synapses with a segmented, completely partitioned postsynaptic density express more AMPA receptors than other axospinous synaptic junctions.* Neuroscience, 2004. **125**(3): p. 615-23.
33. Ganeshina, O., et al., *Differences in the expression of AMPA and NMDA receptors between axospinous perforated and nonperforated synapses are related to the configuration and size of postsynaptic densities.* J Comp Neurol, 2004. **468**(1): p. 86-95.
34. Sala, C., I. Cambianica, and F. Rossi, *Molecular mechanisms of dendritic spine development and maintenance.* Acta Neurobiol Exp (Wars), 2008. **68**(2): p. 289-304.

35. Quitsch, A., et al., *Postsynaptic shank antagonizes dendrite branching induced by the leucine-rich repeat protein Densin-180.* J Neurosci, 2005. **25**(2): p. 479-87.
36. Arikkath, J., et al., *Erbin controls dendritic morphogenesis by regulating localization of delta-catenin.* J Neurosci, 2008. **28**(28): p. 7047-56.
37. Rubio, M.E., et al., *Assembly of the N-cadherin complex during synapse formation involves uncoupling of p120-catenin and association with presenilin 1.* Mol Cell Neurosci, 2005. **30**(1): p. 118-30.
38. Schuman, E.M. and S. Murase, *Cadherins and synaptic plasticity: activity-dependent cyclin-dependent kinase 5 regulation of synaptic beta-catenin-cadherin interactions.* Philos Trans R Soc Lond B Biol Sci, 2003. **358**(1432): p. 749-56.
39. Silverman, J.B., et al., *Synaptic anchorage of AMPA receptors by cadherins through neural plakophilin-related arm protein AMPA receptor-binding protein complexes.* J Neurosci, 2007. **27**(32): p. 8505-16.
40. Izawa, I., et al., *Densin-180 interacts with delta-catenin/neural plakophilin-related armadillo repeat protein at synapses.* J Biol Chem, 2002. **277**(7): p. 5345-50.
41. Martinez, M.C., et al., *Dual regulation of neuronal morphogenesis by a delta-catenin-cortactin complex and Rho.* J Cell Biol, 2003. **162**(1): p. 99-111.
42. Flavell, S.W. and M.E. Greenberg, *Signaling mechanisms linking neuronal activity to gene expression and plasticity of the nervous system.* Annu Rev Neurosci, 2008. **31**: p. 563-90.
43. Saffen, D.W., et al., *Convulsant-induced increase in transcription factor messenger RNAs in rat brain.* Proc Natl Acad Sci U S A, 1988. **85**(20): p. 7795-9.
44. Worley, P.F., et al., *Thresholds for synaptic activation of transcription factors in hippocampus: correlation with long-term enhancement.* J Neurosci, 1993. **13**(11): p. 4776-86.
45. Cole, A.J., et al., *Rapid increase of an immediate early gene messenger RNA in hippocampal neurons by synaptic NMDA receptor activation.* Nature, 1989. **340**(6233): p. 474-6.
46. Kubik, S., T. Miyashita, and J.F. Guzowski, *Using immediate-early genes to map hippocampal subregional functions.* Learn Mem, 2007. **14**(11): p. 758-70.
47. Lanahan, A. and P. Worley, *Immediate-early genes and synaptic function.* Neurobiol Learn Mem, 1998. **70**(1-2): p. 37-43.
48. Lin, Y., et al., *Activity-dependent regulation of inhibitory synapse development by Npas4.* Nature, 2008. **455**(7217): p. 1198-204.
49. Nusser, Z., et al., *Differential synaptic localization of two major gamma-aminobutyric acid type A receptor alpha subunits on hippocampal pyramidal cells.* Proc Natl Acad Sci U S A, 1996. **93**(21): p. 11939-44.
50. Tretter, V., et al., *The clustering of GABA(A) receptor subtypes at inhibitory synapses is facilitated via the direct binding of receptor alpha 2 subunits to gephyrin.* J Neurosci, 2008. **28**(6): p. 1356-65.
51. Apperson, M.L., I.-S. Moon, and M.B. Kennedy, *Characterization of densin-180, a new brain-specific synaptic protein of the O-sialoglycoprotein family.* J. Neurosci., 1996. **16**: p. 6839-6852.
52. Ahola, H., et al., *A novel protein, densin, expressed by glomerular podocytes.* J Am Soc Nephrol, 2003. **14**(7): p. 1731-7.

53. Heikkila, E., et al., *Densin and beta-catenin form a complex and co-localize in cultured podocyte cell junctions.* Mol Cell Biochem, 2007. **305**(1-2): p. 9-18.
54. Rinta-Valkama, J., et al., *Densin and filtrin in the pancreas and in the kidney, targets for humoral autoimmunity in patients with type 1 diabetes.* Diabetes Metab Res Rev, 2007. **23**(2): p. 119-26.